Chapter

6 THEORY AND APPLICATIONS OF SYMMETRY REPRESENTATION PRODUCTS (FINITE GROUPS)

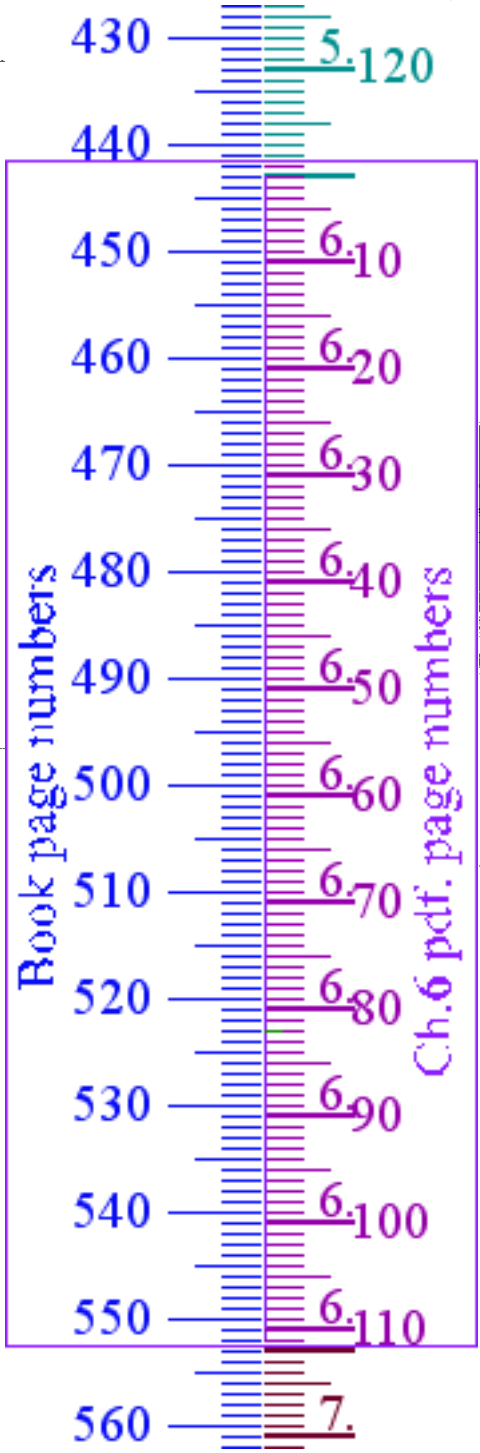

CHAPTER 6

THEORY AND APPLICATIONS OF SYMMETRY REPRESENTATION PRODUCTS (FINITE GROUPS)

So far we have studied the theory in which representations of symmetry can be analyzed into sums ($\oplus$) of irreducible representations (irreps) and have seen how this helps to simplify certain physical problems. This chapter is devoted to a special kind of *product* ($\otimes$) of representations and the study of its physical applications. Let us begin by listing some of the applications of the product analysis which we will treat later in this chapter and elsewhere in the book.

(i) We have seen how the Cartesian coordinates $\{xyz\}$ or unit vectors $\{\hat{x}\hat{y}\hat{z}\}$ are bases for one or more irreps of a symmetry group. For example, in Section 4.2.A the vectors $\{\hat{x}\hat{y}\hat{z}\}$ were shown to be a basis of $\mathscr{D}^{T_{1u}}$ of O_h. Furthermore, the vectors $\{\hat{x}\hat{y}\}$ are a basis of $\mathscr{D}^{E}$ of $\mathscr{D}_4$, while $\hat{z}$ is a basis of $\mathscr{D}^{A_2}$. In Section 6.3 we shall see how product analysis makes similar assignments for polynomials $\cdots x^2y \cdots$ of coordinates and for tensors $\cdots \hat{x}\hat{x}\hat{y} \cdots$ of arbitrary rank.

(ii) We have seen how base states $\left|{}^{\alpha}_{1}\right\rangle, \left|{}^{\alpha}_{2}\right\rangle, \ldots$ that are partners in a basis for a given irrep $\mathscr{D}^{\alpha}$ of a symmetry group are made by projection. Section 6.4 shows how product analysis makes all possible tensor operators out of products $|{}^{\alpha}_{i}\rangle\langle{}^{\beta}_{j}|$ so that they are also partners of various irreps. Certain properties of the matrix elements of these operators called selection rules are derived and the Wigner-Eckart theorem is discussed.

(iii) We have seen how the first quantum excitations of vibrations in molecules are described by a single excitation of a mode belonging to a

definite irrep. Section 6.6 shows how overtone or combination-tone states with two or more excitations are described by product analysis.

(iv) We have seen how the orbital states of a single electron in some symmetry environment will belong to an irrep of the symmetry. Now we shall see how two or more electrons orbiting in the same environment can be described using product analysis. This particular application of product analysis will be used to introduce its mathematical details in Sections 6.1 and 6.2.

6.1 TWO-PARTICLE STATES AND PRODUCTS OF REPRESENTATIONS

In Section 4.3.A we discussed the model for the orbital states of a particle tunneling between potential wells fixed at the vertices of a regular octahedron. In this model there were six states $|1\rangle, |2\rangle, \ldots,$ and $|6\rangle$ corresponding to orbitals more or less localized in wells 1, 2, ..., and 6, respectively, as shown in Figure 4.3.1(b). Then Figure 4.3.2(b) shows which combinations of these states would be eigenstates according to O_h symmetry.

The same model can be made to accommodate two orbiting particles. Each basis of a two-particle system has the form $|i_A, j_B\rangle \equiv |i\rangle_A |j\rangle_B$. There are $6^2 = 36$ two-particle bases:

$$\{|1,1\rangle, |1,2\rangle, \ldots, |1,6\rangle, |2,1\rangle, |2,2\rangle, \ldots, |6,6\rangle\}. \tag{6.1.1}$$

The wave functions for these base states are drawn schematically in Figure 6.1.1. The A and B particle waves are indicated by large and small circles, respectively, in the figure. Each vector $|i_A, j_B\rangle \equiv |i\rangle_A |j\rangle_B$ denotes a state in which the first particle (say particle A) is in state i and the second one (say particle B) is in state j.

One defines a scalar product between state vector $|\phi, \psi\rangle \equiv |\phi\rangle|\psi\rangle$ and vector $\langle i, j| = |i, j\rangle^\dagger = (|i\rangle|j\rangle)^\dagger = \langle j|\langle i|$ as follows:

$$\langle i, j|\phi, \psi\rangle = \langle j|\langle i|\phi\rangle|\psi\rangle = \langle i|\phi\rangle\langle j|\psi\rangle. \tag{6.1.2}$$

This quantity gives the amplitude for the system in state $|\phi, \psi\rangle$ to have particle A in state i and particle B in state j. The probability or intensity $|\langle i, j|\phi, \psi\rangle|^2$ of this coincidence is the product of the probabilities or intensities $|\langle i|\phi\rangle|^2$ and $|\langle j|\psi\rangle|^2$ for the separate events. This is consistent with the axioms for quantum amplitudes given in Chapter 1. Two-particle amplitudes of the form in Eq. (6.1.2) will obey the basic axioms 1–4 in Chapter 1 and the orthonormality and completeness relations will hold:

$$\langle i, j|k, l\rangle = \delta_{ik}\delta_{jl}, \tag{6.1.3a}$$

$$\sum_i \sum_j |i, j\rangle\langle i, j| = 1. \tag{6.1.3b}$$

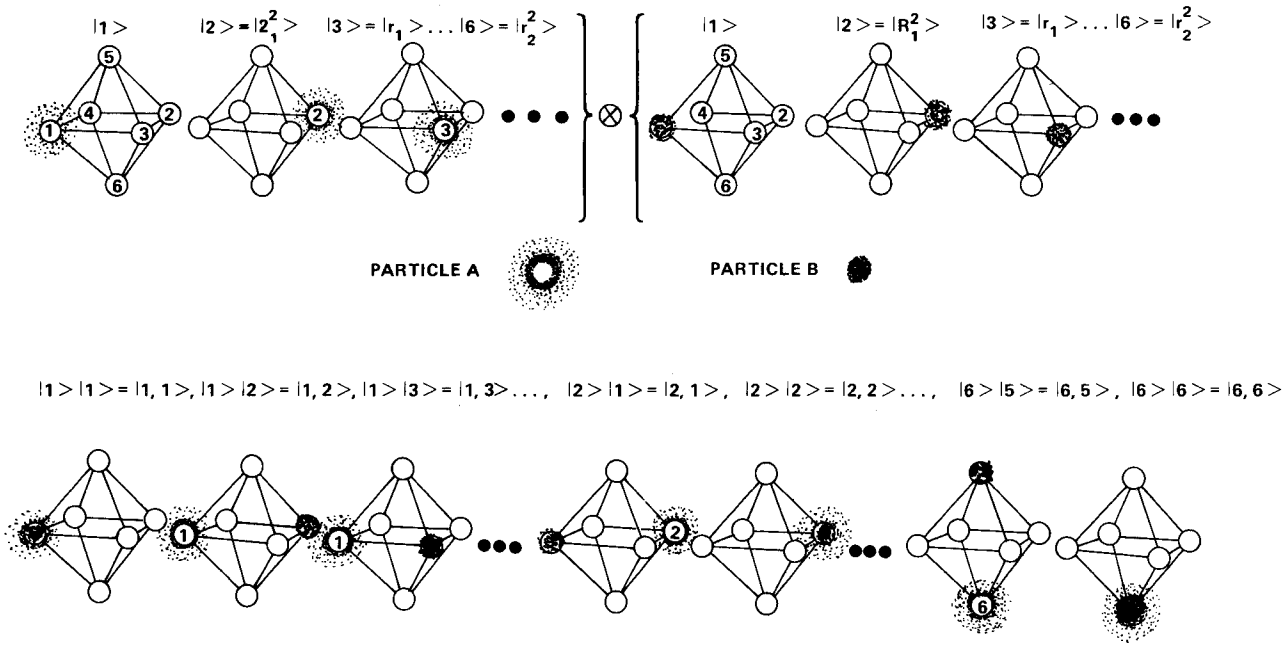

Figure 6.1.1 Sketch of two-particle wave function in octahedral environment. Thirty-six unrestricted two-particle states are possible if particles A and B are distinguishable.

However, if the two particles were identical electrons with the same spin, the states of the form $|j, j\rangle$ would be ruled out by the famous principle of Pauli. We shall discuss Pauli's principle and its consequences later. Meanwhile, we may use the basis in Eq. (6.1.1) without modification if we suppose the two particles are electrons in different spin states or they are different types of particles altogether.

A. Noninteracting Particles

If we suppose that the two particles can orbit around the octahedron without ever feeling each other's presence, then the description of the resulting symmetry analysis is simple. The symmetry operators are all combinations (a, b) of the operators a and b for particles A and B, respectively, as defined by the following:

$$(a, b)|k, l\rangle \equiv (a, b)|k\rangle|l\rangle = a|k\rangle b|l\rangle. \tag{6.1.4a}$$

This defines a representation of the two-particle operators:

$$\begin{aligned}\langle i, j|(a, b)|k, l\rangle &= \langle i|a|k\rangle\langle j|b|l\rangle \\ &= \alpha_{ik}\beta_{jl}.\end{aligned} \tag{6.1.4b}$$

The total symmetry group G of the two-particle system is just the outer product of the individual symmetry groups which in this case are both O_h groups:

$$\begin{aligned}G = O_h^A \times O_h^B &= \{\cdots(a,1)\cdots(a',1)\cdots\} \times \{\cdots(1,b')\cdots(1,b')\cdots\} \\ &= \{\cdots(a,b)\cdots(a,b')\cdots(a',b)\cdots(a',b')\cdots\}.\end{aligned} \tag{6.1.5}$$

This is because the two types of operators work independently through each other. Any $(a, 1)$ commutes with any $(1, b)$ so that

$$(a, b)(a', b') = (aa', bb'). \tag{6.1.6}$$

Therefore, the definition of direct product (Section 2.10) is correctly used in Eq. (6.1.5).

Representations of $G = O^A \times O^B$ such as are indicated in Eq. (6.1.4) or in Eq. (6.1.7) will be called DIRECT PRODUCTS ($\otimes$) of the separate factor group representations. We shall see that all irreps $\mathscr{D}^{\alpha\beta}(a, b) = \mathscr{D}^{\alpha}(a) \otimes$

$\mathscr{D}^{\beta}(b)$ of G can be made in this way:

$$(a,b)\left|\begin{matrix}\alpha & \beta\\ k & l\end{matrix}\right\rangle = a\left|\begin{matrix}\alpha\\ k\end{matrix}\right\rangle b\left|\begin{matrix}\beta\\ l\end{matrix}\right\rangle$$
$$= \left(\sum_{i=1}^{l^{\alpha}} \mathscr{D}^{\alpha}_{ik}(a)\left|\begin{matrix}\alpha\\ i\end{matrix}\right\rangle\right)\left(\sum_{j=1}^{l^{\beta}} \mathscr{D}^{\beta}_{jl}(b)\left|\begin{matrix}\beta\\ j\end{matrix}\right\rangle\right)$$
$$= \sum_{i=1}^{l^{\alpha}}\sum_{j=1}^{l^{\beta}} \mathscr{D}^{\alpha}_{ik}(a)\mathscr{D}^{\beta}_{jl}(b)\left|\begin{matrix}\alpha & \beta\\ i & j\end{matrix}\right\rangle, \qquad (6.1.7a)$$

$$\left\langle\begin{matrix}\alpha & \beta\\ i & j\end{matrix}\right|(a,b)\left|\begin{matrix}\alpha & \beta\\ k & l\end{matrix}\right\rangle = \mathscr{D}^{\alpha}_{ik}(a)\mathscr{D}^{\beta}_{jl}(b) \equiv (\mathscr{D}^{\alpha}(a) \otimes \mathscr{D}^{\beta}(b))_{ij:kl}, \qquad (6.1.7b)$$

$$(\mathscr{D}^{\alpha}(a) \otimes \mathscr{D}^{\beta}(b))_{ij:kl} \equiv \mathscr{D}^{\alpha\beta}_{ij:kl}(a,b). \qquad (6.1.7c)$$

This direct product ($\otimes$) is sometimes called the TENSOR or KRONECKER product of matrices.

One of the difficulties of using the direct product is getting used to the double index notation. Actual construction of this product is quite easy, as demonstrated by the following example:

$$\mathscr{D}^{T_{1g}E_u}(r_2,i_5) = \mathscr{D}^{T_{1g}}(r_2) \otimes \mathscr{D}^{E_u}(i_5) = \begin{pmatrix} 0 & 0 & -1\\ 1 & 0 & 0\\ 0 & -1 & 0\end{pmatrix} \otimes \begin{pmatrix} -\frac{1}{2} & -\frac{\sqrt{3}}{2}\\ -\frac{\sqrt{3}}{2} & \frac{1}{2}\end{pmatrix}.$$

The second factor $\mathscr{D}^{E_u}$ appears in blocks of the outer product multiplied by corresponding components of the first factor $\mathscr{D}^{T_{1g}}$.

$$\begin{pmatrix} 0\begin{pmatrix} -\frac{1}{2} & -\frac{\sqrt{3}}{2}\\ -\frac{\sqrt{3}}{2} & \frac{1}{2}\end{pmatrix} & 0\begin{pmatrix} -\frac{1}{2} & -\frac{\sqrt{3}}{2}\\ -\frac{\sqrt{3}}{2} & \frac{1}{2}\end{pmatrix} & -1\begin{pmatrix} -\frac{1}{2} & -\frac{\sqrt{3}}{2}\\ -\frac{\sqrt{3}}{2} & \frac{1}{2}\end{pmatrix}\\ 1\begin{pmatrix} -\frac{1}{2} & -\frac{\sqrt{3}}{2}\\ -\frac{\sqrt{3}}{2} & \frac{1}{2}\end{pmatrix} & 0\begin{pmatrix} -\frac{1}{2} & -\frac{\sqrt{3}}{2}\\ -\frac{\sqrt{3}}{2} & \frac{1}{2}\end{pmatrix} & 0\begin{pmatrix} -\frac{1}{2} & -\frac{\sqrt{3}}{2}\\ -\frac{\sqrt{3}}{2} & \frac{1}{2}\end{pmatrix}\\ 0\begin{pmatrix} -\frac{1}{2} & -\frac{\sqrt{3}}{2}\\ -\frac{\sqrt{3}}{2} & \frac{1}{2}\end{pmatrix} & -1\begin{pmatrix} -\frac{1}{2} & -\frac{\sqrt{3}}{2}\\ -\frac{\sqrt{3}}{2} & \frac{1}{2}\end{pmatrix} & 0\begin{pmatrix} -\frac{1}{2} & -\frac{\sqrt{3}}{2}\\ -\frac{\sqrt{3}}{2} & \frac{1}{2}\end{pmatrix}\end{pmatrix}$$

$$= \begin{pmatrix} \cdot & \cdot & \cdot & \cdot & \frac{1}{2} & \frac{\sqrt{3}}{2}\\ \cdot & \cdot & \cdot & \cdot & \frac{\sqrt{3}}{2} & -\frac{1}{2}\\ -\frac{1}{2} & -\frac{\sqrt{3}}{2} & \cdot & \cdot & \cdot & \cdot\\ -\frac{\sqrt{3}}{2} & \frac{1}{2} & \cdot & \cdot & \cdot & \cdot\\ \cdot & \cdot & \frac{1}{2} & \frac{\sqrt{3}}{2} & \cdot & \cdot\\ \cdot & \cdot & \frac{\sqrt{3}}{2} & -\frac{1}{2} & \cdot & \cdot\end{pmatrix}. \qquad (6.1.7)_{\mathrm{x}}$$

The double indices for the matrix components of this example are deployed lexicographically, i.e., $\{11, 12, \ldots, 21, 22, \ldots\}$, as shown in the following:

$$\mathscr{D}^{TE} = \mathscr{D}^{T} \otimes \mathscr{D}^{E} = \begin{pmatrix} \mathscr{D}^{TE}_{11:11} & \mathscr{D}_{11:12} & \mathscr{D}_{11:21} & \mathscr{D}_{11:22} & \mathscr{D}_{11:31} & \mathscr{D}_{11:32} \\ \mathscr{D}_{12:11} & \mathscr{D}_{12:12} & \mathscr{D}_{12:21} & \mathscr{D}_{12:22} & \mathscr{D}_{12:31} & \mathscr{D}_{12:32} \\ \mathscr{D}_{21:11} & \mathscr{D}_{21:12} & \mathscr{D}_{21:21} & \mathscr{D}_{21:22} & \mathscr{D}_{21:31} & \mathscr{D}_{21:32} \\ \mathscr{D}_{22:11} & \mathscr{D}_{22:12} & \mathscr{D}_{22:21} & \mathscr{D}_{22:22} & \mathscr{D}_{22:31} & \mathscr{D}_{22:32} \\ \mathscr{D}_{31:11} & \mathscr{D}_{31:12} & \mathscr{D}_{31:21} & \mathscr{D}_{31:22} & \mathscr{D}_{31:31} & \mathscr{D}_{31:32} \\ \mathscr{D}_{32:11} & \mathscr{D}_{32:12} & \mathscr{D}_{32:21} & \mathscr{D}_{32:22} & \mathscr{D}_{32:31} & \mathscr{D}_{32:32} \end{pmatrix}. \tag{6.1.8}$$

The characters of direct products of irreps are just the products of the characters, as seen in the following:

$$\begin{aligned} \chi^{\alpha\beta}(a,b) \equiv \text{TRACE}\, \mathscr{D}^{\alpha\beta}(a,b) &\equiv \sum_{m=1}^{l^\alpha} \sum_{n=1}^{l^\beta} \mathscr{D}^{\alpha\beta}_{mn:mn}(a,b) \\ &= \left(\sum_{m=1}^{l^\alpha} \mathscr{D}^{\alpha}_{mm}(a) \right) \left(\sum_{n=1}^{l^\beta} \mathscr{D}^{\beta}_{nn}(b) \right) \\ &= \chi^{\alpha}(a)\chi^{\beta}(b). \end{aligned} \tag{6.1.9}$$

It turns out that virtually all properties of a direct product group $G = O^A \times O^B$ are derived by product analysis of the corresponding factor groups. This is true for the operators in Eq. (6.1.4), irreps in Eq. (6.1.7), and characters in Eq. (6.1.9).

The Hamiltonian operator for noninteracting particles is just the sum of their two separate single-particle operators. Let us write this operator so it indicates that each term operates exclusively on only one particle:

$$H = (H_A, 1) + (1, H_B). \tag{6.1.10}$$

The irrep basis states of the form $\left| \begin{matrix} \alpha & \beta \\ i & j \end{matrix} \right\rangle$ are eigenstates of the noninteracting Hamiltonian if $\left| \begin{matrix} \alpha \\ i \end{matrix} \right\rangle$ and $\left| \begin{matrix} \beta \\ j \end{matrix} \right\rangle$ were eigenstates of H_A and H_B, respectively:

$$H \left| \begin{matrix} \alpha & \beta \\ i & j \end{matrix} \right\rangle = H_A \left| \begin{matrix} \alpha \\ i \end{matrix} \right\rangle \left| \begin{matrix} \beta \\ j \end{matrix} \right\rangle + \left| \begin{matrix} \alpha \\ i \end{matrix} \right\rangle H_B \left| \begin{matrix} \beta \\ j \end{matrix} \right\rangle = (\varepsilon^\alpha + \varepsilon^\beta) \left| \begin{matrix} \alpha & \beta \\ i & j \end{matrix} \right\rangle. \tag{6.1.11}$$

The energies of two noninteracting particles are simply added to give the energy of the two-particle system.

One may combine the levels and states in Figure 4.3.2(b) as shown on the left-hand side of Figure 6.1.2(a). This gives the level diagram of the noninter-

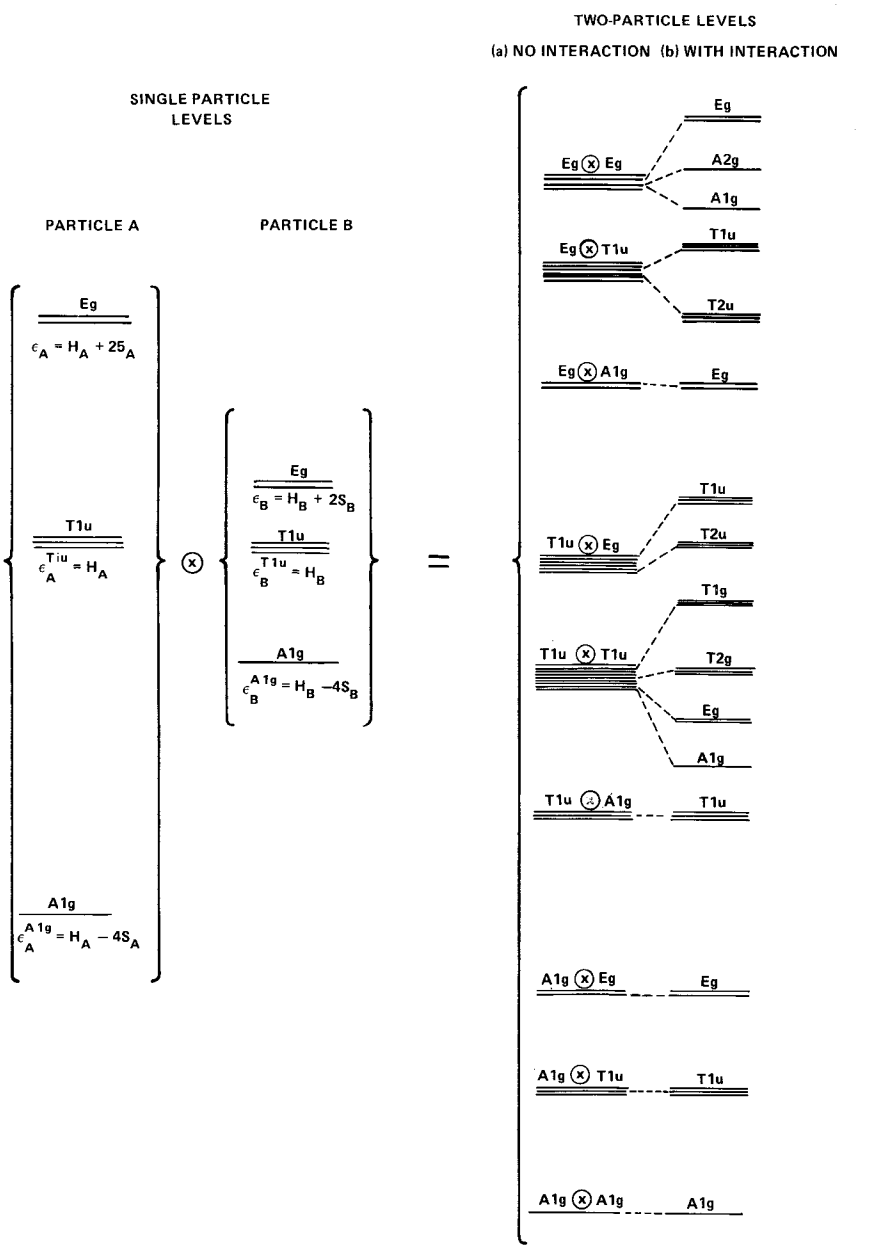

Figure 6.1.2 Eigenlevels of octahedral two-particle system. (a) Two-particle levels are labeled by irreps $(D^{\alpha} \otimes D^{\beta})$ of cross-product symmetry $G^A \times G^B = O_h \times O_h$. (b) Interaction causes levels to split into levels labeled by irreps of $G^{\text{RIGID}} = O_h^{\text{RIGID}}$.

acting two-particle system. The levels have degeneracies $l^\alpha l^\beta$ equal to the dimension irreps of $G = O_h^A \times O_h^B$. Note also that state $\begin{vmatrix} \alpha & \beta \\ i & j \end{vmatrix}\rangle$ would have the same energy as state $\begin{vmatrix} \beta & \alpha \\ j & i \end{vmatrix}\rangle$ if particles A and B were identical electrons. This additional symmetry will be studied when we introduce the Pauli principle. In the next section we explain the level splitting shown on the extreme right-hand side of Figure 6.1.2.

B. Interacting Particles

Suppose we could gradually turn on a repulsive interaction between the two particles orbiting in the octahedral potential such as the Coulomb potential that would exist between two electrons. Mathematically, this can be described by some perturbation operator V added to the Hamiltonian in Eq. (6.1.10).

A matrix element of the form $\langle 1,1|V|1,1\rangle$, for example, would give the expectation value of the repulsion energy for the state $|1,1\rangle$ in which two particles are sharing the first potential well. This energy would be more than for states like $|1,3\rangle$ or $|1,2\rangle$, in which the particles are not so close to each other; i.e., $\langle 1,1|V|1,1\rangle \geq \langle 1,3|V|1,3\rangle \geq \langle 1,2|V|1,2\rangle$. From this it follows that most of the operators in $G = O^A \times O^B = \cdots(a,b)\cdots$ will not commute with V or any Hamiltonian that contains V. Consider the operator $g = (1, R_1)$, for example. If this commutes with V, then the following contradictory relation follows:

$$\langle 1,1|V|1,1\rangle = \langle 1,1|g^\dagger V g|1,1\rangle = \langle 1,3|V|1,3\rangle. \tag{6.1.12}$$

However, all the octahedral sites are still equivalent, and V should have the symmetry O_h. The symmetry operators that still commute with V are just those which move the two particles rigidly together without changing the distance between them, i.e., operators of the form (a,a). Call the resulting group O_h^{RIGID}:

$$O_h^{\text{RIGID}} = \{(1,1)\cdots(a,a)\cdots(b,b)\cdots\}. \tag{6.1.13}$$

Each of the irreducible product representations of the now-defunct symmetry $G = O_h^A \times O_h^B$ will be, in general, only reducible representations of the subgroup O_h^{RIGID}. The techniques of Chapter 3 can be used to reduce them, and this will give the eigenvectors of the new Hamiltonian in the limit of small V.

First, the character analysis will tell which irreps $\mathscr{D}^\gamma$ of O_h^{RIGID} are contained in $\mathscr{D}^{\alpha\beta}$, that is, the frequency $f^\gamma(\mathscr{D}^{\alpha\beta})$. Equations (3.5.11) and

(6.1.9) yield the following frequency formula:

$$f^{\gamma}(\mathscr{D}^{\alpha\beta}) = \frac{1}{48}\sum_{\substack{\text{classes}\\ g}} {}^{\circ}c_g \chi_g^{\gamma *}\,\text{TRACE}\,\mathscr{D}^{\alpha\beta}(g,g),$$

$$= \frac{1}{48}\sum_{\substack{\text{classes}\\ g}} {}^{\circ}c_g \chi_g^{\gamma *}\chi_g^{\alpha}\chi_g^{\beta}. \qquad (6.1.14)$$

Substitution of the O_h characters (4.1.16) for $\alpha = \beta = T_{1u}$ yields the frequencies $f^{A_{1g}} = f^{E_g} = f^{T_{1g}} = f^{T_{2g}} = 1$. All other f^{γ} are zero. This means that some transformation matrix $\mathscr{C}$ exists which effects the following reduction:

$$\mathscr{C}^{\dagger}\mathscr{D}^{T_{1u}T_{1u}}(g,g)\mathscr{C} = \mathscr{D}^{A_{1g}}(g) \oplus \mathscr{D}^{E_g}(g) \oplus \mathscr{D}^{T_{1g}}(g) \oplus \mathscr{D}^{T_{2g}}(g). \quad (6.1.15)$$

It is easy to check that the sum of the four characters add up to the product character $\chi^{T_{1u}}\chi^{T_{1u}}$:

$h = 1$	r	R^2	R	i	I	Ir	IR^2	IR	Ii
$\chi_h^{A_{1g}} = 1$	1	1	1	1	1	1	1	1	1
$\chi_h^{E_g} = 2$	−1	2	0	0	2	−1	2	0	0
$\chi_h^{T_{1g}} = 3$	0	−1	1	−1	3	0	−1	1	−1
$\chi_h^{T_{2g}} = 3$	0	−1	−1	1	3	0	−1	−1	1
$\chi_h^{T_{1u}}\chi_h^{T_{1u}} = 9$	0	1	1	1	9	0	1	1	1

For many cases one may find the correct combinations by trial and inspection of characters in this way. This may be quicker than using the formula (6.1.14).

The appearance of the four irreps in the $T_{1u} \times T_{1u}$ product (6.1.15) means that the (T_{1u}, T_{1u}) level in Figure 4.1.2 will split into four levels when the interaction V is present. The four levels labeled A_{1g}, E_g, T_{1g}, and T_{2g} are shown splitting away from (T_{1u}, T_{1u}) in Figure 6.1.2(b). The form of the eigenstates for these four levels is determined by columns of the $\mathscr{C}$ matrix. Each splitting in Figure 6.1.2(b) corresponds to a different $\mathscr{C}$ matrix.

Let us see how to find the transformation matrix $\mathscr{C}$ that reduces a general product $\mathscr{D}^{\alpha} \otimes \mathscr{D}^{\beta}$ and, particularly, the one in Eq. (6.1.15). Following the theory of Chapter 3, one applies the elementary operators P^{γ}_{mn} of $H = O_h^{\text{RIGID}}$ to the base states of $O_h^A \times O_h^B$. One obtains the following eigenstates:

$$\left|{}^{\gamma}_{m}(\alpha \otimes \beta)\right\rangle \equiv P^{\gamma}_{mn}\left|{}^{\alpha\ \ \beta}_{k\ \ l}\right\rangle \Big/ \sqrt{N^{\gamma\alpha\beta}_{nkl}}$$

$$= (l^{\gamma}/{}^{\circ}H)\sum_{a}\mathscr{D}^{\gamma *}_{mn}(a)(a,a)\left|{}^{\alpha\ \ \beta}_{k\ \ l}\right\rangle \Big/ \sqrt{N^{\gamma\alpha\beta}_{nkl}}, \quad (6.1.16a)$$

where the effect of operator (a, a) is given by Eq. (6.1.7a) as

$$\left|{}^{\gamma}_{m}(\alpha \otimes \beta)\right\rangle = (l^{\gamma}/{}^{o}H)\sum_{a}\sum_{i=1}^{l^{\alpha}}\sum_{j=1}^{l^{\beta}}\mathscr{D}^{\gamma *}_{mn}(a)\mathscr{D}^{\alpha}_{ik}(a)\mathscr{D}^{\beta}_{jl}(a)\left|{}^{\alpha}_{i}\ {}^{\beta}_{j}\right\rangle\Big/\sqrt{N^{\gamma\alpha\beta}_{nkl}}, \tag{6.1.16b}$$

and where the normalization constant is the following:

$$N^{\gamma\alpha\beta}_{nkl} = \left\langle {}^{\alpha}_{k}\ {}^{\beta}_{l}\right|P_{mn}\left|{}^{\gamma}_{k}\ {}^{\beta}_{l}\right\rangle = (l^{\gamma}/{}^{o}H)\sum_{a}\mathscr{D}^{\gamma *}_{nn}(a)\mathscr{D}^{\alpha}_{kk}(a)\mathscr{D}^{\beta}_{ll}(a). \tag{6.1.16c}$$

The indices n, k, and l are chosen to be the first combination which gives nonzero $N^{\gamma\alpha\beta}_{nkl}$. For example, let $\alpha = \beta = T_{1u}$, and $\gamma = T_{1g}$. Substituting tetragonally defined irreps (4.2.14) into Eq. (6.1.16) gives $N_{111} = N_{113} = N_{121} = N_{122} = 0$, and $N_{123} = \frac{1}{2}$. [Note that Eq. (6.1.16) gives the same results whether one sums over group O or $O_h = O \times C_i$.] Now with n, k, and l fixed, one tries different j, i, and m in Eq. (4.1.16b). For this example the following results are obtained:

$$\begin{aligned}
\left|{}^{T_{1g}}_{1}(T_{1u}\otimes T_{1u})\right\rangle &= \frac{1}{\sqrt{2}}\left|{}^{T_{1u}}_{2}\ {}^{T_{1u}}_{3}\right\rangle - \frac{1}{\sqrt{2}}\left|{}^{T_{1u}}_{3}\ {}^{T_{1u}}_{2}\right\rangle,\\
\left|{}^{T_{1g}}_{2}(T_{1u}\otimes T_{1u})\right\rangle &= \frac{1}{\sqrt{2}}\left|{}^{T_{1u}}_{3}\ {}^{T_{1u}}_{1}\right\rangle - \frac{1}{\sqrt{2}}\left|{}^{T_{1u}}_{1}\ {}^{T_{1u}}_{3}\right\rangle,\\
\left|{}^{T_{1g}}_{3}(T_{1u}\otimes T_{1u})\right\rangle &= \frac{1}{\sqrt{2}}\left|{}^{T_{1u}}_{1}\ {}^{T_{1u}}_{2}\right\rangle - \frac{1}{\sqrt{2}}\left|{}^{T_{1u}}_{2}\ {}^{T_{1u}}_{1}\right\rangle.
\end{aligned} \tag{6.1.17}$$

The coefficients in the foregoing example are called COUPLING COEFFICIENTS or CLEBSCH-GORDON COEFFICIENTS $\mathscr{C}^{\alpha\beta\gamma}_{ijm}$. They are defined in terms of the product states $\left|{}^{\alpha}_{i}\ {}^{\beta}_{j}\right\rangle$:

$$\left|{}^{\gamma}_{m}(\alpha \otimes \beta)\right\rangle = \sum_{i=1}^{l^{\alpha}}\sum_{j=1}^{l^{\beta}}\mathscr{C}^{\alpha\beta\gamma}_{ijm}\left|{}^{\alpha}_{i}\ {}^{\beta}_{j}\right\rangle. \tag{6.1.18a}$$

They are transformation amplitudes connecting $\left|{}^{\alpha}_{i}\ {}^{\beta}_{j}\right\rangle$ to states $|{}^{\gamma}_{m}(\alpha \times \beta)\rangle$

belonging to irrep $\mathscr{D}^{\gamma}$:

$$\mathscr{C}^{\alpha\beta\gamma}_{ijm} = \left\langle \begin{matrix} \alpha & \beta \\ i & j \end{matrix} \middle| \begin{matrix} \gamma \\ m \end{matrix} (\alpha \otimes \beta) \right\rangle = \frac{(l^{\gamma}/{}^{o}G)\Sigma_g \mathscr{D}^{\gamma *}_{mn}(g)\mathscr{D}^{\alpha}_{ik}(g)\mathscr{D}^{\beta}_{jl}(g)}{\sqrt{(l^{\gamma}/{}^{o}G)\Sigma_g \mathscr{D}^{\gamma *}_{nn}(g)\mathscr{D}^{\alpha}_{kk}(g)\mathscr{D}^{\beta}_{ll}(g)}}. \tag{6.1.18b}$$

The $\mathscr{C}^{\alpha\beta\gamma}_{ijm}$ are the components of the transformation matrix $\mathscr{C}$ in Eq. (6.1.15) which reduces the product representation $\mathscr{D}^{\alpha} \times \mathscr{D}^{\beta}$. The C transformation which reduces the example with $\alpha = T_{1u} = \beta$ is shown in Eq. (6.1.19). Equation (6.1.17) gives three of the columns of $\mathscr{C}$ and the other six are derived similarly. The $\mathscr{C}$ matrix is the usual format for a table of coupling coefficients as shown in Eq. (6.1.19c):

$$\sum_{i=1}^{l^{\alpha}} \sum_{j=1}^{l^{\beta}} \sum_{k=1}^{l^{\alpha}} \sum_{l=1}^{l^{\beta}} \left(\mathscr{C}^{\alpha\beta\gamma'}_{ijm}\right)^{*} \mathscr{D}^{\alpha\beta}_{ij:kl}(R_1, R_1)\mathscr{C}^{\alpha\beta\gamma}_{kln} = \mathscr{D}^{\gamma}_{mn}(R_1)\delta^{\gamma'\gamma}, \tag{6.1.19a}$$

$$\mathscr{C}^{\dagger} \begin{vmatrix} 1 & \cdot & \cdot & \cdot & \cdot & \cdot & \cdot & \cdot & \cdot \\ \cdot & \cdot & -1 & \cdot & \cdot & \cdot & \cdot & \cdot & \cdot \\ \cdot & 1 & \cdot & \cdot & \cdot & \cdot & \cdot & \cdot & \cdot \\ \cdot & \cdot & \cdot & \cdot & \cdot & \cdot & -1 & \cdot & \cdot \\ \cdot & \cdot & \cdot & \cdot & \cdot & \cdot & \cdot & \cdot & 1 \\ \cdot & \cdot & \cdot & \cdot & \cdot & \cdot & \cdot & -1 & \cdot \\ \cdot & \cdot & \cdot & 1 & \cdot & \cdot & \cdot & \cdot & \cdot \\ \cdot & \cdot & \cdot & \cdot & \cdot & -1 & \cdot & \cdot & \cdot \\ \cdot & \cdot & \cdot & \cdot & 1 & \cdot & \cdot & \cdot & \cdot \end{vmatrix} \mathscr{C} =$$

$$\begin{vmatrix} \boxed{1} = \mathscr{D}^{A_{1g}}(R_1) & & \\ & \boxed{\begin{matrix} -\frac{1}{2} & -\frac{\sqrt{3}}{2} \\ -\frac{\sqrt{3}}{2} & \frac{1}{2} \end{matrix}} = \mathscr{D}^{E_g}(R_1) & \\ & & \boxed{\begin{matrix} 1 & \cdot & \cdot \\ \cdot & \cdot & -1 \\ \cdot & 1 & \cdot \end{matrix}} = \mathscr{D}^{T_{1g}}(R_1) \\ \mathscr{D}^{T_{2g}}(R_1) = & \boxed{\begin{matrix} -1 & \cdot & \cdot \\ \cdot & \cdot & 1 \\ \cdot & -1 & \cdot \end{matrix}} & \end{vmatrix}, \tag{6.1.19b}$$

where:

$\mathscr{C} =$

T_{1u} ⊗ T_{1u}	A_{1g}	E_g 1	E_g 2	T_{1g} 1	T_{1g} 2	T_{1g} 3	T_{2g} 1	T_{2g} 2	T_{2g} 3
T_{1u} T_{1u}									
1 1	$\frac{1}{\sqrt{3}}$	$\frac{1}{\sqrt{6}}$	$-\frac{1}{\sqrt{2}}$	·	·	·	·	·	·
1 2	·	·	·	·	·	$\frac{1}{\sqrt{2}}$	·	·	$\frac{1}{\sqrt{2}}$
1 3	·	·	·	·	$-\frac{1}{\sqrt{2}}$	·	·	$\frac{1}{\sqrt{2}}$	·
2 1	·	·	·	·	·	$-\frac{1}{\sqrt{2}}$	·	·	$\frac{1}{\sqrt{2}}$
2 2	$\frac{1}{\sqrt{3}}$	$\frac{1}{\sqrt{6}}$	$\frac{1}{\sqrt{2}}$	·	·	·	·	·	·
2 3	·	·	·	$\frac{1}{\sqrt{2}}$	·	·	$\frac{1}{\sqrt{2}}$	·	·
3 1	·	·	·	·	$\frac{1}{\sqrt{2}}$	·	·	$\frac{1}{\sqrt{2}}$	·
3 2	·	·	·	$-\frac{1}{\sqrt{2}}$	·	·	$\frac{1}{\sqrt{2}}$	·	·
3 3	$\frac{1}{\sqrt{3}}$	$-\frac{2}{\sqrt{6}}$	·	·	·	·	·	·	·

(6.1.19c)

Note that the irreps (4.2.14), (4.2.15), and (4.2.19) have been used. The coupling coefficients for the "kosher T_2" irreps (4.2.16) have slightly different phases, as we will see in the following section. Note also that the transformation equations (6.1.17) or (6.1.19) only define the coupling coefficients $\mathscr{C}_{ijm}^{\alpha\beta\gamma}$ to within an overall phase that is a function of α, β, and γ. Any l^γ-column section of a C matrix, such as in Eq. (6.1.19), can be multiplied overall by $e^{i\phi}$ without changing the effect of the transformation $\mathscr{C}$.

C. Subgroup Chain Labeling for Coupling Coefficients

The subgroup chain labeling described in Section 4.2.A is also useful for deriving coupling coefficients. The straightforward projection method used in the preceding section becomes quite laborious in some applications. Subgroup structure can be used to divide and conquer many symmetry problems involving large groups or complex representations. The numerical values of coupling coefficients involving multidimensional representations depend on which bases are chosen. We now derive coefficients for two different choices belonging to subgroup chains (a) $O \supset D_4 \supset D_2$ and (b) $O \supset D_3 \supset C_2$.

(a) Tetragonal ($O \supset D_4 \supset D_2$) Coupling Coefficients Subgroup chain calculations begin with the lowest link. Subgroup $D_2 = \{1, R_1^2, R_2^2, R_3^2\}$ is the

lowest link in the tetragonal chain described in Section 4.2.A(a). The lowest link in all the chains is an Abelian group. The coupling coefficients for one-dimensional Abelian irreps are just 1's and 0's, and they are very easy to find. For example, the D_2 characters (4.1.43) yield the following $\otimes$-multiplication table:

$$\begin{array}{rcccc} B = & A_1 & A_2 & B_1 & B_2 \\ D^{A_1} \otimes D^B = & D^{A_1} & D^{A_2} & D^{B_1} & D^{B_2} \\ D^{A_2} \otimes D^B = & D^{A_2} & D^{A_1} & D^{B_2} & D^{B_1} \\ D^{B_1} \otimes D^B = & D^{B_1} & D^{B_2} & D^{A_1} & D^{A_2} \\ D^{B_2} \otimes D^B = & D^{B_2} & D^{B_1} & D^{A_2} & D^{A_1} \end{array} . \tag{6.1.20}$$

The combinations allowed by the table give unit coupling coefficients (viz., $D^{A_2} \otimes D^{B_1} = D^{B_2}$ implies that $\mathscr{C}^{A_2B_1B_2} = 1$), while all others are zero (viz., $0 = \mathscr{C}^{A_2B_1A_1} = \mathscr{C}^{A_2B_1A_2} = \mathscr{C}^{A_2B_1B_1}$).

The zero combinations can be eliminated immediately from coupling coefficients of the next higher subgroup link D_4. The D_4 coupling coefficients $\mathscr{C}^{\alpha\beta\gamma}_{A_2B_1A_1}$, $\mathscr{C}^{\alpha\beta\gamma}_{A_2B_1A_2}$, and $\mathscr{C}^{\alpha\beta\gamma}_{A_2B_1B_1}$ must vanish along with any combination of D_2 labels not allowed by the table of (6.1.20). For example, in the outer product of E bases $\left\{\left|\begin{matrix}E\\1\end{matrix}\right\rangle \equiv \left|\begin{matrix}E\\B_1\end{matrix}\right\rangle, \left|\begin{matrix}E\\2\end{matrix}\right\rangle \equiv \left|\begin{matrix}E\\B_2\end{matrix}\right\rangle\right\}$ the D_4 coupling matrix $\mathscr{C}$ must perform the reduction

$$\mathscr{C}^{\dagger}\mathscr{D}^E \otimes \mathscr{D}^E\mathscr{C} = \mathscr{D}^{A_1} \oplus \mathscr{D}^{B_1} \oplus \mathscr{D}^{A_2} \oplus \mathscr{D}^{B_2} \tag{6.1.21a}$$

according to D_4 characters (3.6.3) and the theory of the preceding section. The D_2 irreps correlated with D_4 irreps A_1, B_1, A_2, and B_2 are A_1, A_1, A_2, and A_2, respectively. Therefore the $E \otimes E$ $\mathscr{C}$ matrix must have the following form:

$$\begin{array}{lcccc} \left|\begin{matrix}\gamma\\k\end{matrix}(E \times E)\right\rangle = & \left|\begin{matrix}A_1\\A_1\end{matrix}\right\rangle & \left|\begin{matrix}B_1\\A_1\end{matrix}\right\rangle & \left|\begin{matrix}A_2\\A_2\end{matrix}\right\rangle & \left|\begin{matrix}B_2\\A_2\end{matrix}\right\rangle & \leftarrow D_4 \text{ label} \\ & & & & & \leftarrow D_2 \text{ label} \\ \left|\begin{matrix}E\\B_1\end{matrix}\right\rangle\left|\begin{matrix}E\\B_1\end{matrix}\right\rangle & a & c & 0 & 0 & \\ \left|\begin{matrix}E\\B_1\end{matrix}\right\rangle\left|\begin{matrix}E\\B_2\end{matrix}\right\rangle & 0 & 0 & e & g & \\ \left|\begin{matrix}E\\B_2\end{matrix}\right\rangle\left|\begin{matrix}E\\B_1\end{matrix}\right\rangle & 0 & 0 & f & h & \\ \left|\begin{matrix}E\\B_2\end{matrix}\right\rangle\left|\begin{matrix}E\\B_2\end{matrix}\right\rangle & b & d & 0 & 0 & \end{array} \tag{6.1.21b}$$

Impossible D_2 products are eliminated by writing zeros and the allowed ones are indicated by unknowns $a, b, c, \ldots, h$. To solve for the unknowns we write

the matrix equation (6.1.21) in the form

$$(\mathscr{D}^E(R) \otimes \mathscr{D}^E(R))\mathscr{C} = \mathscr{C}(\mathscr{D}^{A_1}(R) \oplus \mathscr{D}^{B_1}(R) \oplus \mathscr{D}^{A_2}(R) \oplus \mathscr{D}^{B_2}(R)). \tag{6.1.21c}$$

Using the D_4 irreps (3.6.7) for one operator R outside of the D_2 subgroup gives the following matrix equation:

$$(\mathscr{D}^E(R) \otimes \mathscr{D}^E(R))\,\mathscr{C}$$

$$\begin{pmatrix} 0 & 0 & 0 & 1 \\ 0 & 0 & -1 & 0 \\ 0 & -1 & 0 & 0 \\ 1 & 0 & 0 & 0 \end{pmatrix} \begin{pmatrix} a & c & 0 & 0 \\ 0 & 0 & e & g \\ 0 & 0 & f & h \\ b & d & 0 & 0 \end{pmatrix}$$

$$\mathscr{C}(\mathscr{D}^{A_1}(R) \oplus \mathscr{D}^{B_1}(r) \oplus \mathscr{D}^{A_2}(R) \oplus \mathscr{D}^{B_2}(R))$$

$$= \begin{pmatrix} a & c & 0 & 0 \\ 0 & 0 & e & g \\ 0 & 0 & f & h \\ b & d & 0 & 0 \end{pmatrix} \begin{pmatrix} 1 & 0 & 0 & 0 \\ 0 & -1 & 0 & 0 \\ 0 & 0 & 1 & 0 \\ 0 & 0 & 0 & -1 \end{pmatrix},$$

$$\begin{pmatrix} b & d & 0 & 0 \\ 0 & 0 & -f & -h \\ 0 & 0 & -e & -g \\ a & c & 0 & 0 \end{pmatrix} = \begin{pmatrix} a & -c & 0 & 0 \\ 0 & 0 & e & -g \\ 0 & 0 & f & -h \\ b & -d & 0 & 0 \end{pmatrix}. \tag{6.1.22}$$

This determines the unknowns to within a normalization factor:

$$b = a, \qquad c = -d, \qquad f = -e, \qquad h = g.$$

By normalizing each column the desired coupling coefficient table is obtained:

$E \otimes E$	A_1	B_1	A_2	B_2
	A_1	A_1	A_2	A_2
B_1 B_1	$\frac{1}{\sqrt{2}}$	$\frac{1}{\sqrt{2}}$	0	0
B_1 B_2	0	0	$\frac{1}{\sqrt{2}}$	$\frac{1}{\sqrt{2}}$
B_2 B_1	0	0	$-\frac{1}{\sqrt{2}}$	$\frac{1}{\sqrt{2}}$
B_2 B_2	$\frac{1}{\sqrt{2}}$	$-\frac{1}{\sqrt{2}}$	0	0

(6.1.23)

Consider one more example involving a different D_4 product and $\mathscr{C}$ matrix:

$$\mathscr{C}^{\dagger}\mathscr{D}^{E} \otimes \mathscr{D}^{A_2}\mathscr{C} = \mathscr{D}^{E}. \tag{6.1.24}$$

This $\mathscr{C}$ matrix must have the form

$$\mathscr{C} = \begin{array}{c|c|c} {}^{\gamma}_{k}(E \otimes A_2) & \left|\begin{matrix}E\\B_1\end{matrix}\right\rangle & \left|\begin{matrix}E\\B_2\end{matrix}\right\rangle \\ \hline \left|\begin{matrix}E\\B_1\end{matrix}\right\rangle\left|\begin{matrix}A_2\\A_2\end{matrix}\right\rangle & 0 & b \\ \hline \left|\begin{matrix}E\\B_2\end{matrix}\right\rangle\left|\begin{matrix}A_2\\A_2\end{matrix}\right\rangle & a & 0 \end{array}, \tag{6.1.25}$$

according to (6.1.20). Solving Eq. (6.1.24) and (6.1.25) gives

$$\begin{pmatrix} 0 & -1 \\ 1 & 0 \end{pmatrix}\begin{pmatrix} 0 & b \\ a & 0 \end{pmatrix} = \begin{pmatrix} 0 & b \\ a & 0 \end{pmatrix}\begin{pmatrix} 0 & -1 \\ 1 & 0 \end{pmatrix},$$

$$\begin{pmatrix} -a & 0 \\ 0 & b \end{pmatrix} = \begin{pmatrix} b & 0 \\ 0 & -a \end{pmatrix}$$

for the D_4 operator R. The resulting coupling coefficient table is shown in the following, along with three others:

$$\begin{array}{cc|cc} E \otimes A_2 & & E & E \\ & & B_1 & B_2 \\ \hline B_1 & A_2 & 0 & -1 \\ B_2 & A_2 & 1 & 0 \end{array}, \qquad \begin{array}{cc|cc} E \otimes B_1 & & E & E \\ & & B_1 & B_2 \\ \hline B_1 & A_1 & 1 & 0 \\ B_2 & A_1 & 0 & -1 \end{array}, \qquad \begin{array}{cc|cc} E \otimes B_2 & & E & E \\ & & B_1 & B_2 \\ \hline B_1 & A_2 & 0 & 1 \\ B_2 & A_2 & 1 & 0 \end{array}. \tag{6.1.26}$$

Now we are ready to analyze the highest link (O) in the $O \supset D_4 \supset D_2$ chain. Let us rederive the $T_1 \otimes T_1$ table of (6.1.19c) using the Kosher irreps labeled by this chain. The proper chain labels of O states are now repeated,

following Eqs. (4.2.11), (4.2.17), and (4.2.18):

$$\left\{\left|\begin{matrix}T_1\\E\\B_1\end{matrix}\right\rangle,\left|\begin{matrix}T_1\\E\\B_2\end{matrix}\right\rangle,\left|\begin{matrix}T_1\\A_2\\A_2\end{matrix}\right\rangle\right\}\left\{\left|\begin{matrix}T_2\\E\\B_1\end{matrix}\right\rangle,\left|\begin{matrix}T_2\\E\\B_2\end{matrix}\right\rangle,\left|\begin{matrix}T_2\\B_2\\A_2\end{matrix}\right\rangle\right\}\left\{\left|\begin{matrix}E\\A_1\\A_1\end{matrix}\right\rangle,\left|\begin{matrix}E\\B_1\\A_1\end{matrix}\right\rangle\right\}\left\{\left|\begin{matrix}A_2\\A_2\\A_2\end{matrix}\right\rangle\right\}\left\{\left|\begin{matrix}A_1\\A_1\\A_1\end{matrix}\right\rangle\right\}. \tag{6.1.27a}$$

By combining this with the D_4 couplings [(6.1.23) and (6.1.26)], one may deduce the structure of the $T_1 \otimes T_1$ coupling matrix as follows:

$T_1 \otimes T_1$	$\left\|\begin{matrix}A_1\\A_1\\A_1\end{matrix}\right\rangle$	$\left\|\begin{matrix}E\\A_1\\A_1\end{matrix}\right\rangle$	$\left\|\begin{matrix}B_1\\A_1\end{matrix}\right\rangle$	$\left\|\begin{matrix}T_1\\E\\B_1\end{matrix}\right\rangle$	$\left\|\begin{matrix}E\\B_2\end{matrix}\right\rangle$	$\left\|\begin{matrix}A_2\\A_2\end{matrix}\right\rangle$	$\left\|\begin{matrix}T_2\\E\\B_1\end{matrix}\right\rangle$	$\left\|\begin{matrix}E\\B_2\end{matrix}\right\rangle$	$\left\|\begin{matrix}A_2\\A_2\end{matrix}\right\rangle$
$\left\|\begin{matrix}E\\B_1\end{matrix}\right\rangle\left\|\begin{matrix}E\\B_1\end{matrix}\right\rangle$	$\frac{a}{\sqrt{2}}$	$\frac{c}{\sqrt{2}}$	$\frac{e}{\sqrt{2}}$	0	0	0	0	0	0
$\left\|\begin{matrix}E\\B_1\end{matrix}\right\rangle\left\|\begin{matrix}E\\B_2\end{matrix}\right\rangle$	0	0	0	0	0	$\frac{h}{\sqrt{2}}$	0	0	$\frac{k}{\sqrt{2}}$
$\left\|\begin{matrix}E\\B_1\end{matrix}\right\rangle\left\|\begin{matrix}A_2\\A_2\end{matrix}\right\rangle$	0	0	0	0	$-f$	0	0	$-i$	0
$\left\|\begin{matrix}E\\B_2\end{matrix}\right\rangle\left\|\begin{matrix}E\\B_1\end{matrix}\right\rangle$	0	0	0	0	0	$-\frac{h}{\sqrt{2}}$	0	0	$\frac{k}{\sqrt{2}}$
$\left\|\begin{matrix}E\\B_2\end{matrix}\right\rangle\left\|\begin{matrix}E\\B_2\end{matrix}\right\rangle$	$\frac{a}{\sqrt{2}}$	$\frac{c}{\sqrt{2}}$	$-\frac{e}{\sqrt{2}}$	0	0	0	0	0	0
$\left\|\begin{matrix}E\\B_2\end{matrix}\right\rangle\left\|\begin{matrix}A_2\\A_2\end{matrix}\right\rangle$	0	0	0	f	0	0	i	0	0
$\left\|\begin{matrix}A_2\\A_2\end{matrix}\right\rangle\left\|\begin{matrix}E\\B_1\end{matrix}\right\rangle$	0	0	0	0	$-g$	0	0	$-j$	0
$\left\|\begin{matrix}A_2\\A_2\end{matrix}\right\rangle\left\|\begin{matrix}E\\B_2\end{matrix}\right\rangle$	0	0	0	g	0	0	j	0	0
$\left\|\begin{matrix}A_2\\A_2\end{matrix}\right\rangle\left\|\begin{matrix}A_2\\A_2\end{matrix}\right\rangle$	b	d	0	0	0	0	0	0	0

(6.1.27b)

The first, second, fourth, and fifth rows of the $T_1 \otimes T_1$ table are copied from the $E \otimes E$ table of (6.1.23) for subgroup D_4. The third and sixth rows, as well as the seventh and eighth rows, follow from the $E \otimes A_2$ ($= A_2 \otimes E$) table of (6.1.26). Finally, the ninth row follows since $A_2 \otimes A_2 = A_1$ according to Eq. (6.1.20).

The unknown coefficients $a, b, \ldots, k$ are derived in the same way as before. To save space we shall write the $\mathscr{C}$ matrix only once in the following between the $(\mathscr{D}^{T_1}(R_1) \otimes \mathscr{D}^{T_1}(R_1))$ matrix (6.1.19b) on top and the $(\mathscr{D}^{A_1}(R_1) \oplus \mathscr{D}^{E}(R_1) \oplus \mathscr{D}^{T_1}(R_1) \oplus \mathscr{D}^{T_1}(R_1) \oplus \mathscr{D}^{T_2}(R_1))$ matrix below. [Note that $\mathscr{D}^{T_2}(R_1)$ differs from the nonkosher T_2 irrep given on the lower right-hand side of Eq. (6.1.19b).]

$$\left(\begin{array}{ccc|ccc|ccc}
1 & \cdot & \cdot & \cdot & \cdot & \cdot & \cdot & \cdot & \cdot \\
\cdot & \cdot & -1 & \cdot & \cdot & \cdot & \cdot & \cdot & \cdot \\
\cdot & 1 & \cdot & \cdot & \cdot & \cdot & \cdot & \cdot & \cdot \\
\hline
\cdot & \cdot & \cdot & \cdot & \cdot & \cdot & -1 & \cdot & \cdot \\
\cdot & \cdot & \cdot & \cdot & \cdot & \cdot & \cdot & \cdot & 1 \\
\cdot & \cdot & \cdot & \cdot & \cdot & \cdot & \cdot & -1 & \cdot \\
\hline
\cdot & \cdot & \cdot & 1 & \cdot & \cdot & \cdot & \cdot & \cdot \\
\cdot & \cdot & \cdot & \cdot & \cdot & -1 & \cdot & \cdot & \cdot \\
\cdot & \cdot & \cdot & \cdot & 1 & \cdot & \cdot & \cdot & \cdot
\end{array}\right) : \left(\begin{array}{ccc|ccc|ccc}
a/\sqrt{2} & c/\sqrt{2} & e/\sqrt{2} & \cdot & \cdot & \cdot & \cdot & \cdot & \cdot \\
\cdot & \cdot & \cdot & \cdot & \cdot & h/\sqrt{2} & \cdot & \cdot & k/\sqrt{2} \\
\cdot & \cdot & \cdot & \cdot & -f & \cdot & \cdot & -i & \cdot \\
\hline
\cdot & \cdot & \cdot & \cdot & \cdot & -h/\sqrt{2} & \cdot & \cdot & k/\sqrt{2} \\
a/\sqrt{2} & c/\sqrt{2} & -e/\sqrt{2} & \cdot & \cdot & \cdot & \cdot & \cdot & \cdot \\
\cdot & \cdot & \cdot & f & \cdot & \cdot & i & \cdot & \cdot \\
\hline
\cdot & \cdot & \cdot & \cdot & -g & \cdot & \cdot & -j & \cdot \\
\cdot & \cdot & \cdot & g & \cdot & \cdot & j & \cdot & \cdot \\
b & d & 0 & \cdot & \cdot & \cdot & \cdot & \cdot & \cdot
\end{array}\right)$$

$$: \left(\begin{array}{c|cc|c|c}
1 & & & & \\
\hline
 & -1/2 & -\sqrt{3}/2 & & \\
 & -\sqrt{3}/2 & 1/2 & & \\
\hline
 & & & 1 \cdot \cdot & \\
 & & & \cdot \cdot -1 & \\
 & & & \cdot 1 \cdot & \\
\hline
 & & & & -1 \cdot \cdot \\
 & & & & \cdot \cdot -1 \\
 & & & & \cdot 1 \cdot
\end{array}\right) . \tag{6.1.28}$$

Multiplying first and second factors and then the second and third matrices gives the following matrix equation:

$$\left(\begin{array}{ccc|ccc|ccc}
a/\sqrt{2} & c/\sqrt{2} & e/\sqrt{2} & \cdot & \cdot & \cdot & \cdot & \cdot & \cdot \\
\cdot & \cdot & \cdot & \cdot & f & 0 & \cdot & i & \cdot \\
\cdot & \cdot & \cdot & \cdot & \cdot & h/\sqrt{2} - & \cdot & \cdot & k/\sqrt{2} \\
\hline
\cdot & \cdot & \cdot & \cdot & g & \cdot & \cdot & j & \cdot \\
b & d & 0 & \cdot & \cdot & \cdot & \cdot & \cdot & \cdot \\
\cdot & \cdot & \cdot & -g & \cdot & \cdot & -j & \cdot & \cdot \\
\hline
\cdot & \cdot & \cdot & \cdot & \cdot & -h/\sqrt{2} & \cdot & \cdot & k/\sqrt{2} \\
\cdot & \cdot & \cdot & -f & \cdot & \cdot & -i & \cdot & \cdot \\
a/\sqrt{2} & c/\sqrt{2} & -e/\sqrt{2} & \cdot & \cdot & \cdot & \cdot & \cdot & \cdot
\end{array}\right) =$$

$$\left(\begin{array}{ccc|ccc|ccc}
a/\sqrt{2} & C & E & \cdot & \cdot & \cdot & \cdot & \cdot & \cdot \\
\cdot & \cdot & \cdot & \cdot & h/\sqrt{2} & \cdot & \cdot & k/\sqrt{2} & \cdot \\
\cdot & \cdot & \cdot & \cdot & \cdot & f & \cdot & \cdot & i \\
\hline
\cdot & \cdot & \cdot & \cdot & -h/\sqrt{2} & \cdot & \cdot & k/\sqrt{2} & \cdot \\
a/\sqrt{2} & D & F & \cdot & \cdot & \cdot & \cdot & \cdot & \cdot \\
\cdot & \cdot & \cdot & f & \cdot & \cdot & -i & \cdot & \cdot \\
\hline
\cdot & \cdot & \cdot & \cdot & \cdot & g & \cdot & \cdot & j \\
\cdot & \cdot & \cdot & g & \cdot & \cdot & -j & \cdot & \cdot \\
b & C & -E & \cdot & \cdot & \cdot & \cdot & \cdot & \cdot
\end{array}\right) , \tag{6.1.29}$$

where $C = -c/\sqrt{8} - e\sqrt{3}/\sqrt{8}$, $D = -c/\sqrt{8} + e\sqrt{3}/\sqrt{8}$, $E = -c\sqrt{3}/\sqrt{8} + e/\sqrt{8}$, $F = -c\sqrt{3}/\sqrt{8} - e/\sqrt{8}$. The following equations for the unknown constants result:

$$b = \frac{a}{\sqrt{2}} \qquad \text{(for } A_1 \text{ column)},$$

$$e = -c\sqrt{3}, \qquad d = \frac{c}{\sqrt{2}} \qquad \text{(for } E \text{ columns)},$$

$$g = -f, \qquad h = f\sqrt{2} \qquad \text{(for } T_1 \text{ columns)},$$

$$k = i\sqrt{2}, \qquad j = i \qquad \text{(for } T_2 \text{ columns)}.$$

A single undetermined constant is left for each irrep. This is determined up to a phase by requiring normalized column vectors. Then the coupling coefficient table is written:

		A_1	E		T_1			T_2		
		A_1	A_1	B_1	E			E		
$T_1 \otimes T_1$		A_1	A_1	A_1	B_1	B_2	A_2	B_1	B_2	A_2
B_1	B_1	$\frac{1}{\sqrt{3}}$	$\frac{1}{\sqrt{6}}$	$-\frac{1}{\sqrt{2}}$						
	B_2						$\frac{1}{\sqrt{2}}$			$\frac{1}{\sqrt{2}}$
	A_2					$-\frac{1}{\sqrt{2}}$			$-\frac{1}{\sqrt{2}}$	
B_2	B_1						$-\frac{1}{\sqrt{2}}$			$\frac{1}{\sqrt{2}}$
	B_2	$\frac{1}{\sqrt{3}}$	$\frac{1}{\sqrt{6}}$	$\frac{1}{\sqrt{2}}$						
	A_2				$\frac{1}{\sqrt{2}}$			$\frac{1}{\sqrt{2}}$		
A_2	B_1					$\frac{1}{\sqrt{2}}$			$-\frac{1}{\sqrt{2}}$	
	B_2				$-\frac{1}{\sqrt{2}}$			$\frac{1}{\sqrt{2}}$		
	A_2	$\frac{1}{\sqrt{3}}$	$-\frac{2}{\sqrt{6}}$	0						

(6.1.30)

The table agrees with the previously calculated $(T_1 \otimes T_1)$ coefficients (6.1.19c) in all but the second column from the right-hand side. The differ-

ence in sign there is due to the difference in sign $\left(\left|{}^{T_2}_{2}\right\rangle = -\left|{}^{T_2}_{B_2}\right\rangle\right)$ between nonkosher and kosher bases, respectively.

In Appendix F all the O-group coupling coefficients are tabulated. The O_h coefficients follow immediately from these. One only has to remember that even-even and odd-odd products are even ($g \otimes g = u \otimes u = g$), while odd-even products are odd ($g \otimes u = u \otimes g = u$).

(b) Trigonal ($O \supset D_3 \supset C_2$) Coupling Coefficients Products of the even [(+), A, A_1, A', etc.)] and odd [(−), B, A_2, A'', etc.] irreps of C_2-like groups follow the usual odd-even rules:

$$\begin{array}{rl} B = & A \quad B \\ A \otimes B = & \boxed{\begin{array}{cc} A & B \\ B & A \end{array}} \\ B \otimes B = & \end{array} . \tag{6.1.31}$$

The irrep bases of $D_3 = \{1, r_1, r_1^2, i_2, i_4, i_5\}$ are labeled

$$\left|{}^{E}_{A}\right\rangle, \left|{}^{E}_{B}\right\rangle, \left|{}^{A_2}_{B}\right\rangle, \left|{}^{A_1}_{A}\right\rangle,$$

where the lower indices are irreps of subgroup $C_2 = \{1, i_4\}$. Following the procedures given in the preceding section one deduces the form of the $E \otimes E$ coupling coefficients:

$$\begin{array}{cc|cccc} & & A_1 & A_2 & E & E \\ E & \otimes E & A & B & A & B \\ \hline A & A & a & 0 & e & 0 \\ A & B & 0 & c & 0 & g \\ B & A & 0 & d & 0 & h \\ B & B & b & 0 & f & 0 \end{array} = \mathscr{C}. \tag{6.1.32}$$

The irrep matrix

$$\mathscr{D}^E(r_1) = \mathscr{D}^3(r) = \begin{pmatrix} -\frac{1}{2} & -\frac{\sqrt{3}}{2} \\ \frac{\sqrt{3}}{2} & -\frac{1}{2} \end{pmatrix}$$

is taken from Eq. (3.4.14) and used to solve for the unknown coupling coefficient

$$\mathscr{D}^E(r_1) \otimes \mathscr{D}^E(r_1)\mathscr{C} = \mathscr{C}\left(\mathscr{D}^{A_1}(r_1) \oplus \mathscr{D}^{A_2}(r_1) \oplus \mathscr{D}^E(r_1)\right). \tag{6.1.33}$$

This equation is represented as follows

$$\begin{pmatrix} \frac{1}{4} & \frac{\sqrt{3}}{4} & \frac{\sqrt{3}}{4} & \frac{3}{4} \\ -\frac{\sqrt{3}}{4} & \frac{1}{4} & -\frac{3}{4} & \frac{\sqrt{3}}{4} \\ -\frac{\sqrt{3}}{4} & -\frac{3}{4} & \frac{1}{4} & \frac{\sqrt{3}}{4} \\ \frac{3}{4} & -\frac{\sqrt{3}}{4} & -\frac{\sqrt{3}}{4} & \frac{1}{4} \end{pmatrix} \begin{pmatrix} a & 0 & e & 0 \\ 0 & c & 0 & g \\ 0 & d & 0 & h \\ b & 0 & f & 0 \end{pmatrix}$$

$$= \mathscr{E} \begin{pmatrix} 1 & 0 & 0 & 0 \\ 0 & 1 & 0 & 0 \\ 0 & 0 & -\frac{1}{2} & -\frac{\sqrt{3}}{2} \\ 0 & 0 & \frac{\sqrt{3}}{2} & -\frac{1}{2} \end{pmatrix}. \qquad (6.1.34)$$

Solving this equation and normalizing gives the coupling table:

$E \otimes E$		A_1 A	A_2 B	E A	E B
A	A	$\frac{1}{\sqrt{2}}$	0	$\frac{1}{\sqrt{2}}$	0
A	B	0	$\frac{1}{\sqrt{2}}$	0	$-\frac{1}{\sqrt{2}}$
B	A	0	$-\frac{1}{\sqrt{2}}$	0	$-\frac{1}{\sqrt{2}}$
B	B	$\frac{1}{\sqrt{2}}$	0	$-\frac{1}{\sqrt{2}}$	0

(6.1.35a)

The $E \otimes A_2$ table follows similarly:

$E \otimes A_2$		E A	E B
A	B	0	-1
B	B	1	0

(6.1.35b)

The D_3 tables have very similar form to the D_4 tables. However, the octahedral coupling coefficients for the $O \supset D_3 \supset C_2$ chain are very different in form from those of the $O \supset D_4 \supset D_2$ chain. For example, the $T_2 \otimes T_1$ table is given here:

$T_2 \otimes T_1$	A_1	E 1	2	T_2 1	2	3	T_1 1	2	3
1 1	$\frac{1}{\sqrt{3}}$	$\frac{1}{\sqrt{6}}$	·	$\frac{1}{\sqrt{6}}$	$\frac{1}{\sqrt{3}}$	·	·	·	·
1 2	·	·	$-\frac{1}{\sqrt{6}}$	·	·	$-\frac{1}{\sqrt{3}}$	·	·	$\frac{1}{\sqrt{2}}$
1 3	·	·	$-\frac{1}{\sqrt{3}}$	·	·	$\frac{1}{\sqrt{6}}$	·	$-\frac{1}{\sqrt{2}}$	·
2 1	·	·	$-\frac{1}{\sqrt{6}}$	·	·	$-\frac{1}{\sqrt{3}}$	·	·	$-\frac{1}{\sqrt{2}}$
2 2	$\frac{1}{\sqrt{3}}$	$-\frac{1}{\sqrt{6}}$	·	$\frac{1}{\sqrt{6}}$	$-\frac{1}{\sqrt{3}}$	·	·	·	·
2 3	·	$\frac{1}{\sqrt{3}}$	·	·	$-\frac{1}{\sqrt{6}}$	·	$\frac{1}{\sqrt{2}}$	·	·
3 1	·	·	$-\frac{1}{\sqrt{3}}$	·	·	$\frac{1}{\sqrt{6}}$	·	$\frac{1}{\sqrt{2}}$	·
3 2	·	$\frac{1}{\sqrt{3}}$	·	·	$-\frac{1}{\sqrt{6}}$	·	$-\frac{1}{\sqrt{2}}$	·	·
3 3	$\frac{1}{\sqrt{3}}$	·	·	$-\frac{2}{\sqrt{6}}$	·	·	·	·	·

(6.1.36)

In this table the bases are labeled as follows according to $O \supset D_3 \supset C_2$:

$$\begin{pmatrix} A_1 \end{pmatrix} = \begin{pmatrix} A_1 \\ A_1 \\ A \end{pmatrix};$$

$$\begin{pmatrix} E \\ 1 \end{pmatrix} = \begin{pmatrix} E \\ E \\ A \end{pmatrix}, \qquad \begin{pmatrix} E \\ 2 \end{pmatrix} = \begin{pmatrix} E \\ E \\ B \end{pmatrix};$$

$$\begin{pmatrix} T_2 \\ 1 \end{pmatrix} = \begin{pmatrix} T_2 \\ A \\ A \end{pmatrix}, \qquad \begin{pmatrix} T_2 \\ 2 \end{pmatrix} = \begin{pmatrix} T_2 \\ E \\ A \end{pmatrix}, \qquad \begin{pmatrix} T_2 \\ 3 \end{pmatrix}, \qquad \begin{pmatrix} T_2 \\ E \\ B \end{pmatrix};$$

$$\begin{pmatrix} T_1 \\ 1 \end{pmatrix} = \begin{pmatrix} T_1 \\ E \\ A \end{pmatrix}, \qquad \begin{pmatrix} T_1 \\ 2 \end{pmatrix} = \begin{pmatrix} T_1 \\ E \\ B \end{pmatrix}, \qquad \begin{pmatrix} T_1 \\ 3 \end{pmatrix} = \begin{pmatrix} T_1 \\ A_2 \\ B \end{pmatrix}.$$

The other trigonal coupling tables are given in Appendix F.

6.2 GENERAL CONCEPTS AND MATRIX RELATIONS FOR COUPLING COEFFICIENTS

There are some important algebraic relations between the $\mathscr{C}_{ijk}^{\alpha\beta\gamma}$ coefficients and irreps $\mathscr{D}^{\alpha}$. These are based on important orthogonality and completeness properties. We must review these before considering detailed applications of coupling theory.

A. Products Involving Invariants or Scalars

One irreducible representation called the SCALAR or INVARIANT irrep $\mathscr{D}^{0}$ exists for any group $G = \{g, g', \ldots\}$. It is defined to be unity for all elements:

$$\mathscr{D}^{A_1}(g) = \mathscr{D}^{0}(g) = 1 \qquad \text{(for all } g\text{)}. \tag{6.2.1}$$

It is labeled variously A_1, A_{1g}, A', Σ, or (0) depending on what group is being treated. The coupling coefficients for the product of the scalar with any other irrep are obviously given by

$$\mathscr{C}_{\cdot ij}^{0\alpha\beta} = \delta^{\alpha\beta}\delta_{ij} = \mathscr{C}_{i\cdot j}^{\alpha 0\beta}. \tag{6.2.2}$$

This relation is so simple that we did not bother to write it in table form before.

A somewhat more complicated problem involves representations whose products produce scalars. In order to find which products will yield the scalar, one may use Eq. (6.1.18b) with $\mathscr{D}^{\gamma}$ set equal to 1:

$$\mathscr{C}_{ij\cdot}^{\alpha\beta 0} = \frac{(1/{}^{\circ}G)\Sigma_g 1 \cdot \mathscr{D}_{ik}^{\alpha}(g)\mathscr{D}_{jl}^{\beta}(g)}{(1/{}^{\circ}G)\Sigma_g 1 \cdot \mathscr{D}_{kk}^{\alpha}(g)\mathscr{D}_{ll}^{\beta}(g)}. \tag{6.2.3}$$

By combining Eqs. (3.4.18) and (3.4.19) (see also Appendix G) one derives the irrep orthogonality relation:

$$(l^{\alpha}/{}^{\circ}G)\sum_{g}\mathscr{D}_{ik}^{\alpha}(g)\mathscr{D}_{jl}^{\beta *}(g) = \delta^{\alpha\beta}\delta_{ij}\delta_{kl}. \tag{6.2.4}$$

Comparison with the preceding Eq. (6.2.3) shows that the only nonzero coupling coefficients in Eq. (6.2.3) occur when the product of an irrep $\mathscr{D}^{\alpha}$ is formed with its complex conjugate $\mathscr{D}^{\alpha *}$ or with itself if it is real. The irreps of finite groups fall into three categories with respect to complex conjugation. These are listed in the following:

Type 1 Irrep $\mathscr{D}^{\alpha}$ is real or else can be transformed to be real. $\mathscr{D}^{\alpha}(g)^{*} = \mathscr{D}^{\alpha}(g)$.

Type 2 Irreps $\mathscr{D}^{\alpha} = \mathscr{D}^{\beta *}$ and $\mathscr{D}^{\beta} = \mathscr{D}^{\alpha *}$ are a complex conjugate pair of inequivalent irreps.

Type 3 Irrep $\mathscr{D}^{\alpha}$ is always complex but equivalent to its conjugate $\mathscr{D}^{\alpha *}$.

Irreps that can be transformed to either standing-wave or moving-wave forms belong to type (1). The O, O_h, T_d, and D_n irreps are all of this type. For type (1) irreps ($\mathscr{D}^{\alpha*}(g) = \mathscr{D}^{\alpha}(g)$), we have from Eqs. (6.2.3) and (6.2.4) the following formula for making scalars:

$$\mathscr{D}_{ij\cdot}^{\alpha\beta 0} = \sqrt{1/l^{\alpha}}\,\frac{(l^{\alpha}/{}^{\circ}G)\Sigma_g \mathscr{D}_{ik}^{\alpha}(g)\mathscr{D}_{jl}^{\beta}(g)}{(l^{\alpha}/{}^{\circ}G)\Sigma_g \mathscr{D}_{kk}^{\alpha}(g)\mathscr{D}_{ll}^{\beta}(g)} = \sqrt{1/l^{\alpha}}\,\delta^{\alpha\beta}\delta_{ij}. \quad (6.2.5)$$

This checks with the results in Eq. (6.1.19c), where the scalar of O symmetry is conventionally labeled $\mathscr{D}^0 \equiv \mathscr{D}^{A_{1g}}$.

Complex one-dimensional moving-wave irreps of groups C_n, C_{nh}, and T_h groups belong to type (2). For type (2) one has the following formula, where $(\mathscr{D}^{\alpha})^* = \mathscr{D}(^{\alpha^*})$:

$$\mathscr{C}_{ij\cdot}^{\alpha\beta 0} = \sqrt{1/l^{\alpha}}\,\delta^{\alpha^*\beta}\delta_{ij}. \quad (6.2.6)$$

This form holds for type (3) irreps, too. The spinor and ray representations $\mathscr{D}^{n/2}$, $\mathscr{D}^{G}$, etc., all belong to type (2) or (3). The ones with real characters $\chi^{\alpha^*} = \chi^{\alpha}$ belong to type (3), and a transformation $\mathscr{J}$ exists such that $\mathscr{D}^{\alpha^*} = \mathscr{J}^{\dagger}\mathscr{D}\mathscr{J}$.

B. Symmetry Relations

Notice in Eq. (6.1.1) that for coupling coefficients $\mathscr{C}_{ijk}^{\alpha\alpha\gamma}$ involving the product of irrep T_{1u} with itself, either

$$\mathscr{C}_{ijk}^{\alpha\alpha\gamma} = \mathscr{C}_{jik}^{\alpha\alpha\gamma}, \quad (6.2.7a)$$

or

$$\mathscr{C}_{ijk}^{\alpha\alpha\gamma} = -\mathscr{C}_{jik}^{\alpha\alpha\gamma}, \quad (6.2.7b)$$

for all i, j, k. This follows from a more detailed treatment of permutation symmetry. Generally one says that $\mathscr{D}^{\gamma}$ belongs to the SYMMETRIZED SQUARE of $\mathscr{D}^{\alpha}$ if Eq. (6.2.7a) holds or to the ANTISYMMETRIZED SQUARE of $\mathscr{D}^{\alpha}$ if Eq. (6.2.7b) holds.

Other symmetry relations involving unequal irreps such as the following can be established to within a phase:

$$\mathscr{C}_{ijk}^{\alpha\beta\gamma} = \mathscr{C}_{jik}^{\beta\alpha\gamma}, \quad (6.2.8)$$

$$\mathscr{C}_{ijk}^{\alpha\beta\gamma} = \sqrt{l^{\gamma}/l^{\alpha}}\,\mathscr{C}_{jki}^{\beta\gamma\alpha}. \quad (6.2.9)$$

(Note that for the foregoing, $\mathscr{C}_{jik}^{\alpha\beta\gamma}$ would in general be meaningless.) However, these relations depend upon your choice and convention for overall phases, as we will discuss in detail in Chapter 7.

C. Product Analysis with Repeated Irreps

For most of the point groups and many other symmetry groups, we will find that reduction of any direct product will not yield any irreps $\mathscr{D}^{\gamma}$ more than once. These are called SIMPLY REDUCIBLE groups. There are groups that are not so simple. Two crystal point groups T and T_h are examples. For these the three-dimensional $\mathscr{D}^{T_i}$ ($i = u$ or g) appear twice in the product $\mathscr{D}^{T_i} \times \mathscr{D}^{T_j}$. For example, the T characters give the following product:

$$\mathscr{D}^{T_g} \times \mathscr{D}^{T_g} \cong \mathscr{D}^{A_g} + \mathscr{D}^{E} + \mathscr{D}^{E^*} + 2\mathscr{D}^{T_g}. \tag{6.2.10}$$

Whenever $\mathscr{D}^{\gamma}$ appears n times in the reduction of a product $\mathscr{D}^{\alpha} \times \mathscr{D}^{\beta}$, we will have n sets of coupling coefficients $\mathscr{C}_{ijm}^{\alpha\beta\gamma_1}, \mathscr{C}_{ijm}^{\alpha\beta\gamma_2}, \ldots, \mathscr{C}_{ijm}^{\alpha\beta\gamma_n}$. Each set can be made to give orthonormal sets of (γ) bases:

$$\left| \begin{matrix} (\gamma)_{\omega} \\ m \end{matrix} (\alpha\beta) \right\rangle = \sum_{i=1}^{l^{\alpha}} \sum_{j=1}^{l^{\beta}} \mathscr{C}_{ijm}^{\alpha\beta(\gamma)_{\omega}} \left| \begin{matrix} \alpha & \beta \\ i & j \end{matrix} \right\rangle. \tag{6.2.11}$$

These coefficients will not be uniquely defined until something is done to distinguish the n repeated states. For the two T_g in (6.2.10) one may simply reuse the $\mathscr{C}_{ijm}^{T_1T_1T_1}$ and $\mathscr{C}_{ijm}^{T_1T_1T_2}$ coefficients of the octahedral supergroup. In this case the repeating T's are distinguished by orthogonal irrep labels T_1 and T_2. However, a convenient "supergroup" may not always be available. Indeed, a general treatment of multiplicities in products constitutes an unsolved problem at present. Until this is solved one must sort and orthogonalize repeated product bases arbitrarily.

D. Orthonormality and Completeness

Any set of coupling coefficients are components of a transformation matrix. They are generally expected to be orthonormal and complete with respect to the product basis $\left\{ \left| \begin{matrix} \alpha & \beta \\ 1 & 1 \end{matrix} \right\rangle, \left| \begin{matrix} \alpha & \beta \\ 1 & 2 \end{matrix} \right\rangle, \ldots, \left| \begin{matrix} \alpha & \beta \\ l^{\alpha} & l^{\beta} \end{matrix} \right\rangle \right\}$ that is involved. Different product bases are expected to be orthogonal, as stated by the following:

$$\left\langle \begin{matrix} (\gamma)_{\omega} \\ m \end{matrix} \middle| \begin{matrix} (\gamma')_{\omega'} \\ m' \end{matrix} \right\rangle = \delta_{mm'}\delta^{(\gamma)_{\omega}(\gamma')_{\omega'}} = \sum_{i=1}^{l^{\alpha}} \sum_{j=1}^{l^{\beta}} \left\langle \begin{matrix} (\gamma)_{\omega} \\ m \end{matrix} \middle| \begin{matrix} \alpha\beta \\ ij \end{matrix} \right\rangle \left\langle \begin{matrix} \alpha\beta \\ ij \end{matrix} \middle| \begin{matrix} (\gamma')_{\omega'} \\ m' \end{matrix} \right\rangle$$

$$= \sum_{i=1}^{l^{\alpha}} \sum_{j=1}^{l^{\beta}} \left(\mathscr{C}_{ijm}^{\alpha\beta(\gamma)_{\omega}} \right)^* \left(\mathscr{C}_{ijm'}^{\alpha\beta(\gamma')_{\omega'}} \right). \tag{6.2.12a}$$

The product bases are also expected to be complete, as stated by the

following:

$$\left\langle \begin{matrix} \alpha\beta \\ ij \end{matrix} \middle| \begin{matrix} \alpha\beta \\ i'j' \end{matrix} \right\rangle = \delta_{ii'}\delta_{jj'} = \sum_{\gamma}\sum_{\omega}\sum_{m=1}^{l^\gamma} \left\langle \begin{matrix} \alpha\beta \\ ij \end{matrix} \middle| \begin{matrix} (\gamma)_\omega \\ m \end{matrix} \right\rangle \left\langle \begin{matrix} (\gamma)_\omega \\ m \end{matrix} \middle| \begin{matrix} \alpha\beta \\ i'j' \end{matrix} \right\rangle$$

$$= \sum_{\gamma}\sum_{\omega}\sum_{m=1}^{l^\gamma} \left(\mathscr{C}_{ijm}^{\alpha\beta(\gamma)_\omega}\right)\left(\mathscr{C}_{i'j'm}^{\alpha\beta(\gamma)_\omega}\right)^*. \qquad (6.2.12b)$$

The product reduction equations such as Eq. (6.1.19a) may be written in the following general form:

$$\sum_{i=1}^{l^\alpha}\sum_{j=1}^{l^\beta}\sum_{k=1}^{l^\alpha}\sum_{l=1}^{l^\beta} \left(\mathscr{C}_{ijm}^{\alpha\beta\gamma_\omega}\right)^* \mathscr{D}_{ik}^{\alpha}(g)\mathscr{D}_{jl}^{\beta}(g)\mathscr{C}_{kln}^{\alpha\beta(\gamma')_{\omega'}} = \delta^{(\gamma')_{\omega'}(\gamma)_\omega}\mathscr{D}_{mn}^{\gamma}(g). \qquad (6.2.13)$$

By applying Eq. (6.2.12b) twice, one obtains the inverse relation:

$$\mathscr{D}_{ik}^{\alpha}(g)\mathscr{D}_{jl}^{\beta}(g) = \sum_{\gamma}\sum_{\omega}\sum_{m=1}^{l^\gamma}\sum_{n=1}^{l^\gamma} \mathscr{C}_{ijm}^{\alpha\beta(\gamma)_\omega}\left(\mathscr{C}_{kln}^{\alpha\beta(\gamma)_\omega}\right)^* \mathscr{D}_{mn}^{\gamma}(g). \qquad (6.2.14)$$

Finally, the orthogonality relation Eq. (6.2.4) yields an equation that is quite analogous to Eq. (6.1.18), which was used previously to derive $\mathscr{C}_{ijm}^{\alpha\beta\gamma}$:

$$(l^\alpha/{}^oG)\sum_{g}\mathscr{D}_{ik}^{\alpha}(g)\mathscr{D}_{jl}^{\beta}(g)\mathscr{D}_{mn}^{\gamma*}(g) = \sum_{\omega}\mathscr{C}_{ijm}^{\alpha\beta(\gamma)_\omega}\left(\mathscr{C}_{kln}^{\alpha\beta(\gamma)_\omega}\right)^*. \qquad (6.2.15)$$

This is sometimes called the FACTORIZATION LEMMA. For most crystal point groups, we may drop the sum (Σ_ω) over repeats. Also, the conjugate ($*$) is not needed for real coefficients.

6.3 VECTORS AND TENSORS IN 3-SPACE

The knowledge of symmetry can systematically simplify the treatment of vector and tensor quantities. We discuss how some procedures that work for any spatial symmetry with examples in the symmetries of O_h, C_{3v}, and D_{4h}. Stress-strain tensor relations in solids will be treated in detail.

A. Symmetry-Defined Unit Vectors

As a first step one must define three unit vectors of a Cartesian coordinate system and obtain a 3×3 representation $\mathscr{V}$ of the symmetry operators in this basis which is called the VECTOR representation. It is convenient to

define unit vectors along symmetry axes whenever possible. For example, one choice for O_h or D_{4h} symmetry has the vectors $\hat{x}_j$ lying on the tetragonal axes and was shown in Figure 4.2.1(a). Figure 4.2.2(a) showed another choice of basis centered on a trigonal axis. The latter vectors $\hat{v}_j$ are also a convenient coordinate system in D_{3d} or C_{3v} symmetry.

To find the vector representation of a symmetry operator g, we imagine this operation moves the physical object with the unit vectors attached, as in Figures 4.2.1(b) and 4.2.2(b). Then, since g is a symmetry operator, the object must look as though it had not been moved at all. However, the unit vectors will be moved to new places. The vector representation $\mathscr{V}$ is the transformation matrix as defined by

$$\mathscr{V}_{ij}(g) = x_i \cdot x'_j = x_i \cdot g \cdot x_j,$$
$$\hat{x}'_j \equiv g \cdot \hat{x}_j = \sum_i \mathscr{V}_{ij}(g)\hat{x}_i. \tag{6.3.1}$$

The second step is to establish relations between the vector representation and certain irreps of the symmetry. In some cases a vector representation may be an irrep as in the case of O_h in Figure 4.2.1, where $\mathscr{V}=\mathscr{D}^{T_{1u}}$. In other cases the vector representation may be equal to a direct sum of irreps as in the case of D_3 in Figure 4.2.2, where $\mathscr{V}=\mathscr{D}^{E_u} \oplus \mathscr{D}^{A_{2u}}$. In general, you may have to transform the vector representation into an irrep or sum of irreps, as would be the case if we used the tetragonal vectors in Figure 4.2.1 to represent the D_{3d} symmetry operations in Figure 4.2.2 or vice versa. Recall the transformation (4.2.31) between the tetragonal and trigonal bases.

In any case, the final result should be three unit vectors $\hat{x}_j^\alpha$ with labels $\binom{\alpha}{j}$ of the symmetry irrep. They should have the corresponding transformation character,

$$\hat{x}_j'^\alpha = \sum_i \mathscr{D}_{ij}^\alpha(g)\hat{x}_i^\alpha. \tag{6.3.2}$$

For O_h x_j vectors and D_{3d} v_j vectors we have the following:

$$\hat{x}_1^{T_{1u}} \equiv \hat{x}_1, \qquad \hat{x}_1^3 \equiv \hat{x}_1^{E_u} \equiv \hat{v}_1,$$
$$\hat{x}_2^{T_{1u}} \equiv \hat{x}_2, \qquad \hat{x}_2^3 \equiv \hat{x}_2^{E_u} \equiv \hat{v}_2,$$
$$\hat{x}_3^{T_{1u}} \equiv \hat{x}_3, \qquad \hat{x}^1 \equiv \hat{x}^{A_{2u}} \equiv \hat{v}_3.$$

For some applications it is helpful to use the full subgroup chains $O_h \supset D_{4h} \supset D_{2h}$ or $O_h \supset D_{3d} \supset C_{2v}$ to label the vectors $\hat{x}_j$ or $\hat{v}_j$, respectively, as

given in Eqs. (4.2.23) or (4.2.27):

$$\begin{array}{ccc} T_{1u}:O_h & T_{1u} & T_{1u} \\ \hat{x}_1 \equiv \hat{x}E_u : D_{4h}\,, & \hat{x}_2 \equiv \hat{x}E_u\,, & \hat{x}_3 \equiv \hat{x}A_{2u}\,, \\ B_{1u}:D_{2h} & B_{2u} & A_{2u} \end{array} \tag{6.3.3a}$$

$$\begin{array}{ccc} T_{1u}:O_h & T_{1u} & T_{1u} \\ \hat{v}_1 \equiv \hat{x}E_u : D_{3d}\,, & \hat{v}_2 \equiv \hat{x}E_u\,, & \hat{v}_3 \equiv \hat{x}A_{2u}\,. \\ A_u:C_{2v} & B_u & B_u \end{array} \tag{6.3.3b}$$

B. Symmetry-Defined Unit Tensors

Using coupling coefficients it is easy to make unit vectors $\hat{x}_i^\alpha$ into complete sets of unit tensors as follows:

$$\hat{T}_m^\gamma = \sum_i \sum_j \mathscr{C}_{ijm}^{\alpha\beta\gamma} \hat{x}_i^\alpha \hat{x}_j^\beta. \tag{6.3.4}$$

According to the theory of coupling coefficients, these tensors must transform according to the irreps which label them. First, the x_j^α transformation (6.3.2) gives

$$\begin{aligned} \hat{T}_m'^\gamma &= \sum_i \sum_j \mathscr{C}_{ijm}^{\alpha\beta\gamma} \hat{x}_i'^\alpha \hat{x}_j'^\beta \\ &= \sum_i \sum_j \sum_{i'} \sum_{j'} \mathscr{C}_{ijm}^{\alpha\beta\gamma} \mathscr{D}_{i'i}^\alpha \mathscr{D}_{j'j}^\beta \hat{x}_{i'}^\alpha\, \hat{x}_{j'}^\beta. \end{aligned}$$

Then the coupling relations (6.2.12)–(6.2.14) give

$$\hat{T}_m'^\gamma = \sum_{m'} \mathscr{D}_{m'm}^\gamma \sum_{i'} \sum_{j'} \mathscr{C}_{i'j'm'}^{\alpha\beta\gamma} \hat{x}_{i'}^\alpha \hat{x}_{j'}^\beta,$$

which is the desired transformation relation

$$\hat{T}_m'^\gamma = \sum_{m'} \mathscr{D}_{m'm}^\gamma \hat{T}_{m'}^\gamma \tag{6.3.5}$$

for an irreducible or SYMMETRY-DEFINED tensor set $\{T_1^\gamma, T_2^\gamma, \ldots\}$.

For example, the $(\alpha \otimes \beta) = (T_{1u} \otimes T_{1u})$ tetragonal O_h coupling coefficients (6.1.19c) yield the "nonkosher" symmetry-defined unit tensors here:

$$\begin{aligned}
\hat{\hat{T}}^{A_{1g}} &= \left(\hat{x}_1\hat{x}_1 + \hat{x}_2\hat{x}_2 + \hat{x}_3\hat{x}_3\right)/\sqrt{3}\,, & \hat{\hat{T}}_1^{T_{2g}} &= \left(\hat{x}_2\hat{x}_3 + \hat{x}_3\hat{x}_2\right)/\sqrt{2}\,,\\
\hat{\hat{T}}_1^{E_g} &= \left(\hat{x}_1\hat{x}_1 + \hat{x}_2\hat{x}_2 - 2\hat{x}_3\hat{x}_3\right)/\sqrt{6}\,, & \hat{\hat{T}}_2^{T_{2g}} &= \left(\hat{x}_3\hat{x}_1 + \hat{x}_1\hat{x}_3\right)/\sqrt{2}\,,\\
\hat{\hat{T}}_2^{E_g} &= \left(-\hat{x}_1\hat{x}_1 + \hat{x}_2\hat{x}_2\right)/\sqrt{2}\,, & \hat{\hat{T}}_3^{T_{2g}} &= \left(\hat{x}_1\hat{x}_2 + \hat{x}_2\hat{x}_1\right)/\sqrt{2}\,,\\
\hat{\hat{T}}_1^{T_{1g}} &= \left(\hat{x}_2\hat{x}_3 - \hat{x}_3\hat{x}_2\right)/\sqrt{2}\,, & \hat{\hat{T}}_2^{T_{1g}} &= \left(\hat{x}_3\hat{x}_1 - \hat{x}_1\hat{x}_3\right)/\sqrt{2}\,,\\
\hat{\hat{T}}_3^{T_{1g}} &= \left(\hat{x}_1\hat{x}_2 - \hat{x}_2\hat{x}_1\right)/\sqrt{2}\,. & & \qquad (6.3.6)
\end{aligned}$$

C. Symmetry-Defined Coordinates and Polynomials

In any of the foregoing tensors the vectors $\hat{x}_j$ may be replaced by coordinates $x = x_1$, $y = x_2$, and $z = x_3$ to give symmetry-defined polynomials provided that the transformation character of the coordinates is defined correctly. One way to do this is to let the x_j be coordinates of a field point $\mathbf{r}$ which is unaffected by symmetry operations:

$$\mathbf{r} = x_1\hat{x}_1 + x_2\hat{x}_2 + x_3\hat{x}_3 = x_1'\hat{x}_1' + x_2'\hat{x}_2' + x_3'\hat{x}_3'. \qquad (6.3.7)$$

Substituting the vector transformation (6.3.1) in the foregoing gives the following. In the last step the orthogonality of the $\mathscr{V}$ matrices is used:

$$x_i' = \sum_{j=1}^{3} \mathscr{V}_{ij}(g^{-1})\, x_j = \sum_{j=1}^{3} \mathscr{V}_{ji}(g)\, x_j. \qquad (6.3.8)$$

Then the coordinates transform just like the base vectors. From Eq. (6.3.6) we get the following quadratic polynomials which transform according to definite irreps of O_h (note that the antisymmetric product T_{1g} is missing, since it is zero):

$$\begin{aligned}
p^{A_{1g}} &= \left(x^2 + y^2 + z^2\right)/\sqrt{3}\,, & p_1^{T_{2g}} &= \sqrt{2}\,yz,\\
p_1^{E_g} &= \left(x^2 + y^2 - 2z^2\right)/\sqrt{6}\,, & p_2^{T_{2g}} &= \sqrt{2}\,xz,\\
p_2^{E_g} &= \left(-x^2 + y^2\right)/\sqrt{2} & p_3^{T_{2g}} &= \sqrt{2}\,xy. \qquad (6.3.9)
\end{aligned}$$

Continued application of coupling coefficients then makes a complete set of cubic, quartic, or higher-degree polynomials for each irrep. These are tabulated in Appendix F.

Polynomials made in this way are sometimes called POINT SYMMETRY HARMONICS since any eigenfunction in the symmetry environment must be a combination of only those harmonics belonging to a particular irrep (γ).

D. Symmetry-Defined Bulk Behavior in Solids

(a) Stress Tensor The word "tensor" comes from its application to the study of internal tension or stress in solid bodies. Soon we will be dealing with more abstract tensors in quantum mechanics, so it is instructive to review the original application of these ideas.

Suppose some solid is weighted down with various forces and weights, and these forces are felt at each point or atom within the solid. For any plane P containing an atom, define a vector $\mathbf{F}(P)$ to be the force felt by the plane per (infinitesimal) unit of area due to all the material on one side [Figure 6.3.1(a)]. $\mathbf{F}(P)$ is the vector average of all the forces transmitted by the various springs or fibers that penetrate or touch a unit area of P. Now imagine a single set of parallel fibers or springs all under uniform tension $\mathbf{t}$ or compression $-\mathbf{t}$ [Figure 6.3.1(b)], per unit transverse area. The force on the unit area just due to these fibers is proportional to the projection $\mathbf{t} \cdot \hat{\mathbf{n}}$ of $\mathbf{t}$ on the unit normal $\hat{\mathbf{n}}$ on the chosen side:

$$\mathbf{F}_t(P) = \mathbf{t}\cos(\mathbf{t}, \hat{n}) = \mathbf{t}(\mathbf{t} \cdot \hat{\mathbf{n}})/t = (\mathbf{tt}) \cdot \hat{\mathbf{n}}/t.$$

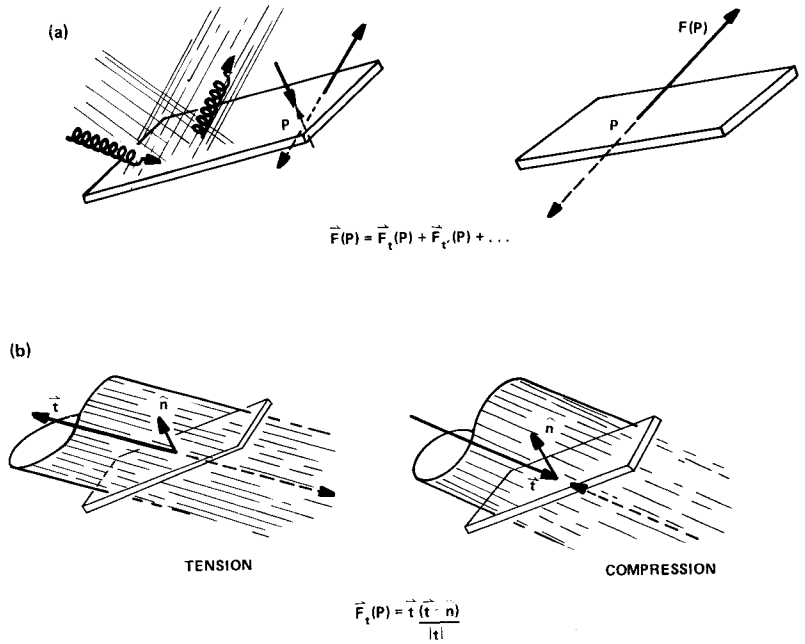

Figure 6.3.1 Representing stress in a solid. (a) The effect of many fibers is represented by the sum $\mathbf{F}(\rho)$ of all the forces pulling on one side of an infinitesimal area. (b) The force due to one set of fibers is expressed by the scalar product of a tensor dyad $\mathbf{tt}$ and the unit surface normal.

This equation simply counts the number of fibers which actually penetrate a unit area with normal $\hat{\mathbf{n}}$, and multiplies this by $t = |\mathbf{t}|$. The quantity $(\mathbf{tt})/t$ is an elementary STRESS TENSOR. The total force $\mathbf{F}(P)$ is given by an n-projected sum of these tensors for all the types of fibers present in the solid:

$$\mathbf{F}(P) = (\mathbf{tt}/t + \mathbf{t}'\mathbf{t}'/t' + \cdots) \cdot \hat{\mathbf{n}} \equiv \overleftrightarrow{T} \cdot \hat{\mathbf{n}}. \tag{6.3.10}$$

The $\overleftrightarrow{T}$ in Eq. (6.3.10) is the stress tensor which describes the tension per area present in a small region of the solid. We see that $\overleftrightarrow{T}$ can be written as a combination of elementary unit tensors $\hat{x}_i\hat{x}_j$ or as a combination of any set of symmetry-defined tensors such as the O_h set T_m^γ in Eq. (6.3.6):

$$\begin{aligned}
\overleftrightarrow{T} = {} & \mathscr{T}_{11}\hat{x}_1\hat{x}_1 + \mathscr{T}_{12}\hat{x}_1\hat{x}_2 + \mathscr{T}_{13}\hat{x}_1\hat{x}_3, \\
& + \mathscr{T}_{21}\hat{x}_2\hat{x}_1 + \mathscr{T}_{22}\hat{x}_2\hat{x}_2 + \mathscr{T}_{23}\hat{x}_2\hat{x}_3 \\
& + \mathscr{T}_{31}\hat{x}_3\hat{x}_1 + \mathscr{T}_{32}\hat{x}_3\hat{x}_2 + \mathscr{T}_{33}\hat{x}_3\hat{x}_3 \\
\overleftrightarrow{T} = {} & \mathscr{T}^{A_{1g}}\hat{T}^{A_{1g}} + \mathscr{T}_1^{E_g}\hat{T}_1^{E_g} + \mathscr{T}_2^{E_g}\hat{T}_2^{E_g} \\
& + \mathscr{T}_1^{T_{2g}}\hat{T}_1^{T_{2g}} + \mathscr{T}_2^{T_{2g}}\hat{T}_2^{T_{2g}} + \mathscr{T}_3^{T_{2g}}\hat{T}_3^{T_{2g}} \\
& + \mathscr{T}_1^{T_{1g}}\hat{T}_1^{T_{1g}} + \mathscr{T}_2^{T_{1g}}\hat{T}_2^{T_{1g}} + \mathscr{T}_3^{T_{1g}}\hat{T}_3^{T_{1g}}.
\end{aligned} \tag{6.3.11}$$

In order to obtain a physical feeling for these components $\mathscr{T}_{1j}$ or $\mathscr{T}_m^\gamma$, we shall discuss their physical representations, which are shown in Figure 6.3.2.

First consider the Cartesian components $\mathscr{T}_{ij}$. Components $\mathscr{T}_{1j}$, $\mathscr{T}_{2j}$, and $\mathscr{T}_{3j}$ are the components of the force $\mathbf{F}(j)$ in Figure 6.3.2(a):

$$\mathbf{F}(j) = \overleftrightarrow{T} \cdot \hat{x}_j = \mathscr{T}_{1j}\hat{x}_1 + \mathscr{T}_{2j}\hat{x}_2 + \mathscr{T}_{3j}\hat{x}_3. \tag{6.3.12}$$

We see that $\mathbf{F}(j)$ is the force per unit area felt by the jth face of the cube due to the outside world on the positive side of the $\hat{x}_j$ axis. It is assumed that the force $F(j)$ is the same for all parallel planes in the neighborhood, so an equal and opposite force $-\mathbf{F}(j)$ can be imagined tugging or pressing on the opposite cube face as indicated by the dotted arrows in the figure.

Now the symmetry-defined components $\mathscr{T}_m^\gamma$ tell how much of a particular type of unit stress $\hat{T}_m^\gamma$ is present. The common names of these symmetry-defined stresses are written in Figure 6.3.2(b). We shall see shortly what is the advantage of these coordinates over the $\mathscr{T}_{ij}$, but for now we can see that one set is easily found in terms of the other using the $(T_{1u} \otimes T_{1u})$ coupling

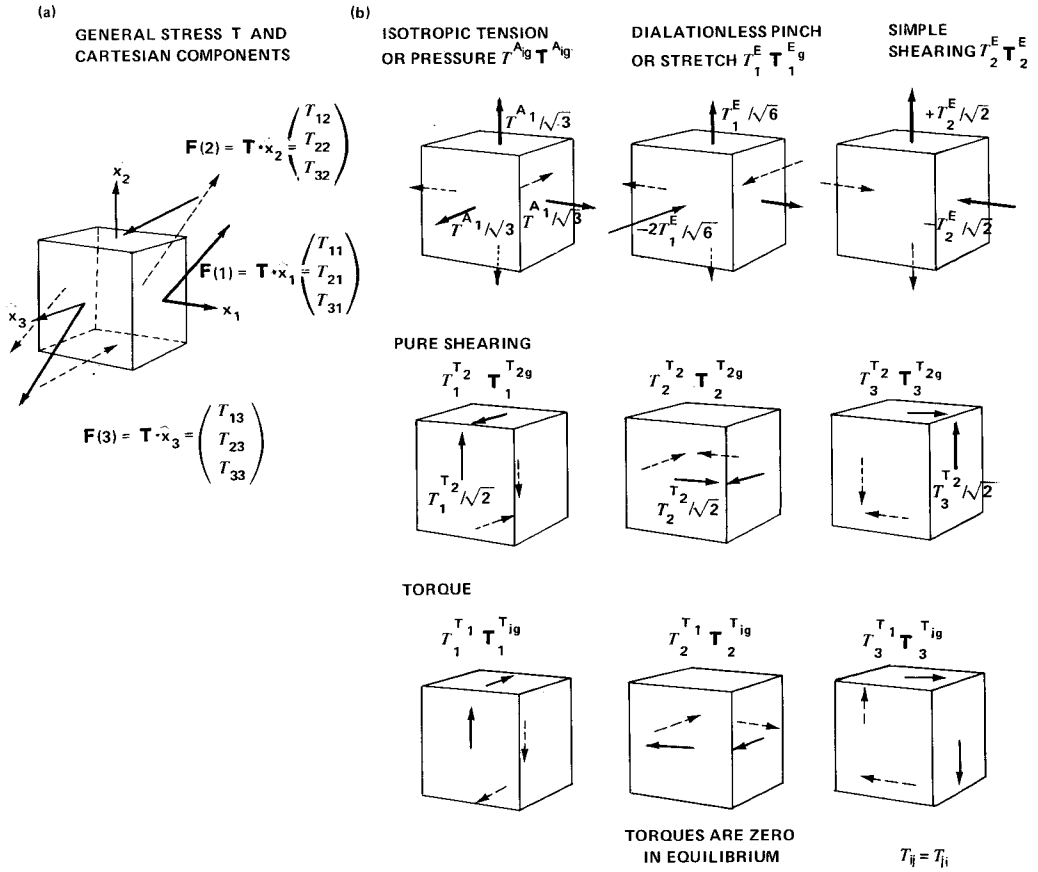

Figure 6.3.2 Tensor representations of stress. (a) The usual Cartesian components T_{ij} are indicated on the left. T_{ij} is the ith component of the total fore $\mathbf{F}(j)$ vector due to stress outside the surface with normal $\hat{x}_j$. (b) The symmetry-defined stresses are shown. The magnitude of each vector is given in terms of the relevant component T_a^α.

coefficients:

$$\mathcal{T}_m^{\gamma} = \sum_i \sum_j \mathcal{C}_{ijm}^{T_{1u}T_{1u}\gamma} \mathcal{T}_{ij}, \tag{6.3.13a}$$

$$\mathcal{T}_{ij} = \sum_{\gamma} \sum_m \mathcal{C}_{ijm}^{T_{1u}T_{1u}\gamma} \mathcal{T}_m^{\gamma}. \tag{6.3.13b}$$

Note that the three torque components, i.e., the three components $\mathcal{T}_1^{T_1}$, $\mathcal{T}_2^{T_1}$, and $\mathcal{T}_3^{T_1}$ will have to be zero for any static or equilibrium stress. If the torques are zero, then the remaining symmetry-defined stress tensors or any combination of them are symmetric,

$$\mathcal{T}_{ij} = \mathcal{T}_{ji},$$

leaving just six independent stress tensor components.

(b) Strain Tensor A similar type of mathematics can be used to define the deformation or STRAIN inside a body. Suppose each point $\mathbf{r}$ inside is moved to some new point $\mathbf{r} + \mathbf{s}(\mathbf{r})$. Strain is a measure of what is happening to neighboring points $\mathbf{r} + d\mathbf{r}$ around a given $\mathbf{r}$. It tells how much the material in the neighborhood is getting crushed or stretched.

Figure 6.3.3 shows that the vector $d\mathbf{r}$ between neighboring points is transformed into $\nabla\mathbf{s} \cdot d\mathbf{r}$ in the limit of small $d\mathbf{r}$. The derivative $\nabla\mathbf{s} \equiv \overleftrightarrow{S}$ is called the STRAIN TENSOR:

$$\overleftrightarrow{S} = \nabla\mathbf{s} = \frac{\partial \mathbf{s}}{\partial x_1}\hat{x}_1 + \frac{\partial \mathbf{s}}{\partial x_2}\hat{x}_2 + \frac{\partial \mathbf{s}}{\partial x_3}\hat{x}_3,$$

$$\begin{aligned}\overleftrightarrow{S} = {} & \frac{\partial s_1}{\partial x_1}\hat{x}_1\hat{x}_1 + \frac{\partial s_1}{\partial x_2}\hat{x}_1\hat{x}_2 + \frac{\partial s_1}{\partial x_3}\hat{x}_1\hat{x}_3 \\ & + \frac{\partial s_2}{\partial x_1}\hat{x}_2\hat{x}_1 + \frac{\partial s_2}{\partial x_2}\hat{x}_2\hat{x}_2 + \frac{\partial s_2}{\partial x_3}\hat{x}_2\hat{x}_3 \\ & + \frac{\partial s_3}{\partial x_1}\hat{x}_3\hat{x}_1 + \frac{\partial s_3}{\partial x_2}\hat{x}_3\hat{x}_2 + \frac{\partial s_3}{\partial x_3}\hat{x}_3\hat{x}_3.\end{aligned} \tag{6.3.14a}$$

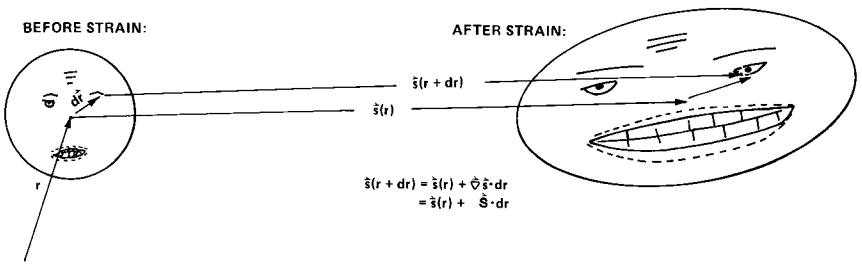

Figure 6.3.3 Defining the strain tensor $\overleftrightarrow{S} = \nabla\mathbf{s}$. The strain causes each point $\mathbf{r}$ to be moved to a new point $\mathbf{r} + \mathbf{s}(r)$.

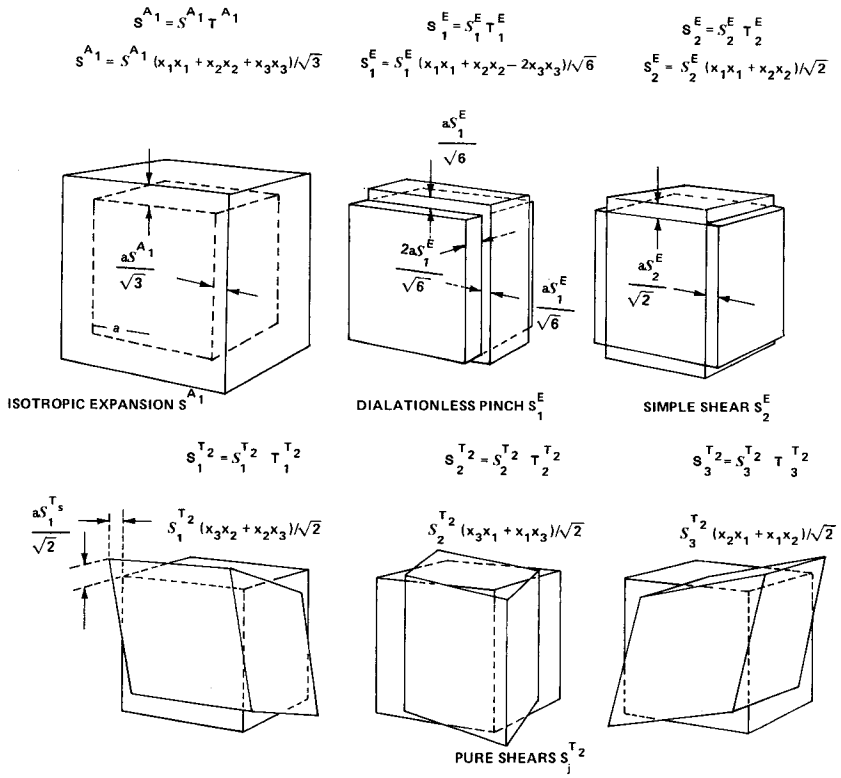

Figure 6.3.4 Symmetry-defined strains and their common names. Rotation motion $S_j^{T_1}$ is not considered to be a strain.

If $\mathbf{s}(\mathbf{r}) = \mathbf{s}$ is constant, then no strain exists ($\mathbf{S} = \mathbf{0}$), and we have just a uniform translation. If $\mathbf{s}(\mathbf{r})$ is linear in the coordinates x_j of $\mathbf{r}$, then $\overleftrightarrow{S}$ is a constant tensor, and we say that a HOMOGENEOUS STRAIN exists.

A homogeneous strain may be defined by the components $\mathscr{S}_{ij} = \partial s_i/\partial x_j$ or by any complete set of symmetry-defined components $\mathscr{S}_m^\gamma$ in exactly the same way that we defined stresses:

$$\vec{\mathbf{S}} = \sum_{i=1}^{3}\sum_{j=1}^{3} \mathscr{S}_{ij}\hat{x}_i\hat{x}_j = \sum_{\gamma}\sum_{m} \mathscr{S}_m^\gamma \hat{T}_m^\gamma. \tag{6.3.14b}$$

The mathematical form of $\hat{T}_m^\gamma$ is the same as before. The physical meaning of each term is different, as seen in Figure 6.3.4.

It is conventional to ignore purely rotational displacement tensors $\overleftrightarrow{S}_1^{T_1} = \mathscr{S}_1^{T_1}(-\hat{x}_3\hat{x}_2 + \hat{x}_2\hat{x}_3)$. These are generally not considered to be strains. Thus, there are only six independent strain components.

E. Symmetry Theory of Tensor Relations (Elastic Constants)

We study now generalizations of Hooke's law ($F = -kx$) for elastic solids in which six stresses are linearly related to six strains. The linear relations may involve either the standard Cartesian tensor components $\mathscr{T}_{hi}$ and $\mathscr{S}_{ik}$ and elastic constants $k_{hi,jk}$ as follows:

$$\mathscr{T}_{hi} = \sum_{j=1}^{3}\sum_{k=1}^{3} k_{hi,jk}\mathscr{S}_{jk}, \tag{6.3.15a}$$

or else symmetry-defined components and constants as follows:

$$\mathscr{T}_m^{\gamma} = \sum_{\delta}\sum_{n} k_{mn}^{\gamma\delta}\mathscr{S}_n^{\delta}. \tag{6.3.15b}$$

At first sight it might appear that the $6^2 = 36$ constants would be needed in either equation. However, this number can be reduced by using symmetry-defined components. For example, in the presence of O_h symmetry, we shall see that only three of the $k_{mn}^{\gamma\delta}$ are needed, namely, $k^{A_1} \equiv k^{A_1A_1}$, $k^{E} \equiv k_{11}^{EE} = k_{22}^{EE}$, and $k^{T_2} \equiv k_{11}^{T_2T_2} = k_{22}^{T_2T_2} = k_{33}^{T_2T_2}$. All others are zero!

Before treating examples, let us prove a general theorem about tensor relations and symmetry. Let us start with a general tensor relation, Eq. (6.3.16a), between two tensors $\mathscr{T}_{hi\ldots}$ and $\mathscr{S}_{kl\ldots}$, where $\mathscr{T}$ and $\mathscr{S}$ have m and n indices, respectively. Symmetry analysis isolates the independent constants from the set of 3^{m+n} constants $k_{hi\ldots kl\ldots}$ in the tensor relation:

$$\mathscr{T}_{hij\ldots} = \sum_{k}\sum_{l}\cdots\sum k_{hi\ldots kl\ldots}\mathscr{S}_{kl\ldots}. \tag{6.3.16a}$$

The idea is to first rewrite this relation using the symmetry-defined components as follows:

$$\mathscr{T}_m^{\omega}(\gamma) = \sum_{\phi}\sum_{\delta}\sum_{n} k_m^{\omega}(\gamma)_n^{\phi}(\delta)\mathscr{S}_n^{\phi}(\delta). \tag{6.3.16b}$$

One could do this whether the symmetry was present or not. However, the new constants $k_m^{\omega}(\gamma)_n^{\phi}(\delta)$ assume a very simple form when the symmetry is present, as proved in the following. First, let us first review the meaning of

the group labeling. Each tensor is labeled by a subgroup chain $\cdots F \supset G \supset H \cdots$ as follows:

$$\begin{aligned} \phi: &\quad \text{Nonsymmetry supergroup } F \text{ label or index,} \\ \mathscr{S}_m \equiv \mathscr{S}(\gamma): &\quad \text{Symmetry group } G \text{ label,} \\ h: &\quad \text{Symmetry subgroup } H \text{ label.} \end{aligned} \tag{6.3.17}$$

For example, the strain tensors in Figure 6.3.4 may be labeled by the tetragonal $O_h \supset D_{4h} \supset D_{2h}$ chain which was introduced in Chapter 4. The six components may be labeled as follows according to this scheme for $G = D_{4h}$:

$$\begin{aligned} &\mathscr{S}^{A_{1g}} = \mathscr{S}\left(\begin{matrix} A_{1g} \\ A_{1g} \end{matrix}\right), \quad \mathscr{S}_1^{E_g} = \mathscr{S}\left(\begin{matrix} E_g \\ A_{1g} \end{matrix}\right), \quad \mathscr{S}_2^{E_g} = \mathscr{S}\left(\begin{matrix} E_g \\ A_1 g \end{matrix}\right), \\ &\mathscr{S}_1^{T_{2g}} = \mathscr{S}\left(\begin{matrix} T_{2g} \\ B_{1g} \end{matrix}\right), \quad \mathscr{S}_2^{T_{2g}} = -\mathscr{S}\left(\begin{matrix} T_{2g} \\ B_{2g} \end{matrix}\right), \quad \mathscr{S}_3^{T_{2g}} = \mathscr{S}\left(\begin{matrix} T_{2g} \\ A_{2g} \end{matrix}\right). \end{aligned} \tag{6.3.18}$$

This scheme was introduced in Eq. (4.2.17). [Remember the slight but terrible difference between "kosher" subgroup labeled components and the "standard" T_{2g} components wherein $\mathscr{S}_2^{T_{2g}} = -\mathscr{S}\left(\begin{matrix} T_{2g} \\ B_{2g} \end{matrix}\right)$.] In the proof of the tensor theorem which follows the (middle) symmetry-group G label is enclosed with parentheses. The upper nonsymmetry supergroup F label is superfluous as long as there are no two independent $\mathscr{S}^{(\gamma)}$ components with the same (γ). Note two $(\gamma) = (A_{1g})$ components exist for D_{4h}, and they are distinguished by the labels $\phi = A_{1g}$ and E_g, respectively, of the next higher link $(F = O_h)$ of the subgroup chain.

If the symmetry group is octahedral $G = O_h$ it may be convenient to include the full rotational group $F = O_3$ in the subgroup chain $(O_3 \supset O_h \supset D_{4h} \cdots)$ and label the strain tensors as follows:

$$\begin{aligned} &\mathscr{S}^{A_{1g}} \equiv \mathscr{S}\left(\begin{matrix} 0^+ \\ A_{1g} \end{matrix}\right), \quad \mathscr{S}_1^{E_g} \equiv \mathscr{S}\left(\begin{matrix} 2^+ \\ A_{1g} \end{matrix}\right), \quad \mathscr{S}_2^{E_g} \equiv \mathscr{S}\left(\begin{matrix} 2^+ \\ B_{1g} \end{matrix}\right), \\ &\mathscr{S}_1^{T_{2g}} \equiv \mathscr{S}\left(\begin{matrix} 2^+ \\ E_g(1) \end{matrix}\right), \quad \mathscr{S}_2^{T_{2g}} \equiv -\mathscr{S}\left(\begin{matrix} 2^+ \\ E_g(2) \end{matrix}\right), \quad \mathscr{S}_3^{T_{2g}} \equiv \mathscr{S}\left(\begin{matrix} 2^+ \\ A_{2g} \end{matrix}\right). \end{aligned} \tag{6.3.19}$$

Here the connection between $J = 0^+$ and 2^+ representations of O_3 and second-order polynomials

$$\{(x^2 + y^2 + z^2) \sim (0^+); (2z^2 - x^2 - y^2, \sqrt{3}(x^2 - y^2), xy, xz, yz) \sim (2^+)\}$$

is used. Recall Eqs. (5.6.15) and (6.3.9).

Tensor Theorem If physical properties of a solid having G symmetry are described by the G-symmetry-defined tensor relation in Eq. (6.3.16b), then there will be at most one independent nonzero constant for each distinct pair of equal symmetry group labels $(\gamma) = (\delta)$ which appear on opposite sides of the relation. These constants obey the following rules:

$$k\begin{matrix}\omega & \phi \\ (\gamma) & (\delta) \\ m & n\end{matrix} = \begin{cases} 0, & \text{if } \delta \neq \gamma \text{ or } m \neq n, \\ k^{(\gamma)^{\omega\phi}}, & \text{for each } m = n \text{ if } \delta = \gamma, \end{cases}$$

and the relation assumes the following form:

$$\mathscr{T}\begin{matrix}\omega \\ (\gamma) \\ m\end{matrix} = \sum_{\phi} k^{(\gamma)^{\omega\phi}} \mathscr{S}\begin{matrix}\phi \\ (\gamma) \\ m\end{matrix} \tag{6.3.20}$$

for each m.

Proof In the presence of symmetry, we may redefine our axes in the solid as indicated in Figure 4.2.2 using any symmetry operator g, without changing the values of the constants $k\begin{matrix}(\gamma)(\delta) \\ m\ n\end{matrix}$ in the relation. Since the axes all end up in equivalent positions with respect to the solid, the constants cannot be different. However, the unit vectors and tensors will be transformed according to their respective irreps as follows:

$$\sum_{m'} \mathscr{D}^{\gamma}_{m'm}(g) \mathscr{T}\begin{matrix}\omega \\ (\gamma) \\ m'\end{matrix}^{\omega} = \sum_{\delta} \sum_{\phi} \sum_{n} k\begin{matrix}\omega & \phi \\ (\gamma) & (\delta) \\ m & n\end{matrix} \sum_{n} \mathscr{D}^{\delta}_{n'n}(g) \mathscr{S}\begin{matrix}\phi \\ (\delta) \\ n\end{matrix}.$$

Since this is true for all g in the group, we may substitute for g the elementary operators P^{α}_{ji} using $\mathscr{D}^{\gamma}_{m'm}(P^{\alpha}_{ji}) = \delta^{\gamma\alpha}\delta_{m'j}\delta_{mi}$, i.e., Eq. (3.4.18).

The resulting relations prove the theorem since each relation

$$\underset{j}{\overset{\omega}{\mathscr{T}}}(\alpha) = \sum_{\phi} \underset{i}{\overset{\omega}{k}}(\alpha)\,\underset{i}{\overset{\phi}{(\alpha)}}\,\underset{j}{\overset{\phi}{\mathscr{S}}}(\alpha)$$

is independent of the choice of subgroup indices i or j.

Equation (6.3.20) is very powerful, and it dictates strong requirements for the k coefficients. For example, if D_{4h} symmetry is present in a crystalline solid then only the following k coefficients survive in the stress-strain tetradic relation:

$\langle k(D_{4h})\rangle$

	$\underset{A_{1g}}{\mathscr{S}(A_{1g})}$	$\underset{A_{1g}}{\mathscr{S}(A_{1g})}$	$\underset{A_{1g}}{\mathscr{S}(B_{1g})}$	$\underset{B_{1g}}{\mathscr{S}(E_g)}$	$\underset{B_{2g}}{\mathscr{S}(E_g)}$	$\underset{A_{2g}}{\mathscr{S}(A_{2g})}$
$\underset{A_{1g}}{\mathscr{T}(A_{1g})}$	$k^{(A_{1g})^{AA}}$	$k^{(A_{1g})^{AE}}$	·	·	·	·
$\underset{A_{1g}}{\mathscr{T}(A_{1g})}$	$k^{(A_{1g})^{EA}}$	$k^{(A_{1g})^{EE}}$	·	·	·	·
$= \underset{A_{1g}}{\mathscr{T}(B_{1g})}$	·	·	$k^{(B_{1g})}$	·	·	·
$\underset{B_{1g}}{\mathscr{T}(E_g)}$	·	·	·	$k^{(E_g)}$	·	·
$\underset{B_{2g}}{\mathscr{T}(E_g)}$	·	·	·	·	$k^{(E_g)}$	·
$\underset{A_{2g}}{\mathscr{T}(A_{2g})}$	·	·	·	·	·	$k^{(A_{2g})}$

(6.3.21)

In O_h symmetry the constants are more restricted so that only three independent constants are left out of the original 36:

$\langle k(O_h) \rangle =$

	0^+ $\mathscr{S}(A_{1g})$ A_{1g}	2^+ $\mathscr{S}(E_g)$ A_{1g}	2^+ $\mathscr{S}(E_g)$ B_{1g}	2^+ $\mathscr{S}(T_{2g})$ $E_g(1)$	2^+ $\mathscr{S}(T_{2g})$ $E_g(2)$	2^+ $\mathscr{S}(T_{2g})$ A_{2g}
0^+ $\mathscr{T}(A_{1g})$ A_{1g}	$k^{(A_{1g})}$	.	.	.	.	.
2^+ $\mathscr{T}(E_g)$ A_{1g}	.	$k^{(E_g)}$	.	.	.	.
2^+ $\mathscr{T}(E_g)$ B_{1g}	.	.	$k^{(E_g)}$	.	.	.
2^+ $\mathscr{T}(T_{2g})$ $E_g(1)$	.	.	.	$k^{(T_{2g})}$	.	.
2^+ $\mathscr{T}(T_{2g})$ $E_g(2)$	.	.	.	.	$k^{(T_{2g})}$	.
2^+ $\mathscr{T}(T_{2g})$ A_{2g}	.	.	.	.	.	$k^{(T_{2g})}$

(6.3.22)

Note that if full rotational (O_2) symmetry is present, then the constants are further restricted so that only two remain: $k^{0^+} = k^{(A_{1g})}$ and $k^{2^+} = k^{(T_{2g})}$. This is the case for amorphous or sintered solids which are isotropic on the average.

For lower-symmetry materials one expects a larger number of off-diagonal k coefficients even if symmetry-defined tensors are used. Then it is helpful to reduce the number of these coefficients by using energy considerations. If the stresses and strains are CONSERVATIVE then the energy E may be written as a function of some set of symmetry-defined strains $\{\mathscr{S}_1 \mathscr{S}_2 \cdots\}$ only. Then one has

$$dE = \sum_j \frac{\partial E}{\partial \mathscr{S}_j} d\mathscr{S}_j = -\sum_j \mathscr{T}_j \, d\mathscr{S}_j, \tag{6.3.23a}$$

where one *defines* the stresses by

$$\mathscr{T}_j = -\frac{\partial E}{\partial \mathscr{S}_j}. \tag{6.3.23b}$$

This definition is supposed to be valid even for large strains for which $\mathscr{T}_j$ is not a linear function of $\mathscr{S}_i$'s. In any case small changes in the stress should be related to small changes in the strains through the following linear relation:

$$d\mathscr{T}_j = \frac{\partial \mathscr{T}_j}{\partial \mathscr{S}_i} d\mathscr{S}_i = \sum_i -\frac{\partial^2 E}{\partial \mathscr{S}_i \partial \mathscr{S}_j} d\mathscr{S}_i. \tag{6.3.24}$$

The coefficients of this relation are generalized k coefficients

$$k_{ij} = -\frac{\partial^2 E}{\partial \mathscr{S}_i \partial \mathscr{S}_j} = k_{ji}, \tag{6.3.25}$$

which will be constants only for small strains $\mathscr{S}_j = d\mathscr{S}_j \sim 0$. Otherwise they are complicated functions of $\mathscr{S}_j$'s. However, even then they satisfy the RECIPROCITY RELATIONS $k_{ij} = k_{ji}$ if the stresses are conservative. This reduces the number of off-diagonal k coefficients by one-half. Only six D_{4h} coefficients in Eq. (6.3.21) are independent if reciprocity holds, since then $k^{(A_{1g})^{AE}} = k^{(A_{1g})^{EA}}$.

The orthonormality and completeness relations of any symmetry definition make it easy to relate back and forth between Cartesian components and constants $k_{hi,jk}$ and the symmetry-defined quantities $k_{mn}^{(\gamma)_\omega(\delta)_\phi}$. This is true even without the presence of symmetry; however, the simplification of the constants makes this transformation very convenient.

Consider, for example, some of the Cartesian components of the O_h-symmetric elasticity relation:

$$k_{hi,jk} = \sum_\gamma \sum_m \mathscr{C}_{him}^{T_{1u}T_{1u}\gamma} \mathscr{C}_{jkm}^{T_{1u}T_{1u}\gamma} k^\gamma. \tag{6.3.26}$$

Now only the symmetric coupling coefficients are used: ($\mathscr{C}_{jkm}^{T_1T_1\gamma} = \mathscr{C}_{kjm}^{T_1T_1\gamma}$). We do not deal with the antisymmetric $\mathscr{C}_{jkm}^{T_1T_1T_1} = -\mathscr{C}_{kjm}^{T_1T_1T_1}$ coefficients since $k^\gamma = k^{T_1}$ is not considered. This gives

$$k_{hi,jk} = k_{ih,jk} = k_{hi,kj} = k_{ih,kj},$$

and leaves only 36 independent $k_{hi,jk}$. From either (6.3.26) or the reciprocity relation (6.3.25) one has

$$k_{hi,jk} = k_{jk,hi},$$

leaving 21 independent components. By substituting the values of the coupling coefficients from Eq. (6.1.19c) one obtains relations between Cartesian k coefficients and the three independent octahedrally defined coefficients k^{A_1}, k^{E}, and k^{T_2}:

$$\begin{aligned} k_{11,11} &= k_{22,22} = k_{33,33} = k^{A_1}/3 + 2k^{E}/3, \\ k_{11,22} &= k_{11,33} = k_{22,33} = k^{A_1}/3 - k^{E}/3, \\ k_{12,12} &= k_{13,13} = k_{23,23} = k^{T_2}/2 + k^{T_1}/2 = k^{T_2}/2. \end{aligned} \tag{6.3.27}$$

In the last line we assume the rotational constant k^{T_1} is zero. The coupling coefficients immediately give us all the relations between the Cartesian components that are a result of symmetry. The inverse transformations are sometimes useful, too:

$$k^{\gamma} = \sum_h \sum_i \sum_j \sum_k \mathscr{C}^{T_{1u}T_{1u}\gamma}_{him} \mathscr{C}^{T_{1u}T_{1u}\gamma}_{jkm} k_{hi,jk}. \tag{6.3.28}$$

For octahedral symmetry one has the following:

$$\begin{aligned} k^{A_1} &= k_{11,11} + 2k_{11,12}, \\ k^{E} &= k_{11,11} - k_{11,22}, \\ k^{T_2} &= 2k_{12,12}. \end{aligned} \tag{6.3.28}_x$$

In order to simplify the relations in Eq. (6.3.28), one may use the relations derived in Eq. (6.3.27) to sort out the Cartesian components that were equal to others or else zero.

We now review the relation between the O_h-symmetry-defined elastic constants k^{γ} and some of the elastic moduli commonly used in physics and engineering.

(a) Bulk Modulus The bulk modulus B is defined in the following, where $\Delta V/V$ is relative change in volume due to an addition of a uniform pressure having force ΔF per area A:

$$\Delta F/A = B\,\Delta V/V. \tag{6.3.29}$$

We make the correspondence between this equation of the symmetry-defined relation $\mathscr{T}^{A_1} = k^{A_1}\mathscr{S}^{A_1}$. According to Figure 6.3.2(b) the pressure is given by the following:

$$\Delta F/A = -\mathscr{T}^{A_1}/\sqrt{3}.$$

According to Figure 6.3.4 the volume strain is given by the following, where it

is assumed that the strain coordinate $\mathscr{S}^{A_1}$ is small:

$$\Delta V/V = \frac{\left[(2a)^3(1-\mathscr{S}^{A_1}/\sqrt{3})^3 - (2a)^3\right]}{[2a]^3} \sim -\sqrt{3}\mathscr{S}^{A_1}.$$

Combining the last two equations with $\mathscr{T}^{A_1} = k^{A_1}\mathscr{S}^{A_1}$ shows that k^{A_1} is three times the bulk modulus.

$$B = k^{A_1}/3 = (k_{11,11} + 2k_{11,22})/3. \tag{6.3.30}$$

(b) Shear Modulus Using the quantities labeled in Figure 6.3.5, we define the shear modulus μ as follows:

$$\Delta F/A = \mu d/h,$$
$$\Delta F/(2a)^2 = \mu d/2a. \tag{6.3.31}$$

We recognize this to belong to one of the symmetry-defined relations $\mathscr{T}^{T_2} = k^{T_2}\mathscr{S}^{T_2}$. Using Figures 6.3.2(b) and 6.3.4 for (T_2) stress and strain definitions, respectively, we obtain the following relations:

$$\mathscr{T}^{T_2}/\sqrt{2} = \Delta F/(2a)^2, \qquad \mathscr{S}^{T_2}a/\sqrt{2} = d/4.$$

Substituting these in Eq. (6.3.31), we find that k^{T_2} is twice the shear modulus:

$$\mu = k^{T_2}/2. \tag{6.3.32}$$

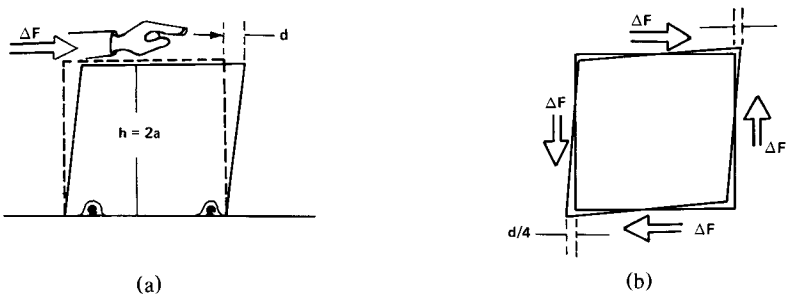

(a) (b)

Figure 6.3.5 Defining shear of a cubical block. (a) Standard definition involves a sideways motion d of the upper surface of the block with the base fixed. (b) A more symmetrical picture of the same distortion shows that the corners each move a distance $d/4$. Here the center of gravity and the diagonal axis of the block do not move.

(c) Young's Modulus and Poisson's Ratio If a pure tension $\vec{\vec{T}} = (F/A)\hat{x}_3\hat{x}_3$ is applied to the cube, we can expect the 3-axis to lengthen. However, we may also expect a change along the transverse 1 and 2 axes since this tensor is a combination of T^{A_1} and T_1^E which affect these dimensions:

$$\begin{aligned}\vec{\vec{T}} &= (F/A)\hat{x}_3\hat{x}_3 = (F/A)\left(\hat{T}^{A_1}/\sqrt{3} - 2\hat{T}_1^E/\sqrt{6}\right) \\ &\equiv \mathcal{T}^{A_1}\hat{T}^{A_1} + \mathcal{T}_1^E\hat{T}_1^E. \end{aligned} \tag{6.3.33}$$

We now find what the strain will be in terms of the symmetry-defined constants k^{A_1} and k^E using the following relations:

$$(F/A)/\sqrt{3} = \mathcal{T}^{A_1} = k^{A_1}\mathcal{S}^{A_1}, \qquad -2(F/A)/\sqrt{6} = \mathcal{T}_1^E = k^E\mathcal{S}_1^E \tag{6.3.34}$$

This yields the strain indicated in Figure 6.3.6, where the changes Δa_L and Δa_T of the longitudinal and transverse semiaxes are given by Eq. (6.3.35):

$$\begin{aligned}\Delta a_L/a &= \mathcal{S}^{A_1}/\sqrt{3} - 2\mathcal{S}_1^E/\sqrt{6} = (F/A)(1/3k^{A_1} + 4/6k^E), \\ \Delta a_T/a &= \mathcal{S}^{A_1}/\sqrt{3} + \mathcal{S}_1^E/\sqrt{6} = (F/A)(1/3k^{A_1} - 2/6k^E). \end{aligned} \tag{6.3.35}$$

Now, Young's modulus Y and Poisson's ratio σ are defined in the following. The definition of σ uses a negative sign since Δa_L and Δa_T always turn out to have opposite signs:

$$\begin{aligned} Y &\equiv (F/A)/(\Delta a_L/a) \\ &= 1/(1/3k^{A_1} + 2/3k^E) \\ &= 3k^Ek^{A_1}/(2k^{A_1} + k^E), \end{aligned} \tag{6.3.36a}$$

$$\begin{aligned}\sigma &\equiv -(\Delta a_T/a)(\Delta a_L/a) \\ &= -(1/3k^{A_1} - 1/3k^E)/(1/3k^{A_1} + 2/3k^E) \\ &= (k^{A_1} - k^E)/(2k^{A_1} + k^E). \end{aligned} \tag{6.3.36b}$$

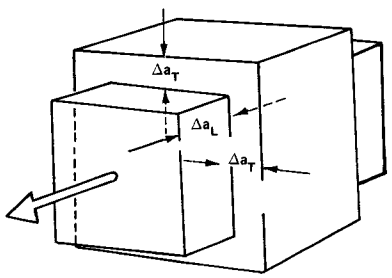

Figure 6.3.6 General strain caused by pure tension. Block elongates by $2\Delta a_L$ while the transverse dimensions shrink by $2\Delta a_T$.

Solving for the k^γ gives the following:

$$k^{A_1} = Y/(1 - 2\sigma), \qquad k^E = Y/(1 + \sigma). \tag{6.3.37}$$

(d) Isotropic Solids In an isotropic material in which crystal order is randomized or nonexistent, we found that $k^E = k^{T_2}$. This will happen in any solid that has no preferential directions. This corresponds to the presence of the infinite rotational symmetry O_3. In order to visualize the fact that $k^E = k^{T_2}$ in this case, observe that the $\mathscr{S}_2^E$ strain in Figure 6.3.4 is the same as the $\mathscr{S}^{T_2}$ strain rotated by 45° around the 3-axis. The same applies to the corresponding stresses in Figure 6.3.2(b). If the 45° rotation is a symmetry operation in addition to all the O_h operations, then we must have $k^E = k^{T_2}$. This is the case in isotropic solids, so there are only two constants which are needed to describe their elastic properties. Combining Eqs. (6.3.30), (6.3.32), and (6.3.37) gives the following relations between them:

$$B = Y/3(1 - 2\sigma), \qquad \mu = Y/2(1 + \sigma) \tag{6.3.38}$$

(e) More Spring Constant Theory Consider a model of solid strontium titanate $SrTiO_3$ as shown in Figure 6.3.7(a) with the interatomic nearest-neighbor forces represented by three different springs. This rather simplified rigid-ion model neglects the bending and long-range Coulomb forces as well as the ion polarizabilities—all of which are considered in more sophisticated shell models. However, we shall see that our model illustrates the group-theoretical techniques inherent in more complicated models and leads to proper order of magnitudes for the elastic constants.

Let us compute the elastic constants k^γ in terms of the interatomic spring constants j, k, and l by imposing one of the symmetry-defined strains belonging to irrep (γ) and summing the forces per unit area on the center plane in Figure 6.3.7(b) due to its nearest-neighbor atoms on one side. By

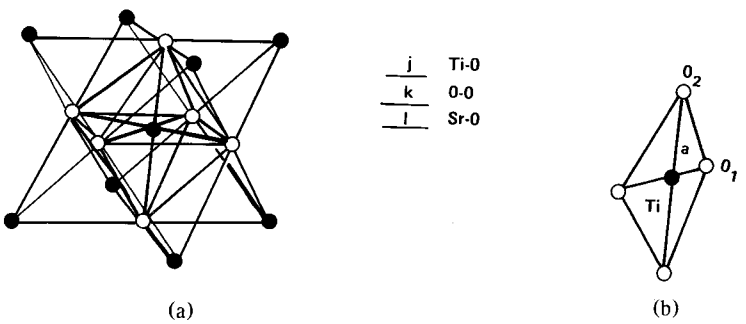

(a) (b)

Figure 6.3.7 (a) Model for strontium titanate $SrTiO_3$. Three different springs used for interatomic bonds. (b) One-half unit cell in Sr plane has area $2a^2$. Unit cell contains one Ti atom and two O atoms [O(1) and O(2)].

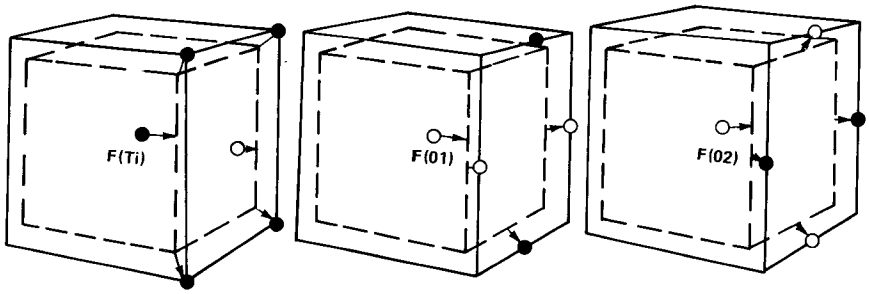

Figure 6.3.8 Atomic forces due to A_{1g} strain on (a) Ti atom, (b) O(1) atom, and (c) O(2) atom.

relating this force to the corresponding components of stress $\mathcal{T}^\gamma$, one obtains elastic constant $k^\gamma = \mathcal{S}^\gamma/\mathcal{T}^\gamma$. The central plane considered contains one Ti atom and two O atoms per unit area $4a^2$, where a is half the lattice parameter ($2a = 3.9 \times 10^{-8}$ cm) or the distance between the Ti and O atoms in this cubic lattice.

Now, an A_{1g} strain gives rise to forces **F**(Ti), **F**(01), and **F**(02) in the plane considered, as shown in Figure 6.3.8. Thus we have

$$\mathcal{T}^{A_1}/\sqrt{3} = \frac{|\mathbf{F}(\mathrm{Ti})| + |\mathbf{F}(01)| + |\mathbf{F}(02)|}{4a^2}, \tag{6.3.39}$$

where the various forces are computed in the following:

$$\begin{aligned} |F(\mathrm{Ti})| &= F_1(\mathrm{Ti}) = j\mathcal{S}^{A_1}a/\sqrt{3}, \\ |F(01)| &= F_1(01) = (2k + 2l)\mathcal{S}^{A_1}a/\sqrt{3}, \\ |F(02)| &= F_1(02) = (2k + 2l)\mathcal{S}^{A_1}a/\sqrt{3}. \end{aligned} \tag{6.3.40}$$

[Note that $F_1(02)$ may always be derived from $F_1(01)$ by interchanging k and l.] From the foregoing two equations, we find

$$k^{A_1} = \mathcal{T}^{A_1}/\mathcal{S}^{A_1} = (j + 4k + 4l)/4a. \tag{6.3.41a}$$

Similar treatment involving the other two types of strain gives the elastic constants k^E and k^{T_2} (we may choose any component of the symmetry type):

$$k^E = (j + k + l)/4a, \tag{6.3.41b}$$

$$k^{T_2} = (2k + 2l)/4a. \tag{6.3.41c}$$

In our calculations, we could equally well have chosen a plane containing strontium atoms with the same result.

Now, it is interesting to observe that these three k^{γ} are not linearly independent. In particular, two of the Cartesian elastic constants, $k_{11,22}$ and $k_{12,12}$, will be equal for all k, j, and l. From Eq. (6.3.27), we find

$$k_{11,11} = (2k + j + 2l)/4a,$$

$$k_{11,22} = (k + l)/4a,$$

$$k_{12,12} = (k + l)/4a. \tag{6.3.42}$$

If we include bending constants or "covalent" forces in our model in addition to the central or "ionic" forces, then $k_{11,22}$ no longer equals $k_{12,12}$.

Plotting the observed values of $k_{11,22}$ versus $k_{12,12}$ for various cubic solids gives us some idea of which have ionic bonds and which have covalent bonds. This is done in Figure 6.3.9. Note that NaCl and similar salts are very close to the $k_{11,22} = k_{12,12}$ line, with exception of AgCl and LiF. Most metals and crystals like diamond are considerably removed from the center line.

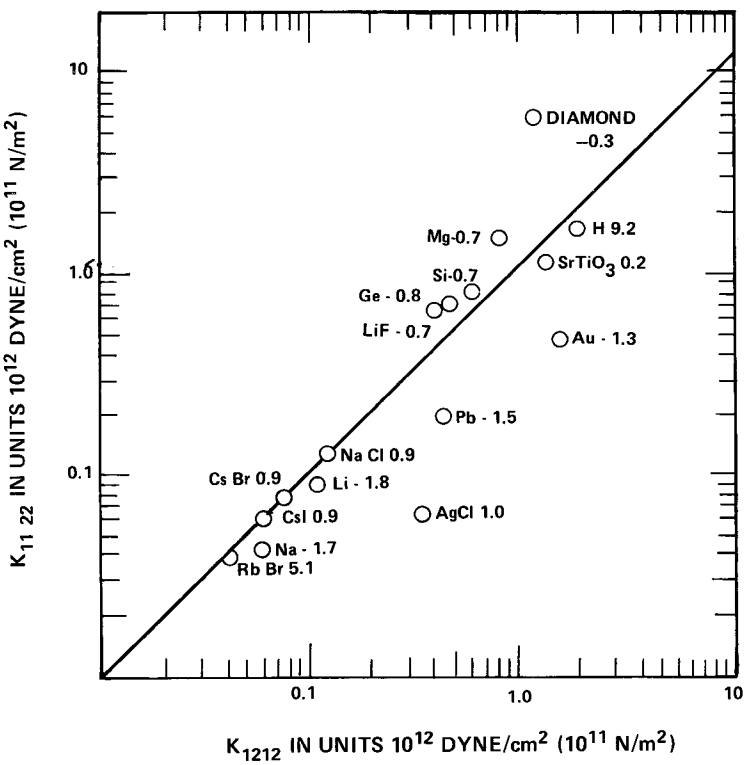

Figure 6.3.9 Plot of observed values of $k_{11,22}$ vs $k_{12,12}$ for various cubic solids.

Next to each point is written an "anisotropy" number A defined as follows:

$$A = \frac{k^E - k^{T_2}}{(k^{T_2}/2)} = \frac{k_{11,11} - k_{11,22} - 2k_{12,12}}{k_{12,12}}. \tag{6.3.43}$$

The closer this is to zero, the more closely the solid will imitate an isotropic material, as far as its bulk properties are concerned. Interestingly, diamond is the most "isotropic."

(f) Elasticity in C_{3v} Symmetry For C_{3v} one may use the trigonally defined ($O_h \supset D_{3d} \supset C_{2v}$) unit vectors shown in Figure 4.2.2: $\hat{v}_1 \equiv \hat{x}^3 \equiv \hat{x}_1^E$, $\hat{v}_2 \equiv \hat{x}^3 \equiv \hat{x}_2^E$, and $\hat{v}_3 \equiv \hat{x}^1 \equiv \hat{x}^{A_1}$. Using C_{3v} coupling coefficients (6.1.35a) we can assemble the symmetry-defined unit tensors and use them to describe stress and strain:

rotation

	$T^{(1)_1}$	$T^{(1)_2}$	$T_1^{(3)_1}$	$T_2^{(3)_1}$	$T_1^{(3)_2}$	$T_2^{(3)_2}$	T^2	$T_1^{(3)_3}$	$T_2^{(3)_3}$
v_1v_1	$\sqrt{\frac{1}{2}}$	·	$\sqrt{\frac{1}{2}}$	·	·	·	·	·	·
v_1v_2	·	·	·	$-\sqrt{\frac{1}{2}}$	·	·	$\sqrt{\frac{1}{2}}$	·	·
v_1v_3	·	·	·	·	$\sqrt{\frac{1}{2}}$	·	·	$\sqrt{\frac{1}{2}}$	·
v_2v_1	·	·	·	$-\sqrt{\frac{1}{2}}$	·	·	$-\sqrt{\frac{1}{2}}$	·	·
v_2v_2	$\sqrt{\frac{1}{2}}$	·	$-\sqrt{\frac{1}{2}}$	·	·	·	·	·	·
v_2v_3	·	·	·	·	·	$\sqrt{\frac{1}{2}}$	·	·	$\sqrt{\frac{1}{2}}$
v_3v_1	·	·	·	·	$\sqrt{\frac{1}{2}}$	·	·	$-\sqrt{\frac{1}{2}}$	·
v_3v_2	·	·	·	·	·	$\sqrt{\frac{1}{2}}$	·	·	$-\sqrt{\frac{1}{2}}$
v_3v_3	·	1	·	·	·	·	·	·	·

(6.3.44)

In the foregoing table of tensors, we have separated those three tensors on the right, which correspond to rotations from the others on the left. As usual, elasticity theory makes no use of rotations.

Using the components of the tensors on the left side of the table and the tensor theorem [Eq. (6.3.20)], we find the following elasticity relations will occur in C_{3v} solids:

$$\mathscr{T}^{(1)_1} = k^{(1)_{11}}\mathscr{S}^{(1)_1} + k^{(1)_{12}}\mathscr{S}^{(1)_2}, \qquad \mathscr{T}_m^{(3)_1} = k^{(3)_{11}}\mathscr{S}_m^{(3)_1} + k^{(3)_{12}}\mathscr{S}_m^{(3)_2},$$
$$\mathscr{T}^{(1)_2} = k^{(1)_{21}}\mathscr{S}^{(1)_1} + k^{(1)_{22}}\mathscr{S}^{(1)_2}, \qquad \mathscr{T}_m^{(3)_2} = k^{(3)_{21}}\mathscr{S}_m^{(3)_1} + k^{(3)_{22}}\mathscr{S}_m^{(3)_2},$$
$$m = 1, 2. \quad (6.3.45)$$

Here the $O_h \supset D_{3d} \supset C_{3v}$ supergroup labeling has been ignored. The repeated $A_1 = (1)$ and $E = (3)$ species have simply been tagged by numbers $(\cdot)_1$ and $(\cdot)_2$.

F. Symmetry-Defined Electric and Magnetic Fields

It is commonly said that an electric field is a vector while a magnetic field is a pseudovector. It is instructive to find to which irreps of C_{3v} they belong using physical arguments. One asks what happens to an electric field **E** or a magnetic field **B** under symmetry operations of C_{3v}. To do a symmetry by "thought experiment" operation, let us imagine that everything connected with the physical object gets transformed including the source charges or currents that make **E** or **B**.

Consider C_{3v} geometry and some electric or magnetic fields $\hat{E}_3$ and $\hat{B}_3$ which point along the $\hat{v}_3$ symmetry axis. Figure 6.3.10 shows what happens to

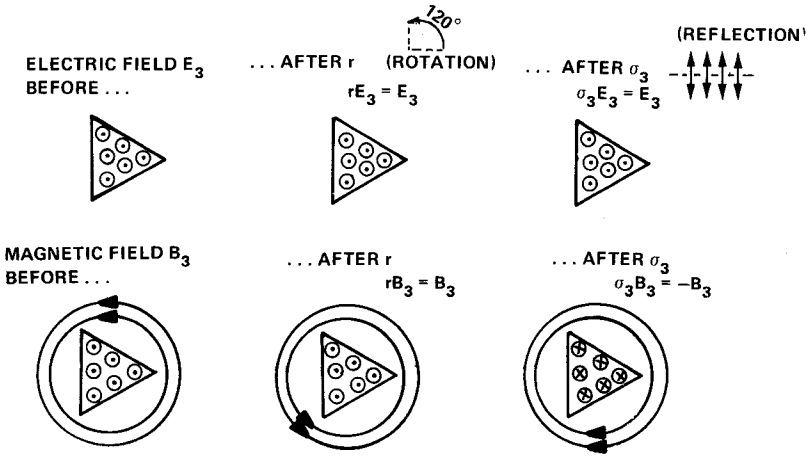

Figure 6.3.10 Effect of C_{3v} symmetry operations on electric field $\mathbf{E}_3$ and magnetic field $\mathbf{B}_3$ along symmetry axis. (a) $\mathbf{E}_3$ and $\mathbf{B}_3$ before symmetry operations. (b) After r. (c) After σ_3.

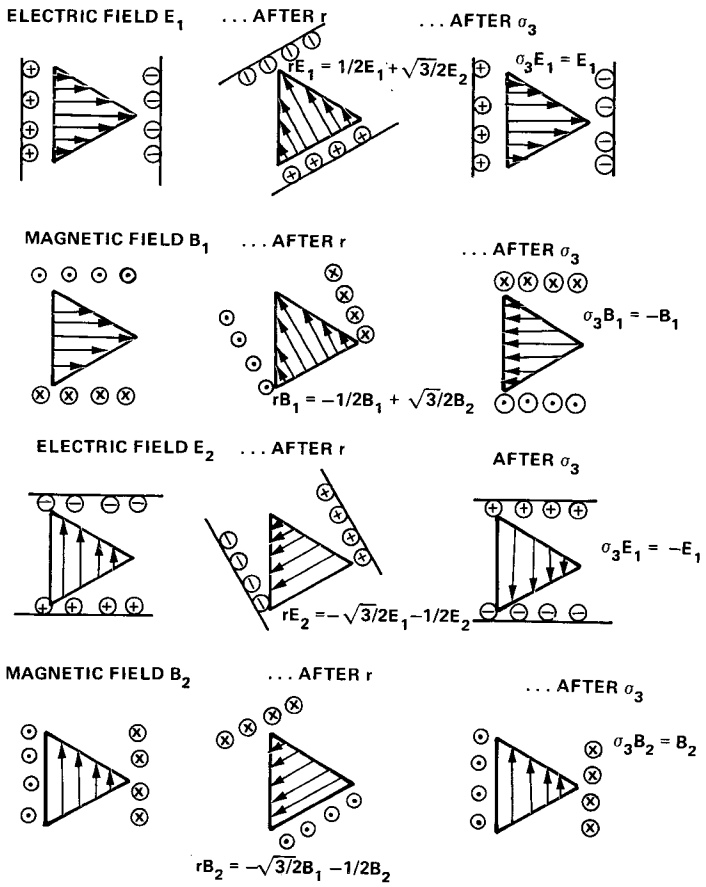

Figure 6.3.11 Effect of C_{3v} symmetry operations on electric fields $\mathbf{E}_1\mathbf{E}_2$ and magnetic fields $\mathbf{B}_1\mathbf{B}_2$ transverse to symmetry axis. (a) $\mathbf{E}_1$, $\mathbf{B}_1$, $\mathbf{E}_2$ and $\mathbf{B}_2$ before symmetry operations. (b) After r. (c) After σ_3.

$\hat{E}_3$ or $\hat{B}_3$ after operations by r (120° rotations) and σ_3 (reflection). The idea is to imagine what happens to sources or currents that give rise to $\mathbf{B}_3$ or the charges that give rise to $\mathbf{E}_3$. In Figure 6.3.10, reflection σ_3 reverses the current loop and thereby reverses $\mathbf{B}$. In Figure 6.3.11, we perform a similar analysis for fields $\mathbf{E}_1$ and $\mathbf{B}_1$ in the transverse directions.

The unit electric fields $\hat{E}_1$, $\hat{E}_2$, and $\hat{E}_3$ transform just like the unit vectors v_j in Figure 4.2.2, and so the symmetry definition of them is as follows:

$$\hat{E}_1 = \hat{E}_1^3 = \hat{E}_1^E, \qquad \hat{E}_2 = \hat{E}_2^3 = \hat{E}_2^E, \qquad \hat{E}_3 = \hat{E}^1 = \hat{E}^{A_1}. \quad (6.3.46)$$

The magnetic fields behave a little differently, as seen in the preceding

figures. In Figure 6.3.10, we see that $\hat{B}_3$ transforms according to irrep $\mathscr{D}^2 = \mathscr{D}^{A_2}$ of C_{3v}. In Figure 6.3.11, we see that some combinations of $\hat{B}_1$ and $\hat{B}_2$ will serve as bases for the irrep $\mathscr{D}^3 = \mathscr{D}^E$ of C_{3v}. To find this combination one applies the elementary operators.

$$\begin{aligned} P_{12}^3 \hat{B}_1 &= \tfrac{1}{3}\left[-\tfrac{3}{2} r \hat{B}_1 + \tfrac{3}{2} r^2 \hat{B}_1 - \tfrac{3}{2}\sigma_1 \hat{B}_1 + \tfrac{3}{2}\sigma_2 \hat{B}_1 \right] \\ &= \tfrac{1}{3}\left[-\tfrac{3}{2}\left(-\tfrac{1}{2}\hat{B}_1 + \tfrac{3}{2}\hat{B}_2 \right) + \tfrac{3}{2}\left(-\tfrac{1}{2}\hat{B}_1 - \tfrac{3}{2}\hat{B}_2 \right) \right. \\ &\qquad \left. -\tfrac{3}{2}\left(\tfrac{1}{2}\hat{B}_1 + \tfrac{3}{2}\hat{B}_2 \right) + \tfrac{3}{2}\left(\tfrac{1}{2}\hat{B}_1 - \tfrac{3}{2}\hat{B}_2 \right) \right] \\ &= -\hat{B}_2, \\ P_{22}^3 \hat{B}_1 &= \hat{B}_1. \end{aligned} \tag{6.3.47}$$

This gives the correct symmetry definition of the three magnetic fields:

$$\hat{B}_1 = \hat{B}_2^3 = \hat{B}_2^E, \qquad \hat{B}_2 = -\hat{B}_1^3 = -\hat{B}_1^E, \qquad \hat{B}_3 = \hat{B}^2 = \hat{B}^{A_2}. \tag{6.3.48}$$

Now one may define "external" fields **E** and **B** that are totally unaffected by symmetry operations and write them in terms of the symmetry-defined fields:

$$\mathbf{E} = \sum_{\gamma, m} \mathscr{E}_m^\gamma \hat{E}_m^\gamma = \sum_{\gamma, m} \mathscr{E}_m^{\gamma'} \hat{E}_m^{\gamma'}, \qquad B = \sum_{\gamma, m} \mathscr{B}_m^\gamma \hat{B}_m^\gamma = \sum_{\gamma, m} \mathscr{B}_m^{\gamma'} \hat{B}_m^{\gamma'}. \tag{6.3.49}$$

This defines components $\mathscr{E}_m^\gamma$ and $\mathscr{B}_m^\gamma$ which have the irrep transformation properties which label them.

Magnetostriction and Electrostriction

Some solids respond to external electric fields by distorting or even shattering into pieces. This effect is called ELECTROSTRICTION. Magnetic fields can cause analogous MAGNETOSTRICTION effects.

From the symmetry of the crystal, you may quickly tell what is possible by assuming a linear or tensor relation such as Eq. (6.3.50) between the field and strain components where $\varepsilon_{ij,k}$ and $\mu_{ij,k}$ are constants of electro- and magnetostriction, respectively.

$$\mathscr{S}_{ij} = \sum_k \varepsilon_{ij,k} \mathscr{E}_k, \tag{6.3.50a}$$

$$\mathscr{S}_{ij} = \sum_k \mu_{ij,k} \mathscr{B}_k. \tag{6.3.50b}$$

The situation becomes clearer if we use the symmetry-defined components and the tensor theorem. The labeling of Eq. (6.3.44) is used here:

$$\begin{aligned}
&\mathscr{S}^{(1)_1} = \varepsilon^{(1)_1}\mathscr{E}^1 = \varepsilon^{(1)_1}\mathscr{E}_3, \\
&\mathscr{S}^{(1)_2} = \varepsilon^{(1)_2}\mathscr{E}^1 = \varepsilon^{(1)_2}\mathscr{E}_3, \\
&\mathscr{S}_1^{(3)_1} = \varepsilon^{(3)_1}\mathscr{E}_1^3 = \varepsilon^{(3)_1}\mathscr{E}_1, \qquad \mathscr{S}_1^{(3)_1} = \mu^{(3)_1}\mathscr{B}_1^3 = -\mu^{(3)_1}\mathscr{B}_2, \\
&\mathscr{S}_2^{(3)_1} = \varepsilon^{(3)_1}\mathscr{E}_2^3 = \varepsilon^{(3)_1}\mathscr{E}_2, \qquad \mathscr{S}_2^{(3)_1} = \mu^{(3)_1}\mathscr{B}_2^3 = \mu^{(3)_1}\mathscr{B}_1, \\
&\mathscr{S}_1^{(3)_2} = \varepsilon^{(3)_2}\mathscr{E}_1^3 = \varepsilon^{(3)_2}\mathscr{E}_1, \qquad \mathscr{S}_1^{(3)_2} = \mu^{(3)_2}\mathscr{B}_1^3 = -\mu^{(3)_2}\mathscr{B}_2, \\
&\mathscr{S}_2^{(3)_2} = \varepsilon^{(3)_2}\mathscr{E}_2^3 = \varepsilon^{(3)_2}\mathscr{E}_2, \qquad \mathscr{S}_2^{(3)_2} = \mu^{(3)_2}\mathscr{B}_2^3 = \mu^{(3)_2}\mathscr{B}_1. \qquad (6.3.51)
\end{aligned}$$

Note that each of the three electric fields $\hat{E}_1$, $\hat{E}_2$, and $\hat{E}_3$ is capable of inducing two kinds of strain described by four independent parameters in all. However, the magnetic field $\hat{B}_3$ cannot cause any strain that is linear in B_3 and only two parameters are needed to describe transverse strains. Furthermore, note that electric field $\hat{E}_2$ can cause the strain $\mathscr{S}_2^{(3)_1}$ and $\mathscr{S}_2^{(3)_2}$, while the magnetic field $\hat{B}_2$ induces the strain $-\mathscr{S}_1^{(3)_1}$ or $-\mathscr{S}_1^{(3)_2}$, and similarly for $\hat{E}_1$ and $\hat{B}_1$.

It is easy to prove that no linear striction effects can occur in cubic symmetry O or O_h. $\mathscr{E}_j$ and $\mathscr{B}_j$ can be shown to take the symmetry definitions of T_{1u} and T_{1g}, respectively, under O_h symmetry:

$$\mathscr{E}_j = \mathscr{E}_j^{T_{1u}}, \qquad \mathscr{B}_j = \mathscr{B}_j^{T_{1g}}. \qquad (6.3.52)$$

No $\mathscr{S}^{T_{1u}}$ strain exists, and there is no $\mathscr{S}^{T_{1g}}$ strain without rotations.

6.4 THEORY OF QUANTUM OPERATORS AND IRREDUCIBLE TENSORS

A common approach to physical models involves the manipulation or variation of parameters in a model operator and equation of motion. One tries to define and evaluate the most important parameters of a model in such a way that the theory gives some insight into the behavior of the system being studied. We have seen examples of parameters such as the spring constants in models of molecular vibration (cf. NH_3, UF_6, SF_6, in Chapters 3 and 4 and energy or tunneling coefficients in electronic orbital models.

Now we see how to tell exactly how many independent parameters are possible in a given model from symmetry theory and how to systematically enumerate and relate different systems of parameters. We shall do this by reviewing the general structure of operators. This will include an introduction to transition operators and selection rules and the Wigner-Eckart theorem.

A. Symmetry-Defined Operators

The mathematics of quantum mechanics reviewed in Chapter 1 revolves around sets of base vectors $\{|1\rangle,|2\rangle,\cdots|n\rangle\}$ or $\{\langle 1|,\langle 2|,\cdots\langle n|\}$ and operators $A, B, \ldots$ which transform these vectors.

As we observed in Chapter 1, all operators can be expressed as linear combinations of "elementary" or "unit" operators $e_{ij} = |i\rangle\langle j|$ made from outer products of bras and kets:

$$A = \sum_{i=1}^{n}\sum_{j=1}^{n}|i\rangle\langle i|A|j\rangle\langle j| = \sum_{i=1}^{n}\sum_{j=1}^{n}\mathscr{A}_{ij}|i\rangle\langle j|. \tag{6.4.1}$$

This is true for any basis which is complete.

In particular this is true for any symmetry-defined basis

$$\left\{\left|\begin{matrix}\alpha\\1\end{matrix}\right\rangle\left|\begin{matrix}\alpha\\2\end{matrix}\right\rangle\cdots\left|\begin{matrix}\alpha\\l^\alpha\end{matrix}\right\rangle\cdots\left|\begin{matrix}\beta\\1\end{matrix}\right\rangle\cdots\right\},$$

where the basis vectors are made to be irrep bases for a group of unitary symmetry operators $G = \{1, g, g', \ldots\}$ as follows:

$$g\left|\begin{matrix}\alpha\\k\end{matrix}\right\rangle = \sum_{i=1}^{l^\alpha}\mathscr{D}^{\alpha}_{ik}(g)\left|\begin{matrix}\alpha\\i\end{matrix}\right\rangle. \tag{6.4.2}$$

Now consider the transformation of a unit operator $\left|\begin{matrix}\alpha\\k\end{matrix}\right\rangle\left\langle\begin{matrix}\beta\\l\end{matrix}\right|$:

$$\begin{aligned}\left|\begin{matrix}\alpha\\k\end{matrix}\right\rangle\left\langle\begin{matrix}\beta\\l\end{matrix}\right| \to g\left|\begin{matrix}\alpha\\k\end{matrix}\right\rangle\left\langle\begin{matrix}\beta\\l\end{matrix}\right|g^\dagger &= g\left|\begin{matrix}\alpha\\k\end{matrix}\right\rangle\left(g\left|\begin{matrix}\beta\\l\end{matrix}\right\rangle\right)^\dagger\\ &= \sum_{i=1}^{l^\alpha}\sum_{j=1}^{l^\beta}\mathscr{D}^{\alpha}_{ik}(g)\left|\begin{matrix}\alpha\\k\end{matrix}\right\rangle\left(\mathscr{D}^{\beta}_{jl}(g)\left|\begin{matrix}\beta\\j\end{matrix}\right\rangle\right)^\dagger\\ &= \sum_{i=1}^{l^\alpha}\sum_{j=1}^{l^\beta}\mathscr{D}^{\alpha}_{ik}(g)\mathscr{D}^{\beta}_{jl}(g)^*\left|\begin{matrix}\alpha\\i\end{matrix}\right\rangle\left\langle\begin{matrix}\beta\\j\end{matrix}\right|.\end{aligned} \tag{6.4.3}$$

For real irreps $[\mathscr{D}^{\beta}_{jl}(g) = \mathscr{D}^{\beta *}_{jl}(g)]$ this last equation takes the same form as the transformation of a two-particle state. [Compare it with Eq. (6.1.7a) with $g = a = b$.] Since most multidimensional point symmetry irreps can be made real we shall assume $\mathscr{D} = \mathscr{D}^*$ for the following discussion.

In this case we can construct SYMMETRY-DEFINED UNIT OPERATORS V^γ_m by summing with coupling coefficients as follows:

$$V^\gamma_m \equiv \sum_{i=1}^{l^\alpha}\sum_{j=1}^{l^\beta}C^{\alpha\beta\gamma}_{ijm}\left|\begin{matrix}\alpha\\i\end{matrix}\right\rangle\left\langle\begin{matrix}\beta\\j\end{matrix}\right|. \tag{6.4.4}$$

According to the theory of Section 6.3.B V_m^γ will transform as follows:

$$gV_m^\gamma g^\dagger = \sum_{l=1}^{l^\gamma} \mathscr{D}_{lm}^\gamma(g) V_l^\gamma. \tag{6.4.5}$$

These operators are a complete set from which all operators can be made if the $\left|\begin{smallmatrix}\alpha\\ i\end{smallmatrix}\right\rangle\left\langle\begin{smallmatrix}\beta\\ j\end{smallmatrix}\right|$ or, before that, the $|1\rangle\langle 1|, |1\rangle\langle 2|, \ldots$ are complete. There may be two or more independent operators for each irrep label (γ), so it may be necessary to distinguish between them in some way. We use (reluctantly) another subscript and write $V_m^{(\gamma)_\omega}$. Any operator A must be a linear combination of the $V_m^{(\gamma)_\omega}$:

$$A = \sum_\gamma \sum_\omega \sum_m \mathscr{A}_m^{(\gamma)_\omega} V_m^{(\gamma)_\omega}. \tag{6.4.6}$$

Sometimes the V_m^γ are called IRREDUCIBLE TENSORIAL SETS or TENSOR OPERATORS. Their stress tensor ancestors (recall Section 6.3) are remembered in name only here.

(a) Invariant Operators Recall the Hamiltonian operators H for the octahedral orbit model in Eq. (4.3.3). H must be a linear combination of $V_m^{(\gamma)_\omega}$, where (γ) are O_h IR labels. In particular, it can only be combinations of those which have $\gamma = A_{1g}$, i.e., the *invariant* irrep since H is O_h symmetric $(gHg^\dagger = H)$:

$$H = \sum_\omega \mathscr{H}^{(A_{1g})_\omega} V^{(A_{1g})_\omega}. \tag{6.4.7}$$

Now the question is: How many independent invariant operators $V^{(A_{1g})_1}, V^{(A_{1g})_2}, \ldots$ exist in that basis? That is exactly the number of parameters $\mathscr{H}^{(A_{1g})_\omega}$ for the Hamiltonian.

According to Section 6.2.A [see Eq. (6.2.5)], just one invariant can be made from a product $\mathscr{D}^\alpha \times \mathscr{D}^\beta$ of real irreps for each $\alpha = \beta$ and none for $\alpha \neq \beta$. For the octahedral model we have $\alpha = A_{1g}, T_{1u}$, and E_g, so there are three invariants and three independent parameters.

Let us construct the first rows of these matrices using Eq. (6.2.5) and the eigenvectors from Eqs. (4.3.20), (4.3.22), (4.3.23), and (4.3.27):

$$V^{(A_{1g})_1} \equiv \left|A_{1g}\right\rangle\left\langle A_{1g}\right| \qquad \leftrightarrow \boxed{\tfrac{1}{6}\ \tfrac{1}{6}\ \tfrac{1}{6}\ \tfrac{1}{6}\ \tfrac{1}{6}\ \tfrac{1}{6}}\ , \tag{6.4.8a}$$

$$V^{(A_{1g})_2} \equiv \sum_{j=1}^{3} \left|\begin{smallmatrix}T_{1u}\\ j\end{smallmatrix}\right\rangle\left\langle\begin{smallmatrix}T_{1u}\\ j\end{smallmatrix}\right| / \sqrt{3} \leftrightarrow \boxed{\tfrac{1}{2}\ \tfrac{1}{2}\ 0\ 0\ 0\ 0}\ /\sqrt{3}\,, \tag{6.4.8b}$$

and

$$V^{(A_{1g})_3} \equiv \sum_{j=1}^{2} \left|\begin{matrix} E_g \\ j \end{matrix}\right\rangle\left\langle\begin{matrix} E_g \\ j \end{matrix}\right| /\sqrt{2} \leftrightarrow \left| \begin{matrix} \frac{1}{3} & \frac{1}{3} & \frac{1}{6} & \frac{1}{6} & \frac{1}{6} & \frac{1}{6} \end{matrix} \right| /\sqrt{2}. \quad (6.4.8c)$$

In the discussion of this physical model two parameters were used: The local energy (H) and the nearest-neighbor tunneling amplitude ($-S$). A third parameter exists since there are three invariants. In fact, we mentioned a next-nearest-neighbor tunneling amplitude ($-T$). The corresponding Hamiltonian

$$H \leftrightarrow \left| \begin{matrix} H & -T & -S & -S & -S & -S \end{matrix} \right| . \quad (6.4.9)$$

It is instructive to write H abstractedly in terms of $V^{(A_{1g})_\omega}$. This shows the relations that exist between parameters and eigenvalues in this case:

$$H = \varepsilon^{A_{1g}} V^{(A_{1g})_1} + \varepsilon^{T_{1u}}\sqrt{3}\, V^{(A_{1g})_2} + \varepsilon^{E_g}\sqrt{2}\, V^{(A_{1g})_3},$$

$$H \leftrightarrow \left| \begin{matrix} \frac{\varepsilon^{A_{1g}} + 3\varepsilon^{T_{1u}} + 2\varepsilon^{E_g}}{6} & \frac{\varepsilon^{A_{1g}} - 3\varepsilon^{T_{1u}} + 2\varepsilon^{E_g}}{6} & \frac{\varepsilon^{A_{1g}} - \varepsilon^{E_g}}{6} & \frac{\varepsilon^{A_{1g}} - \varepsilon^{E_g}}{6} & \frac{\varepsilon^{A_{1g}} - \varepsilon^{E_g}}{6} & \frac{\varepsilon^{A_{1g}} - \varepsilon^{E_g}}{6} \end{matrix} \right| \quad (6.4.10)$$

If the ε^α were given by some experiment, then comparison of Eqs. (6.4.9) and (6.4.10) would immediately give the values of parameters H, S, and T.

This is a special example of a more general theorem.

Parameter Theorem The maximum number of independent parameters for a Hermitian matrix or physical operator is exactly enough to determine all its eigenvalues and all its eigenvectors that are not already fixed by symmetry. This number n is given by

$$n = \sum_\alpha f^\alpha(f^\alpha + 1)/2 \quad (6.4.11a)$$

for a Hermitian operator or matrix, and for an arbitrary operator by

$$n = \sum_\alpha (f^\alpha)^2, \quad (6.4.11b)$$

where f^α is the frequency of irrep (α) in the basis being considered.

Proof The number of independent invariant operators in any basis is completely determined by the product analysis of the basis. Let f^α be the number of orthogonal sets of bases

$$\left\{ \left|\begin{matrix} \alpha \\ 1 \end{matrix}\right\rangle^{(1)} \left|\begin{matrix} \alpha \\ 2 \end{matrix}\right\rangle^{(1)} \cdots \left|\begin{matrix} \alpha \\ l^\alpha \end{matrix}\right\rangle^{(1)} \right\}, \left\{ \left|\begin{matrix} \alpha \\ 1 \end{matrix}\right\rangle^{(2)}, \left|\begin{matrix} \alpha \\ 2 \end{matrix}\right\rangle^{(2)}, \ldots, \left|\begin{matrix} \alpha \\ l^\alpha \end{matrix}\right\rangle^{(2)} \right\}, \ldots, \left\{ \left|\begin{matrix} \alpha \\ 1 \end{matrix}\right\rangle^{(f^\alpha)}, \ldots \right\}$$

that transform according to irrep (α). Using these, we may construct exactly

$(f^\alpha)^2$ invariants

$$V^{(\alpha)_{\omega\phi}} \equiv \sum_{j=1}^{l^\alpha} \left|\begin{matrix}\alpha \\ j\end{matrix}\right\rangle^{(\omega)(\phi)} \left\langle\begin{matrix}\alpha \\ j\end{matrix}\right| / \sqrt{l^\alpha}$$

and a general invariant operator I must be expressible in terms of just these, using $(f^\alpha)^2$ coefficients $\mathcal{I}^{(\alpha)}_{\omega\phi}$:

$$I \equiv \sum_\alpha \sum_\omega \sum_\phi \mathcal{I}^{(\alpha)}_{\omega\phi} V^{(\alpha)_{\omega\phi}}.$$

If I is Hermitian $(\mathcal{I}^{(\alpha)}_{\omega\phi} = (\mathcal{I}^{(\alpha)}_{\phi\omega})^*)$ then the number of parameters is reduced to $f^\alpha(f^\alpha + 1)/2$. In this case, the $\mathcal{I}^{(\alpha)}_{\omega\phi}$ determine the eigenvectors not fixed by symmetry and vice versa.

The UF_6, SF_6, ... molecular vibration models are examples of parameter treatments. One obtains fair results using two or three parameters j, k, and b by making physical pictures involving special arrangements of springs. However, the real molecule is held together by electrons and electrostatic forces instead of springs so it is a wonder that the spring model is even close.

It is instructive to derive the maximum number of parameters for any SF_6 model that uses the same basis. From Eq. (6.4.11a) the SF_6 result is $1 + 1 + 3 + 1 + 1 = 7$. Now one could go looking for other places to stick four more springs in SF_6, but this leads to an empty victory. There are better ways to approach the problem. A generalization of the parameter analysis in Eqs. (6.4.9) and (6.4.10) will be employed later.

(b) Noninvariant Operators If a basis is n dimensional, there are $n(n + 1)/2$ independent Hermitian operators that transform the basis into itself. The preceding section accounted for the invariant operators. Now, the other operators must be labeled by noninvariant irreps if they are going to be defined by symmetry. For example, the six-dimensional octahedron basis will have 21 operators, 18 of which belong to some irrep besides A_{1g}.

Electric multipole operators are examples of noninvariant tensor operators. Suppose the effect of an electromagnetic wave on the energy of a charge (q) orbiting at position $\mathbf{x}$ is given by

$$V = q\mathbf{E}(\mathbf{x}, t) \cdot \mathbf{x} = q(E_1x_1 + E_2x_2 + E_3x_3)e^{i(k\cdot\mathbf{x}-\omega t)}, \quad (6.4.12)$$

where x_1, x_2, and x_3 are quantum position operators for the x, y, and z coordinates. The effects of the *magnetic* field on the *momentum* of the particle will be neglected here. Expanding the exponential gives the following:

$$\begin{aligned} V &= qe^{-i\omega t}\sum_j E_jx_j\left(1 + i\mathbf{k}\cdot\mathbf{x} - \tfrac{1}{2}(\mathbf{k}\cdot\mathbf{x})^2 + \cdots\right) \\ &= qe^{-i\omega t}\left(\sum_j E_jx_j + i\sum_i\sum_j k_iE_jx_ix_j - \tfrac{1}{2}\sum_i\sum_j\sum_k k_ik_jE_kx_ix_jx_k + \cdots\right). \end{aligned} \quad (6.4.13)$$

If the wavelength $\lambda = 2\pi/k$ is long compared to the excursion $\langle x_j \rangle$ of the particle, then terms involving products of k and x_j may be neglected. This leaves only the first terms of V such as

$$V_j^{T_{1u}} \equiv qe^{-i\omega t}E_j x_j, \tag{6.4.14}$$

which transforms like coordinate x_j, i.e., as $T_{1u} - (j)$. Such operators are called ELECTRIC DIPOLE operators. The dipole operator $V_j^{T_{1u}}$ expresses the effect of a j-polarized electric wave of very long wavelength. The assumption of long wavelength corresponds to the DIPOLE APPROXIMATION. Long ocean waves would make a raft bob up and down, but would have no tendency to tip or bend it in the dipole approximation. The raft could not detect the direction of slope and propagation or curvature of waves that are much longer than it is.

Terms which tend to tip the raft are like the second terms in Eq. (6.4.13) and are called QUADRUPOLE terms. The transformation behavior of $x_i x_j$ operators are those of a second-rank tensor. The O_h-defined second-rank tensor operators belong to irreps A_{1g}, E_g, T_{1g}, and T_{2g}, as explained in Section 6.3.B. The third-rank OCTAPOLE terms $x_i x_j x_k$ would belong to A_{1u}, A_{2u}, E_u, T_{1u}, and T_{2u} irreps of O_h.

Now we see how to quickly evaluate the effect of various types of irreducible tensor operators on a quantum system.

B. Wigner-Eckart Theorem and Transition Selection Rules

A powerful theorem relates tensor operator matrix elements for different components or polarizations. First we prove and explain the theorem, and then we apply it using the dipole moment in the octahedron as an example.

Wigner-Eckart Theorem If operator T_i^α belongs to a set $\{T_1^\alpha T_2^\alpha \cdots T_{l^\alpha}^\alpha\}$ which transform according to an irrep of symmetry group $G = \{1, g, g', \ldots\}$ as follows:

$$gT_i^\alpha g^\dagger = \sum_{i'} T_{i'}^\alpha \mathscr{D}_{i'i}(g)$$

then the matrix elements between irrep bases will all be of the following form:

$$\left\langle \begin{matrix} \gamma \\ k \end{matrix} \middle| T_i^\alpha \middle| \begin{matrix} \beta \\ j \end{matrix} \right\rangle = \sum_\omega \mathscr{C}_{ijk}^{\alpha\beta(\gamma)_\omega} \langle \gamma | \, |T^\alpha| \, |\beta\rangle_\omega, \tag{6.4.15a}$$

where the $\mathscr{C}_{ijk}^{\alpha\beta(\gamma)_\omega}$ are coupling coefficients and the constant $\langle \gamma | \, |T^\alpha| \, |\beta\rangle_\omega$ is independent of the components i, j, or k.

Proof First insert the operator $1 = g^\dagger g$ in the matrix element and expand the result according to the assumed transformation properties:

$$\left\langle \begin{matrix} \gamma \\ k \end{matrix} \middle| T_i^\alpha \middle| \begin{matrix} \beta \\ j \end{matrix} \right\rangle = \left\langle \begin{matrix} \gamma \\ k \end{matrix} \middle| g^\dagger g T_i^\alpha g^\dagger g \middle| \begin{matrix} \beta \\ j \end{matrix} \right\rangle$$

$$= \sum_{k'} \sum_{i'} \sum_{j'} \mathscr{D}^\gamma_{k'k}(g)^* \mathscr{D}^\alpha_{i'i}(g) \mathscr{D}^\beta_{j'j}(g) \left\langle \begin{matrix} \gamma \\ k' \end{matrix} \middle| T_{i'}^\alpha \middle| \begin{matrix} \beta \\ j' \end{matrix} \right\rangle.$$

One may sum over all group elements without affecting the left side, if we divide by ${}^oG$ and use Eq. (6.2.15):

$$\left\langle \begin{matrix} \gamma \\ k \end{matrix} \middle| T_i^\alpha \middle| \begin{matrix} \beta \\ j \end{matrix} \right\rangle = \sum_{k'} \sum_{i'} \sum_{j'} \left(1/{}^oG \sum_g \mathscr{D}^\gamma_{k'k}(g)^* \mathscr{D}^\alpha_{i'i}(g) \mathscr{D}^\beta_{j'j}(g) \right) \left\langle \begin{matrix} \gamma \\ k' \end{matrix} \middle| T_{i'}^\alpha \middle| \begin{matrix} \beta \\ j' \end{matrix} \right\rangle$$

$$= \sum_\omega \mathscr{C}^{\alpha\beta(\gamma)_\omega}_{ijk} \left[(1/l^\alpha) \sum_{i'} \sum_{j'} \sum_{k'} \mathscr{C}^{\alpha\beta(\gamma)_\omega}_{i'j'k'} \left\langle \begin{matrix} \gamma \\ k' \end{matrix} \middle| T_{i'}^\alpha \middle| \begin{matrix} \beta \\ j' \end{matrix} \right\rangle \right].$$

The theorem is proved since the bracketed term is not a function of the components.

$$\langle \gamma | \, | T^\alpha | \, | \beta \rangle_\omega \equiv \left[(1/l^\alpha) \sum_{i'} \sum_{j'} \sum_{k'} \mathscr{C}^{\alpha\beta(\gamma)_\omega}_{i'j'k'} \left\langle \begin{matrix} \gamma \\ k' \end{matrix} \middle| T_{i'}^\alpha \middle| \begin{matrix} \beta \\ j' \end{matrix} \right\rangle \right]. \quad (6.4.15b)$$

The constants $\langle \gamma | \, | T^\alpha | \, | \beta \rangle_\omega$ in Eq. (6.4.15a) or (6.4.15b) are usually called REDUCED MATRIX ELEMENTS. They are the "parameters" of the α-tensor operators. For groups with nonsimply reducible products the repetition index (ω) needs to be attached, and the matrix elements are combinations of parameters belonging to different (ω). However, for most of the symmetry groups we will be studying (ω) can be deleted from Eqs. (6.4.15). Then the matrix elements for different polarizations are all simply proportional to one reduced matrix element $\langle \gamma | \, | T^\alpha | \, | \beta \rangle$ for each α transition between manifold $\{\ldots, |{}^\beta_j\rangle, \ldots\}$ and $\{\ldots, |{}^\gamma_k\rangle, \ldots\}$. The proportionality factors are just the coupling coefficients $\mathscr{C}^{\alpha\beta\gamma}_{ijk}$ in each transition $\left| \begin{matrix} \beta \\ j \end{matrix} \right\rangle \leftrightarrow \left| \begin{matrix} \gamma \\ k \end{matrix} \right\rangle$ induced by (ith) polarization component T_i^α.

The Wigner-Eckart theorem provides a way to factor a matrix element into a geometrical part and a physical part. The coupling coefficient is the geometrical part and for it one only needs to know the group transformation properties of the states and transition operator. The reduced matrix element is the physical part and to evaluate it one needs more detailed knowledge of states and operator. The theorem allows one to still make certain predictions when detailed physical knowledge is lacking.

As an example, let us apply the Wigner-Eckart theorem to evaluate electric-dipole ($V_i^{T_{1u}}$) transition rates between the A_{1g}, T_{1u}, and E_g orbital states of the octahedral tunneling eigenstates in Figure 4.3.2(b). The matrix elements are given by

$$\left\langle \begin{matrix} \gamma \\ k \end{matrix} \middle| V_i^{T_{1u}} \middle| \begin{matrix} \beta \\ j \end{matrix} \right\rangle = C_{ijk}^{T_{1u}\beta\gamma} \langle \gamma | \, | V^{T_{1u}} | \, | \beta \rangle. \tag{6.4.16}$$

The squares $\left| \left\langle \begin{matrix} \gamma \\ k \end{matrix} \middle| V_i^{T_{1u}} \middle| \begin{matrix} \beta \\ j \end{matrix} \right\rangle \right|^2$ of the matrix elements are proportional to the probability of absorption of light or intensity of emission according to Fermi's Golden Rule. (This will be treated in Chapter 8 Section 6.)

The first thing to notice is that all dipole or (T_{1u}) transitions are FORBIDDEN between the levels A_{1g} and E_g, since $C_{ijk}^{T_{1u}E_gA_{1g}}$ is identically zero. This is an example of a SELECTION RULE. Remember that a product $u \otimes g$ always gives u states and never g. However, this particular matrix element would be zero even if the transition operator was a *magnetic* dipole ($V_i^{T_{1g}}$) with even (g) parity since the product $T_1 \otimes E$ does not contain A_1. The next possible avenue for an ($E_g \leftrightarrow A_{1g}$) transition is by a quadrupole operator ($V_i^{E_g}$). Note that ($E_g \leftrightarrow E_g$) and ($T_{1u} \leftrightarrow T_{1u}$) transitions are electric-dipole forbidden, also.

The ($A_{1g} \leftrightarrow T_{1u}$) and ($T_{1u} \leftrightarrow E_g$) transitions are electric-dipole allowed, however. The Wigner-Eckart theorem gives the matrix elements for all possibilities in terms of two reduced matrix elements $\langle T_1 | \, | T_1 | \, | E \rangle$ and $\langle T_1 | \, | T_1 | \, | A_1 \rangle$. All the combinations are given in the following. The O_h coupling coefficients in the Appendix F.3.1d are used.

$$\left\langle \begin{matrix} T_1 \\ 1 \end{matrix} \middle| V_1^{T_1} \middle| \begin{matrix} E \\ 1 \end{matrix} \right\rangle = -\frac{1}{2} \langle T_1 | \, | T_1 | \, | E \rangle, \qquad \left\langle \begin{matrix} T_1 \\ 2 \end{matrix} \middle| V_2^{T_1} \middle| \begin{matrix} E \\ 1 \end{matrix} \right\rangle = -\frac{1}{2} \langle T_1 | \, | T_1 | \, | E \rangle,$$

$$\left\langle \begin{matrix} T_1 \\ 3 \end{matrix} \middle| V_3^{T_1} \middle| \begin{matrix} E \\ 1 \end{matrix} \right\rangle = \langle T_1 | \, | T_1 | \, | E \rangle,$$

$$\left\langle \begin{matrix} T_1 \\ 1 \end{matrix} \middle| V_1^{T_1} \middle| \begin{matrix} E \\ 2 \end{matrix} \right\rangle = \frac{\sqrt{3}}{2} \langle T_1 | \, | T_1 | \, | E \rangle, \qquad \left\langle \begin{matrix} T_1 \\ 2 \end{matrix} \middle| V_2^{T_1} \middle| \begin{matrix} E \\ 2 \end{matrix} \right\rangle = -\frac{\sqrt{3}}{2} \langle T_1 | \, | T_1 | \, | E \rangle,$$

$$\left\langle \begin{matrix} T_1 \\ 3 \end{matrix} \middle| V_3^{T_1} \middle| \begin{matrix} E \\ 2 \end{matrix} \right\rangle = 0,$$

$$\left\langle \begin{matrix} T_1 \\ 1 \end{matrix} \middle| V_1^{T_1} \middle| A_1 \right\rangle = \langle T_1 | \, | T_1 | \, | A_1 \rangle, \qquad \left\langle \begin{matrix} T_1 \\ 2 \end{matrix} \middle| V_2^{T_1} \middle| A_1 \right\rangle = \langle T_1 | \, | T_1 | \, | A_1 \rangle,$$

$$\left\langle \begin{matrix} T_1 \\ 3 \end{matrix} \middle| V_3^{T_1} \middle| A_1 \right\rangle = \langle T_1 | \, | T_1 | \, | A_1 \rangle. \tag{6.4.17}$$

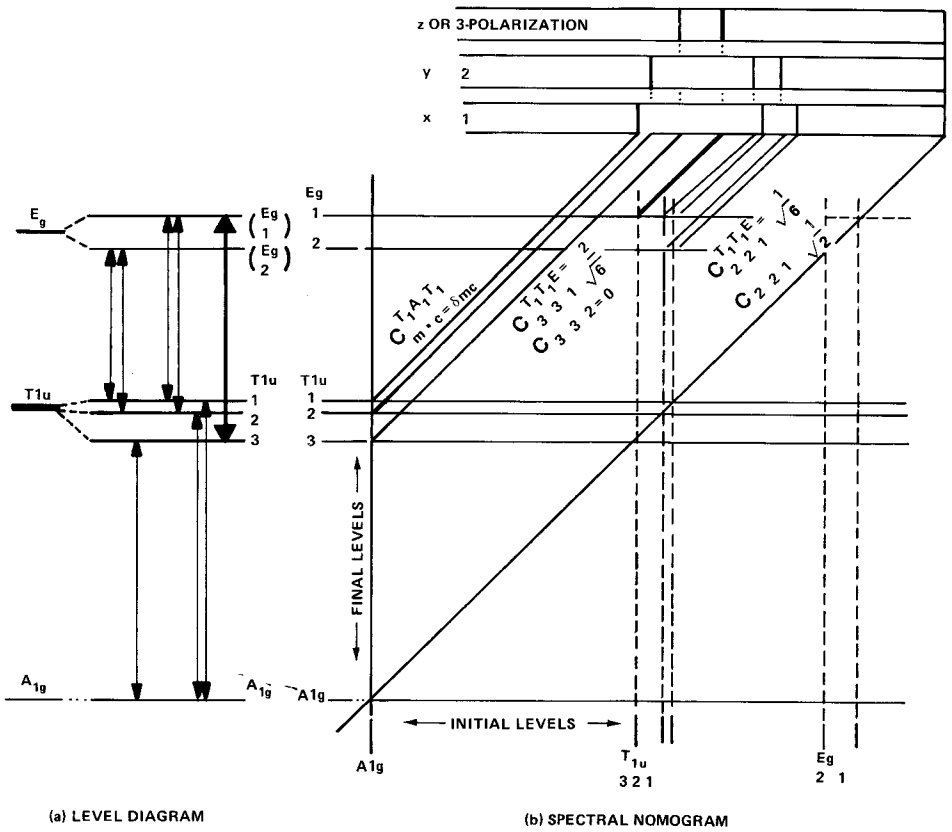

Figure 6.4.1 Intracluster transitions predicted by Wigner-Eckart theorem. (a) Level diagram. Transitions are indicated by arrows drawn between levels. (b) Spectral nomogram. Spectra are indicated by lines drawn at 45° from each intersection that represents an allowed transition.

In the $(T_{1u} \leftrightarrow E_g)$ transition one predicts an intensity ratio of $|1/2|^2 : |\sqrt{3}/2|^2 = 1:3$ between the $\begin{pmatrix} E_{1g} \\ 1 \end{pmatrix}$ and $\begin{pmatrix} E_{1g} \\ 2 \end{pmatrix}$ levels, respectively, using polarization 1 or 2 and a ratio of $1:0$ using polarization 3. In order for a spectroscopist to observe such intensity ratios it would be necessary to partially split the E_g and T_{1u} degeneracies as indicated on the left-hand side of Figure 6.4.1. This could be done using some external perturbation such as a weak Q field as discussed in Section 4.3.D. (Recall the splitting indicated near the center of Figure 4.3.5.) It is very important to polarize or otherwise prepare the octahedral system by some external means. It will not make any difference which polarization component $V_1^{T_1}$, $V_2^{T_1}$, or $V_3^{T_1}$ causes the $(T_{1u} \leftrightarrow E_g)$ transition if one cannot distinguish the three substates $\left|\begin{matrix} T_{1u} \\ 1 \end{matrix}\right\rangle$, $\left|\begin{matrix} T_{1u} \\ 2 \end{matrix}\right\rangle$, or $\left|\begin{matrix} T_{1u} \\ 3 \end{matrix}\right\rangle$

within the T_{1u} manifold or the two substates $\left|\begin{matrix}E_g\\1\end{matrix}\right\rangle$ and $\left|\begin{matrix}E_g\\2\end{matrix}\right\rangle$ within the E_g manifold. The detailed Wigner-Eckart intensity predictions are useless unless the system is oriented somehow with respect to the polarization of the dipole field causing the transition.

In case the system is polarized one would obtain a very different spectrum from 3-polarized light than from 1- or 2-polarized light. This is indicated by the 1, 2, and 3 bands of spectral lines shown in the upper portion of Figure 6.4.1. The *lines* are obtained from the *levels* according to geometrical nomogram drawn below in the central portion of the figure. Here the final levels are plotted along the x axis and are extended by lines parallel to the y axis. The final levels are plotted along the y axis and extended by lines parallel to the x axis. (This trick is useful even if the manifold of final levels is completely different from the initial ones.) Whenever an initial level intersects a final level of higher (lower) energy that represents a possible absorption (emission) transition. If the transition is allowed the spectral line is located by a 45° line drawn upward and to the right from that point. The parallel displacement of the 45° lines is proportional to the *difference* between levels and hence models the spectrum.

In this way the $(A_{1g} \rightarrow T_{1u})$ and $(T_{1u} \rightarrow E_g)$ absorption spectra are drawn in Figure 6.4.1. The leftmost lines belong to the $(A_{1g} \rightarrow T_{1u})$ absorption. The others belong to various allowed $(T_{1u} \rightarrow E_g)$ transitions with darker lines indicating larger $\mathscr{C}_{ijk}^{T_{1u}T_{1u}E_g}$ coefficients and greater intensity I where

$$I_i\begin{pmatrix}T_{1u}\\j\end{pmatrix} \rightarrow \begin{pmatrix}E_g\\k\end{pmatrix} \sim \left(\mathscr{C}_{ijk}^{T_{1u}T_{1u}E_g}\langle E| \,|T_1|\, |T_1\rangle\right)^2. \tag{6.4.18}$$

Note that if the $\left|\begin{matrix}T_{1u}\\1\end{matrix}\right\rangle$ and $\left|\begin{matrix}T_{1u}\\2\end{matrix}\right\rangle$ levels become degenerate then the 1- and 2-polarization spectral patterns become indistinguishable. Finally, if the $\left|\begin{matrix}T_{1u}\\3\end{matrix}\right\rangle$ level joins the other T_{1u} pair and the splitting of E_g is zero then all three polarizations look the same. Each spectrum will have two lines with intensity ratios given by

$$I(A_{1g} \rightarrow T_{1u})/I(T_{1u} \rightarrow E_g) = \left(\langle T_1| \,|T_1|\, |A_1\rangle / \langle T_1| \,|T_1|\, |E\rangle\right)^2, \tag{6.4.19}$$

and the Wigner-Eckart theorem predicts nothing of the detail. In the next chapter there will be situations in which symmetry analysis can be used to evaluate reduced matrix elements. However, the reduced matrix elements in Eq. (6.4.19) are simply undetermined physical parameters in this example.

Note that individual intensities such as given by Eq. (6.4.18) may not agree with the spectral experiment if too much splitting is present. As shown in

Section 4.3.D a large Q splitting mixes the $\left|\begin{matrix}E_g\\1\end{matrix}\right\rangle$ and $\left|\begin{matrix}A_{1g}\\\cdot\end{matrix}\right\rangle$ states. When this occurs one says that one line "borrows" intensity from another. The effect of changing Q on the 3-spectrum would be a change of relative intensity as well as position. As the $\left|\begin{matrix}E_g\\1\end{matrix}\right\rangle$ picked up more or less $|A_{1g}\rangle$ the intensity of the transition $\left[\left|\begin{matrix}T_{1u}\\3\end{matrix}\right\rangle \rightarrow \left|\begin{matrix}E_g\ (\text{modified})\\1\end{matrix}\right\rangle\right]$ would depend on the square of the matrix element

$$\left\langle \begin{matrix}T_{1u}\\3\end{matrix}\middle|V_3^{T_{1u}}\middle|\begin{matrix}E_g\ (\text{modified})\\1\end{matrix}\right\rangle = \varepsilon\left\langle \begin{matrix}T_{1u}\\3\end{matrix}\middle|V_3^{T_{1u}}\middle|\begin{matrix}E_g\\1\end{matrix}\right\rangle + \alpha\left\langle \begin{matrix}T_{1u}\\3\end{matrix}\middle|V_3^{T_{1u}}\middle|A_{1g}\right\rangle$$

$$= \varepsilon\langle T_1|\,|T_1|\,|E\rangle + \alpha\langle T_1|\,|T_1|\,|A\rangle,$$

where α is the mixing amplitude of the $|A_{1g}\rangle$ and $|\varepsilon|^2 = 1 - |\alpha|^2$. In this way the two large induced dipole moments can interfere.

One should try to get a qualitative physical picture of the significance of a matrix element whenever possible. For example, the fact that the pair of states $\left|\begin{matrix}E_g\\1\end{matrix}\right\rangle$ and $\left|\begin{matrix}T_{1u}\\3\end{matrix}\right\rangle$ would have a large matrix element of the dipole operator $V_3^{T_{1u}}$ implies that their mixture $\alpha\left|\begin{matrix}E_g\\1\end{matrix}\right\rangle + \beta\left|\begin{matrix}T_{1u}\\3\end{matrix}\right\rangle$ corresponds to large charge displacement or dipole moment in the 3-direction as shown in Figure 6.4.2. Indeed, if the two states have different phases in time, say $e^{i\omega_{E_g}t}$ and $e^{i\omega_{T_{1u}}t}$, this dipole moment will oscillate with angular frequency $(\omega_{E_g} - \omega_{T_{1u}})$, and radiate or absorb accordingly. In the following section we discuss the significance of oscillating dipoles in some detail.

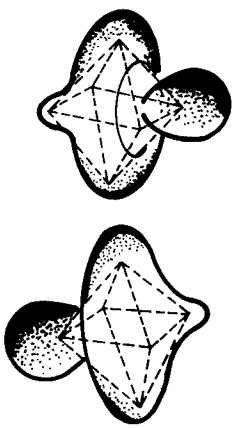

Figure 6.4.2 Sketch of time behavior of wave function for mixture of $\left|\begin{matrix}E_g\\1\end{matrix}\right\rangle$ and $\left|\begin{matrix}T_{1u}\\3\end{matrix}\right\rangle$.

6.5 CLASSICAL APPROACH TO OPTICAL RESONANCE AND SELECTION RULES

We consider now the classical theory of resonance and its application to optical spectroscopy. Resonance may very well be the single most important phenomenon involved in the observation and study of our immediate physical world. Without it we might all be blind, deaf, and dumb, since seeing, hearing, and speaking all involve resonant transfer of energy containing high-quality (i.e., coherent) signals and information. Most physical stimuli in nature are very weak and need to be amplified in order to cause observable responses. Resonance provides a way for a weak stimulus to cause a relatively large response.

Spectroscopic lines or peaks all involve some form of resonance. To understand many types of spectroscopy it is sufficient to know just the classical theory of spectroscopic resonance as developed by Lorentz and others in the late 1800s. In any case classical resonance and radiation theory is a very important prerequisite to the understanding of semiclassical and quantum theory of resonance, which will be taken up in Chapter 8, Section 8.6B. In view of the importance of classical resonance theory, it is surprising how little coverage it receives in many physics or chemical physics texts, particularly the beginning ones. Here we shall try to make up for this.

This section will include an introduction to concepts of polarization, polarizability, susceptibility, absorption, and indices of refraction. A review of some graphical aids such as phasors (first discussed in Sections 2.3.B, 2.6, and 2.7), Smith charts, and Feynman's radiation lever will be introduced. Two well-known forms of spectroscopy, (1) infrared or optical absorption, and (2) Raman spectroscopy, will be discussed in this section. Physical interpretations of infrared and Raman selection rules will be given along with the group-theoretical methods of derivation.

A. Introduction to the Effect of Light on Matter

The Lorentz theory was based on a simple model for an atom or molecule. In this model electrons are imagined to be bound to more massive nuclei in such a way that they behave like harmonic oscillators with certain natural frequencies $\{\omega_0\omega_0' \cdots\}$. The small mass of the electron ($\mu_e = 9.1 \times 10^{-31}$ kg) compared to that of the nuclei (a single proton has a mass of $M_p \cong 1836\mu_e \cong 6\pi^5\mu_e$) means that electrons would usually respond more easily to an externally applied electric field than the nuclei. The electronic charge of $q = e = -1.6 \times 10^{-19}$ coulomb is equal but opposite to that of the proton, so that the electric forces $\mathbf{F} = q\mathbf{E}$ would be of the same magnitude.

One should keep in mind how large is the so-called "tiny" charge of an electron or proton. A mole of an element with atomic number $Z(= 1 - 103)$ has N_0Z electrons where $N_0 = 6.02 \times 10^{23}$ is Avogadro's number. This amounts to nearly -10^5Z coulombs of electronic charge often confined to

within a few cubic centimeters. According to Coulomb's law the force ($F = qq'/(4\pi\varepsilon_0 r^2)$) or energy ($V = qq'/(4\pi\varepsilon_0 r)$) between a pair of charges of just 1 coulomb each separated by one meter is about nine billion newtons or joules, respectively! ($1/4\pi\varepsilon_0 = 9.0 \times 10^9$ Nm^2/C^2.) This explains why so much energy can arise if atomic ions of the same charge are formed with separations of a few angstroms ($r \simeq 1$ Å $= 10^{-10}$ m) or (much worse!) if nuclei split into parts that are separated by a few Fermis or femtometers ($r \simeq 1$ F $= 10^{-15}$ m). The atomic bomb is really an electric bomb!

Optical resonance provides a way to excite the negative or electronic part of the enormous charge that resides in atoms and molecules. Many of the hues we see in nature involve resonantly excited electrons in molecules that reside in the objects as well as in our retinas. On the other hand, infrared or microwave resonance allows one to "see" nuclear vibrational or rotational excitations using other kinds of detectors.

The Lorentz model for resonance assumes that an electron's spatial coordinate x obeys a forced damped harmonic oscillator equation of the form

$$\ddot{x} + 2\Gamma\dot{x} + \omega_0^2 x = (q/\mu)E(\mathbf{r}, t), \tag{6.5.1}$$

where ω_0 represents a natural oscillation frequency, Γ is a phenomenological decay constant, and the radiation stimulus is represented by the time-dependent acceleration $(q/\mu)E(\mathbf{r}, t)$ of an electric field $\mathbf{E}$ on a charge q and mass μ. It will be shown in Section 8.4c that the Lorentz oscillator model agrees with the quantum theory for small oscillations of x. It worked very well until the laser was invented and oscillations with much greater amplitudes could be excited.

In discussing the solutions of (6.5.1) it is helpful to consider a monochromatic stimulus, i.e., an E field oscillating at one frequency ω_s. It is also convenient to represent oscillating quantities by complex numbers or phasors. The stimulating field will be written

$$E(t) = E_0 e^{-i\omega_s t + i\phi}. \tag{6.5.2}$$

One first considers the solutions to the zero-field or homogeneous equation (6.5.1) by substituting the trial expression

$$x_T = ae^{-i(\omega t - \alpha)} \tag{6.5.3}$$

into (6.5.1) with ($E = 0$). Solving the resulting equation,

$$\left(-\omega^2 - 2i\Gamma\omega + \omega_0^2\right)\alpha e^{-i(\omega t - \alpha)} = 0,$$

yields

$$\omega = -i\Gamma + \left(\omega_0^2 - \Gamma^2\right)^{1/2} \equiv -i\Gamma + \omega_\Gamma$$

and

$$x_T = ae^{-\Gamma t}e^{-i(\omega_\Gamma t-\alpha)}. \tag{6.5.4}$$

This is called the transient part of the solution since the damping factor $e^{-\Gamma t}$ will eventually kill it off if $\Gamma > 0$.

The other part of the solution is called the inhomogeneous or steady-state response. Substituting

$$x_S = Re^{-i(\omega_s t-\rho)} \tag{6.5.5a}$$

into (6.5.1) with (6.5.2) yields

$$Re^{i\rho}\left(-\omega_s^2 - i2\Gamma\omega_s + \omega_0^2\right)e^{-i\omega_s t} = (q/\mu)E_0e^{-i\omega_s t+i\phi}. \tag{6.5.5b}$$

Solving this gives the complex response function

$$Re^{i\rho} = \frac{(q/\mu)E_0e^{i\phi}}{\omega_0^2 - \omega_s^2 - i2\Gamma\omega_s}. \tag{6.5.5c}$$

The response function can be written in Cartesian $(x + iy)$ form

$$Re^{i(\rho-\phi)} = \frac{(q/\mu)E_0\left(\omega_0^2 - \omega_s^2\right)}{\left(\omega_0^2 - \omega_s^2\right)^2 + (2\Gamma\omega_s)^2} + i\frac{(q/\mu)E_0(2\Gamma\omega_s)}{\left(\omega_0^2 - \omega_s^2\right)^2 + (2\Gamma\omega_s)^2}, \tag{6.5.5d}$$

or in the original polar form, where

$$R = \frac{(q/\mu)E_0}{\left[\left(\omega_0^2 - \omega_s^2\right)^2 + (2\Gamma\omega_s)^2\right]^{1/2}} \tag{6.5.5e}$$

and

$$\rho = \tan^{-1}\frac{2\Gamma\omega_s}{\omega_0^2 - \omega_s^2} + \phi \tag{6.5.5f}$$

are the magnitudes and phase lags, respectively, of the response function $Re^{i\rho}$. The general complex solution takes the form

$$\begin{aligned} x(t) &= x_S(t) + x_T(t) \\ &= ae^{-\Gamma t}e^{-i(\omega_\Gamma t-\alpha)} + Re^{-i(\omega_s t-\rho)}, \end{aligned} \tag{6.5.6}$$

where the transient amplitude a and phase lag α depend upon the initial conditions $x = \mathrm{Re}(x(0))$ and $v_0 = \mathrm{Re}(\dot{x}(0))$. It should be remembered [recall Section 2.3(B)] that only the real part $(\mathrm{Re}(x))$ of the complex coordinate

represents the real physical position. The same applies to complex velocity and force.

Setting ($t = 0$) in the real part of (6.5.6) and its derivative gives

$$x_0 = a\cos\alpha + R\cos\rho,$$
$$v_0 = a(\omega_\Gamma \sin\alpha - \Gamma\cos\alpha) + R\omega_s \sin\rho.$$

Solving for a and α gives the transient amplitude

$$\begin{aligned} a &= (x_0 - R\cos\rho)/\cos\alpha \\ &= -R\cos\rho/\cos\alpha \qquad (\text{for } x_0 = 0 = v_0) \end{aligned} \tag{6.5.7}$$

and phase lag

$$\begin{aligned} \alpha &= \tan^{-1}\left[\frac{(v_0 - R\omega_s\sin\rho)}{(x_0 - R\cos\rho)\omega_\Gamma} + \frac{\Gamma}{\omega_\Gamma}\right] \\ &= \tan^{-1}\left[\frac{\omega_s\sin\rho}{\omega_\Gamma\cos\rho} + \frac{\Gamma}{\omega_\Gamma}\right] \qquad (\text{for } x_0 = 0 = v_0). \end{aligned} \tag{6.5.8}$$

Figure 6.5.1 shows plots of the response (6.5.6) of an initially cold oscillator ($x_0 = 0 = v_0$) to a ($\cos\omega_s t$) stimulus turned on at $t = 0$. The oscillator parameters are $\Gamma = 0.5\ \text{s}^{-1}$, $\omega_0 = 10\pi$, and ω_s is set at (a) $8\ \pi$, (b) 9π, (c) 9.8π, (d) 10π, (e) 10.5π, and (f) $12\ \pi$. The first six or so seconds of each plot shows one or more "beats" (recall also Figure 2.3.2), which occur with a frequency equal to the difference $(\omega_0 - \omega_s)/2\pi$ between the interfering natural and stimulating frequencies. This interference is called transient behavior and it is analogous to "quantum beats" which occur in quantum excitations, as will be discussed in Chapter 8.

Lorentz theory is generally concerned with steady-state oscillator behavior after the transient amplitude $ae^{-\Gamma t}$ has died off. In Figure 6.5.1 $e^{-\Gamma t}$ decays to less than 5% ($e^{-3} = 0.05$) after $t = 6$ s. Then the steady-state response x_s, which has the same frequency (ω_s) as the stimulus, is all that remains after the natural frequency (ω_0) part dies away. The magnitude R and relative phase ρ of the responding oscillator coordinate x_S is of prime importance for Lorentz theory.

In particular we know that the stimulating force transfers the maximum power to the oscillator when the phase ρ of x_S is 90° behind the stimulus. This was explained in Section 2.3.A. According to (6.5.5f) this occurs when $\omega_s = \omega_0$, i.e., when the stimulus is exactly in resonance with the oscillator. This is the point where the real part of the response function (6.5.5d) changes sign as shown in Figure 6.5.2(a) and the imaginary part (Figure 6.5.2(b)) is near its maximum value. For a stimulus frequency below resonance ($\omega_s < \omega_0$) the response is almost in phase or only lagging slightly

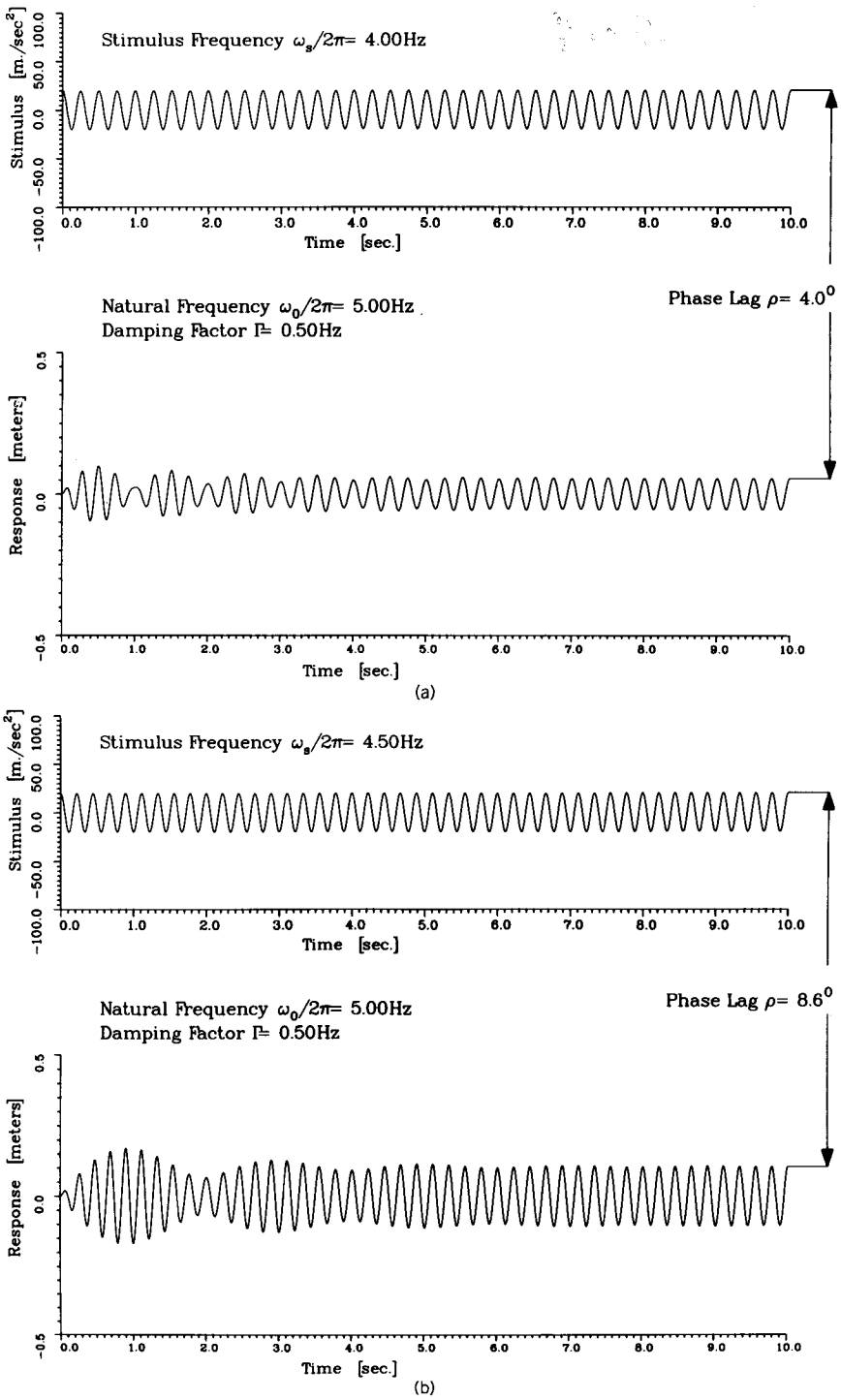

Figure 6.5.1 Time plots of stimulus and response of oscillator for various values of the stimulus frequency. (a)–(c) Below resonance; (d) resonance; (e) and (f) above resonance.

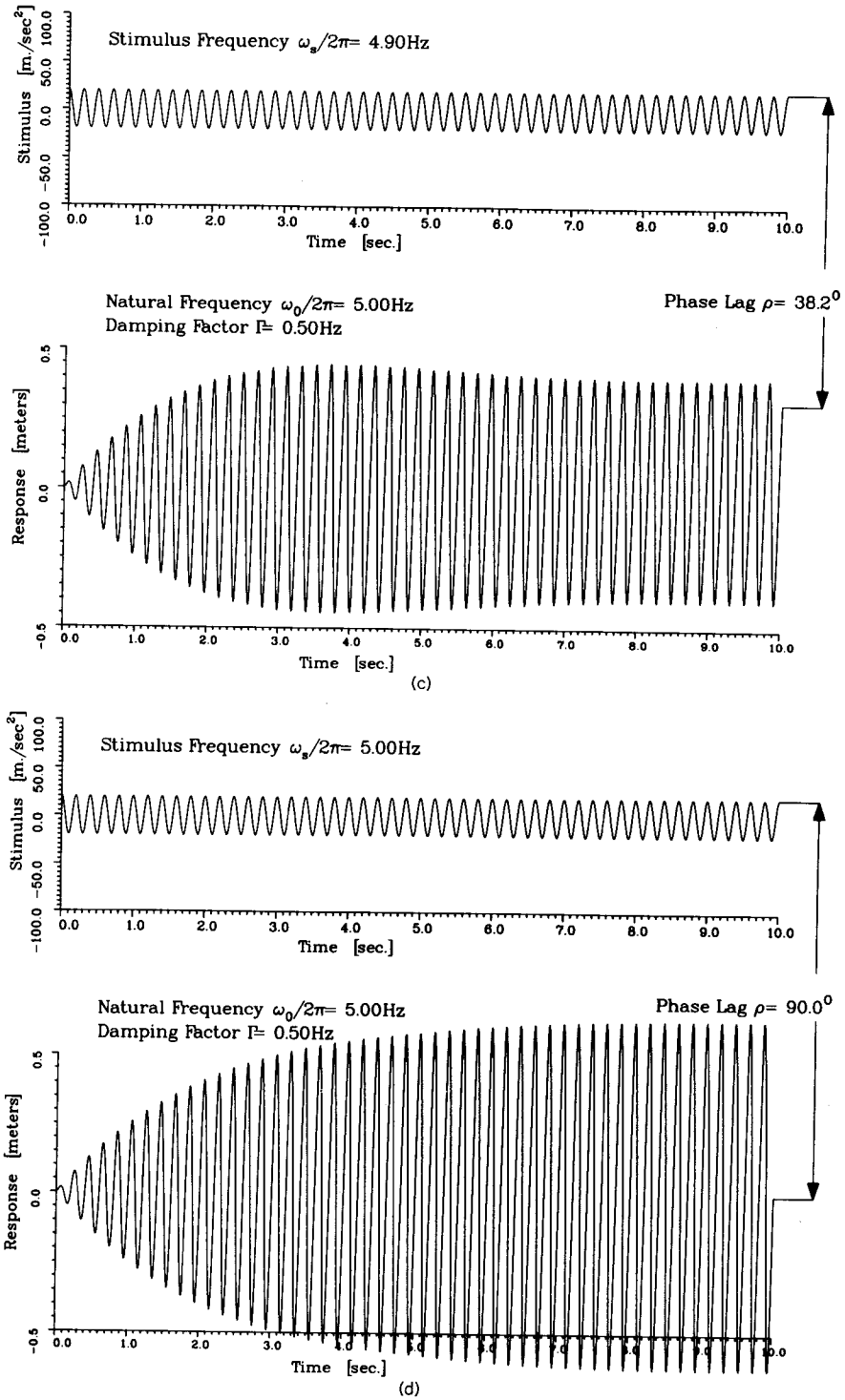

Figure 6.5.1 Time plots of stimulus and response of oscillator for various values of the stimulus frequency *(Continued)*.

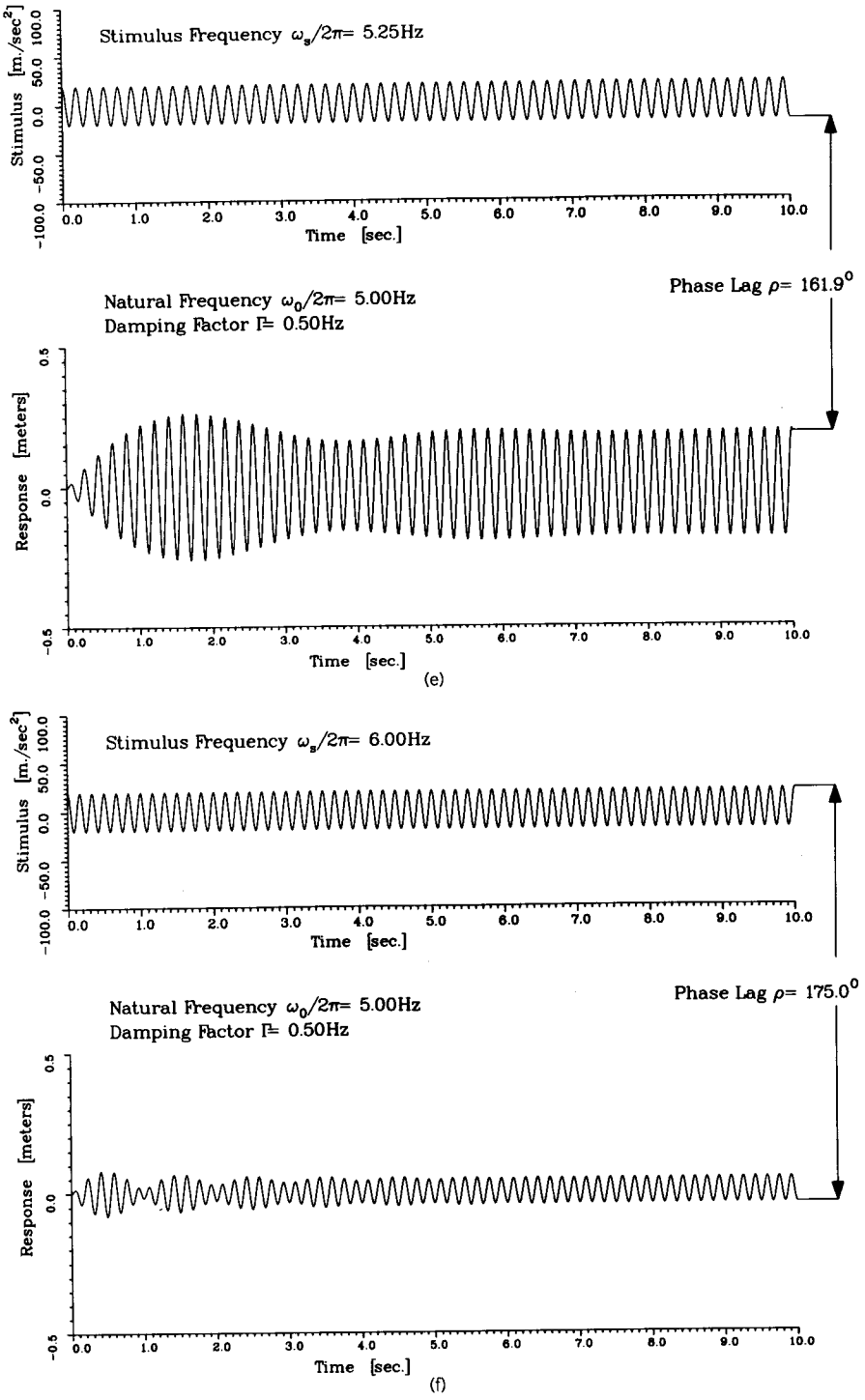

Figure 6.5.1 *(Continued).*

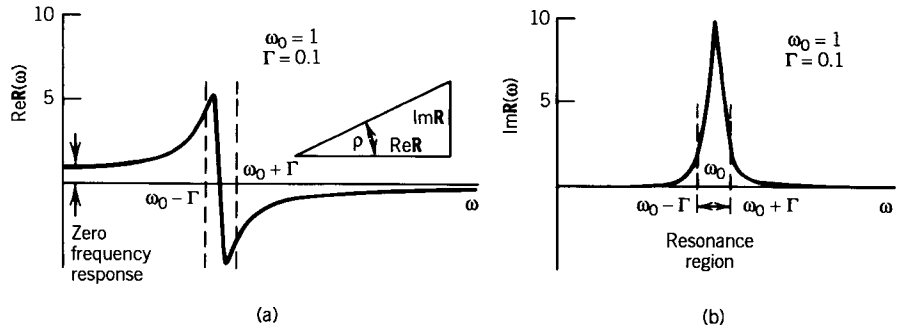

Figure 6.5.2 Classical oscillator response function $R(\omega)$. (a) Real part has a zero value and maximum slope at resonance. (b) Imaginary part has maximum value at resonance.

behind the stimulus ($\rho = 0^+$). Above resonance ($\omega_s > \omega_0$) the response falls almost completely out of phase ($\rho = 180^-$). Only near resonance ($\omega_s = \omega_0$) does the stimulus lead by the magic 90° and feed maximum power into the oscillator, which promptly wastes it through some damping mechanism characterized by the coefficient Γ. (More about this shortly.)

For reasonably low values of Γ (say $\Gamma < \omega_0/10$) it may be helpful to display the response quantities using an approximation and a monogram known as the Smith chart. The near-resonance approximation allows us to write

$$\begin{aligned} \omega_0^2 - \omega_s^2 &= (\omega_0 - \omega_s)(\omega_0 + \omega_s) \\ &\simeq (\omega_0 - \omega_s)2\omega_0, \end{aligned}$$

so that the response function (6.5.5c) may be approximated by

$$Re^{i\rho} \simeq \frac{(q/\mu)E_0}{(\omega_0 - \omega_s - i\Gamma)2\omega_0} = \frac{S}{\Delta - i\Gamma}, \tag{6.5.9a}$$

where we define

$$S = (q/2\mu\omega_0)E_0 \tag{6.5.9b}$$

as the stimulus strength and

$$\Delta = \omega_0 - \omega_s \tag{6.5.9c}$$

as the resonance detuning. Now the complex response can be written

$$Re^{i\rho} = R\cos\rho + iR\sin\rho = \frac{S\Delta}{\Delta^2 + \Gamma^2} + i\frac{S\Gamma}{\Delta^2 + \Gamma^2}, \tag{6.5.10a}$$

and its absolute square is a Lorentzian function of Δ:

$$R^2 = S^2/(\Delta^2 + \Gamma^2). \tag{6.5.10b}$$

Equating real and imaginary parts leads to the relation

$$R = (S/\Delta)\cos\rho = (B/\Gamma)\sin\rho. \tag{6.5.11}$$

From Figure 6.5.3 it is easy to see that the R phasor lies at the intersection of two circles with diameters (S/Δ) and (S/Γ) placed along the real and imaginary axes, respectively, and intersecting at origin. Note that for constant Γ and S the $\mathrm{Re}^{i\rho}$ phasor would follow the Γ circle to the top as $\Delta \to 0$ and $\rho \to \pi/2$. For negative detuning ($\omega_s > \omega_0$ or $\Delta < 0$) it would continue into the second quadrant as $|R|$ passed its maximum value, and finally the phase lag ρ would approach 180°. Graphs whose coordinates are (Δ, Γ) circles are called SMITH CHARTS and are used for many different purposes. The amplitude (6.5.9a) and Lorentzian function (6.5.10) will turn out to be quantum resonance functions in Chapter 8, and the Smith constructions may be used to help understand line shapes.

One should note that the Smith chart approximation (6.5.9) is completely wrong for the classical response at low frequency. The ($\omega_s \sim 0$) or DC response given by (6.5.5c),

$$R_{\mathrm{DC}} \simeq \left(q/\mu\omega_0^2\right)E_0, \tag{6.5.12}$$

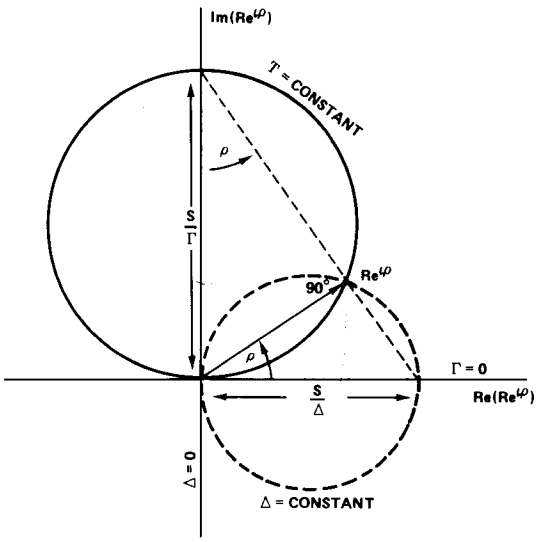

Figure 6.5.3 Geometry of a Smith chart. A nomogram for displaying response $|R|e^{ip}$ near resonance is based upon intersecting circles whose diameters are inversely proportional to damping (Γ) and detuning (Δ).

represents the displacement in equilibrium caused by a static or slowly moving field. [See the left-hand side of Figure 6.5.2(a).] It is also wrong for very high frequencies, since the correct R (6.5.5) vanishes as $(1/\omega_s^2)$ not as $(1/\omega_s)$.

B. Introduction to the Effect of Matter on Light

The displacement and separation or oscillation of electronic charge from the nuclei gives rise to dipole moments and currents which affect Maxwell's equations and light propagation. In the Lorentz model the dipole moments are taken to be directly proportional to the oscillator coordinate x, and the volume polarization is

$$\mathbf{P} = N\mathbf{p} = Nq\mathbf{x} \tag{6.5.13}$$

for N dipoles per unit volume. This enters as an extra current term $\mathbf{i} = Nq(\partial\mathbf{x}/\partial t)$ in Ampere's equation,

$$\nabla \times \mathbf{B} = \mu_0\left(\varepsilon_0\frac{\partial \mathbf{E}}{\partial t} + \mathbf{i}\right) = \mu_0\left(\varepsilon_0\frac{\partial \mathbf{E}}{\partial t} + \frac{\partial \mathbf{P}}{\partial t}\right).$$

Using Faraday's equation ($\nabla \times \mathbf{E} = -(\partial\mathbf{B}/\partial t)$) and the vector identity $\nabla(\nabla \cdot \mathbf{E}) - \nabla^2\mathbf{E} = \nabla \times (\nabla \times \mathbf{E})$ one obtains the electric wave equation

$$\begin{aligned}\nabla(\nabla \cdot \mathbf{E}) - \nabla^2\mathbf{E} &= -\frac{\partial}{\partial t}[\nabla \times \mathbf{B}] \\ &= -\mu_0\left(\varepsilon_0\frac{\partial^2 E}{\partial t^2} + \frac{\partial^2 P}{\partial t^2}\right).\end{aligned} \tag{6.5.14}$$

This can be simplified by relating volume dipole response to the $\mathbf{E}$ field using (6.5.5) and (6.5.13) and writing

$$\mathbf{P} = N\alpha\varepsilon_0\mathbf{E} = \chi\varepsilon_0\mathbf{E} \tag{6.5.15a}$$

where the POLARIZABILITY (α) and VOLUME SUSCEPTIBILITY (χ) are defined by

$$\chi = N\alpha = \left(Nq^2/\mu\varepsilon_0\right)/\left(\omega_0^2 - \omega_s^2 - i2\Gamma\omega_s\right). \tag{6.5.15b}$$

Dropping the $\nabla \cdot \mathbf{E}$ term (assuming equal positive and negative charge density) in (6.5.14), one obtains the wave equation:

$$\nabla^2\mathbf{E} = \mu_0\varepsilon_0(1 + \chi)\frac{\partial^2 \mathbf{E}}{\partial t^2}. \tag{6.5.16}$$

The susceptibility χ has the steady-state form if the stimulating electric field has a steady oscillation such as the plane wave

$$\mathbf{E} = E_0 \hat{y} e^{i(k_s z - \omega_s t)}. \tag{6.5.17}$$

Substituting this into the wave equation yields the following complex dispersion relation [henceforward we shall drop the subscript (s) from ω or k]:

$$k^2 = \mu_0 \varepsilon_0 (1 + \chi)\omega^2 = (1 + \chi)\omega^2/c^2. \tag{6.5.18}$$

The resulting wave phase velocity is

$$\omega/k = c/(1 + \chi)^{1/2} = c/\varepsilon^{1/2}, \tag{6.5.19}$$

where the complex DIELECTRIC CONSTANT (ε) and INDEX OF REFRACTION (n) are defined by

$$n = \varepsilon^{1/2} = (1 + \chi)^{1/2}. \tag{6.5.20}$$

From (6.5.15b) one has the following expression for the dielectric constant:

$$\varepsilon(\omega) = \left[1 + \frac{(Nq^2/\mu\varepsilon_0)(\omega_0^2 - \omega^2)}{(\omega_0^2 - \omega^2)^2 + 4\Gamma^2\omega^2}\right] + i\left[\frac{\Gamma(Nq^2/\mu\varepsilon_0)\omega}{(\omega_0^2 - \omega^2)^2 + 4\Gamma^2\omega^2}\right]. \tag{6.5.21}$$

For zero damping ($\Gamma = 0$) ε and $\varepsilon^{1/2}$ are positive and real, respectively, everywhere except between the resonance frequency $\omega = \omega_0$ and the frequency ω_c. The ω_c is called the CUTOFF FREQUENCY and is defined by

$$\omega_0^2 - \omega_c^2 + Nq^2/m\varepsilon_0 = 0$$

or

$$\omega_c^2 = \omega_0^2 + \omega_p^2, \tag{6.5.22a}$$

where

$$\omega_p = (Nq^2/\mu\varepsilon_0)^{1/2} \tag{6.5.22b}$$

is called the PLASMA FREQUENCY. Inside the region $\omega_0 < \omega < \omega_c$ the value of ε is negative. Therefore, $\varepsilon^{1/2}$ and k [recall Eq. (6.5.19)] are pure imaginary. This means that the wave will not propagate along z since it is damped according to $e^{-|k|z}$. For a free plasma where there is no mechanical restoring force; i.e., ω_0 vanishes. However, there is still a Coulomb electrostatic restoring force which gives the plasma a natural frequency of ω_p, and it will therefore respond 180° out of phase to a field oscillating at $\omega < \omega_p$ and tend to cancel the field.

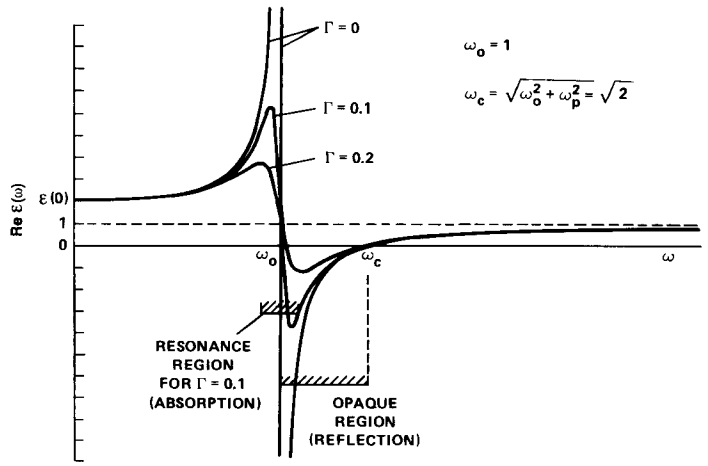

Figure 6.5.4 Real part of dielectric function for various values of damping Γ.

For charges bound to atoms, the wave can propagate unattenuated (in the limit $\Gamma \to 0$) with phase velocity c/n on either side of the cutoff region between ω_0 and ω_c. The phase velocity is less than the vacuum speed of light ($c = 3 \times 10^8$ m/s) on one side ($\omega < \omega_0$), and greater than c on the other side ($\omega > \omega_c$). The group velocity $d\omega/dk$ is less than c on either side.

If damping Γ is nonzero, then ε and $\varepsilon^{1/2}$ are complex. Whenever the wave propagates, it does so with an attenuation factor $e^{-|\text{Im } k|z}$. However, we have seen that the attenuation or absorption due to the imaginary part of ε is appreciable only for frequency ω in the neighborhood ($|\omega - \omega_0| < \Gamma$) of the resonance. Figure 6.5.4 shows the form of Re $\varepsilon(\omega)$ for different values of the damping Γ. The different curves overlap except near the resonance frequency ω_0.

(a) Polarization Mechanisms The polarizability of materials can be due to three basic mechanisms which change the dipole moment. The three categories are sketched in Figure 6.5.5.

The first mechanism involves the rotation of a molecule having a permanent dipole moment. Detailed discussion of this phenomenon really requires an extension of the quantum-mechanical treatment of Chapter 5, which will be pursued again in Chapters 7 and 8. The resonant frequencies associated with rotation are small, usually about 5–50 cm^{-1}.

The second method for changing a dipole moment involves motion of the ions, i.e., the normal modes of vibration in a molecule or solid as indicated in the figure. There will be a resonant frequency for each normal mode generally between 100 and 1000 cm^{-1}—although strong covalent molecules like NH_3 (recall Section 3.7) will resonate above 3000 cm^{-1}.

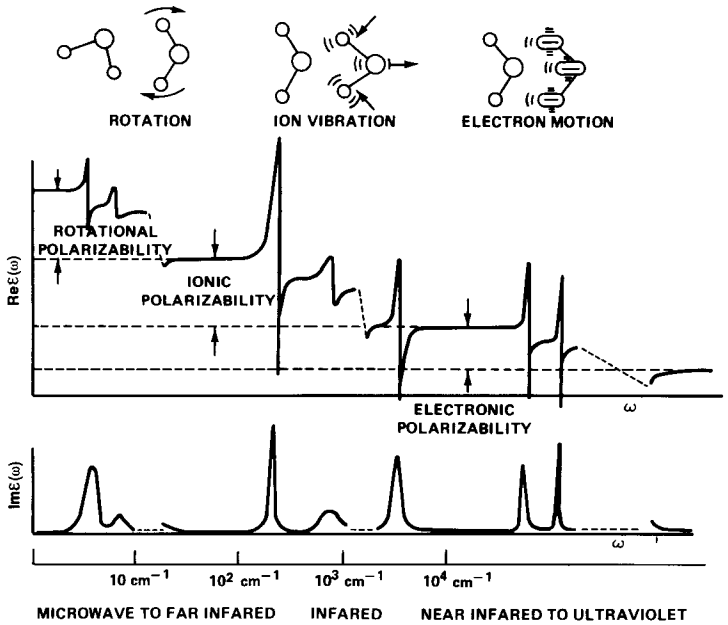

Figure 6.5.5 Classical sketch of three categories of response and dielectric behavior for molecular media.

Finally, the third mechanism of dipole change involves the motion of the electrons with respect to the nuclei. The resonant frequencies for this type of motion will usually be around 10,000 cm^{-1} or higher. Again, the details concerning this type of resonance really require a quantum-mechanical discussion, as seen later.

Nevertheless, in Figure 6.5.5 it is imagined that the entire spectrum of some material could be understood by simply summing dielectric response functions of the form in Eq. (6.5.21) for each "oscillator" or each normal mode, electronic transition, etc., which the material system has. Although the details of the frequency dependence of $\varepsilon(\omega)$, particularly near resonances, require a quantum analysis, it turns out that a classical analysis is qualitatively a good one. In addition, it can give a semiquantitative estimate for polarizability of a given molecule at a frequency that is not near resonance.

For example, if we want to estimate the electronic polarizability of atomic hydrogen at low frequencies ($\omega \to 0$) we may substitute the ultraviolet ionization energy (13.6 eV) in units of frequency ($\omega_0 = 2 \times 10^{16}$ rad/s) into Eq. (6.5.15):

$$\alpha_e \sim \frac{e^2/m\varepsilon_0}{\omega_0^2 - \omega^2} = 7.95 \times 10^{-30}\ \mathrm{m}^3.$$

Electronic mass ($m = 9.11 \times 10^{-31}$ kg) charge ($e = 1.60 \times 10^{-19}$ coulomb), and electrostatic constant ($\varepsilon_0 = 8.84 \times 10^{-12}$) are used.

To estimate the zero-frequency polarizability of a system of ions, suppose we take an ionic mass of 30 amu ($m = 5.0 \times 10^{-26}$ kg), the same charge as above, and an infrared resonance frequency of $\omega_0 = 9.4 \times 10^{13}$ rad/s (500 cm^{-1}) with ($\omega \to 0$):

$$\alpha_v \sim \frac{q^2/m\varepsilon_0}{\omega_0^2 - \omega^2} = 6.6 \times 10^{-30}\ \mathrm{m}^3. \tag{6.5.23}$$

On the other hand, at optical frequencies ($\omega = 3.7 \times 10^{15}$ rad/s ~ 5000 Ä), the polarizability of the same ionic system is negligible by comparison; i.e., $\alpha_v \sim -4 \times 10^{-33}$ m^3, while the electronic polarizability will be growing, particularly if ω is approaching an electronic resonance at ω_0.

Note that a good unit for polarizability is the cubic angstrom $(10^{-10}\ \mathrm{m})^3$. Indeed, the polarizability of something is proportional to its volume, as a general rule.

(b) Effect of Matter on Matter For dense materials such as solids, liquids, and even high-pressure gases, the electric field $\mathbf{E}_{\text{local}}$ affecting a given molecule or atom may differ appreciably from the "applied" $\mathbf{E}$ field. In texts on electromagnetism one finds the following expression for $\mathbf{E}_{\text{local}}$ in isotropic materials and cubic solids:

$$\mathbf{E}_{\text{local}} = \mathbf{E} + \frac{1}{3\varepsilon_0}\mathbf{P}.$$

If the polarizable atom or molecule responds to $\mathbf{E}_{\text{local}}$, we have

$$P = \chi\varepsilon_0 E_{\text{local}} = \chi\varepsilon_0\left(\mathbf{E} + \frac{1}{3\varepsilon_0}\mathbf{P}\right)$$

or, solving for $\mathbf{P}$,

$$\mathbf{P} = \frac{\chi\varepsilon_0}{1 - \chi/3}\mathbf{E},$$

where χ is the same susceptibility as before [Eq. (6.5.9)]. This changes the dielectric constant ε defined by

$$\mathbf{D} = \varepsilon\mathbf{E} = \mathbf{E} + \mathbf{P}/\varepsilon_0$$

to the following:

$$\varepsilon = (1 + \chi/(1 - \chi/3)). \tag{6.5.24}$$

Note that if $\chi \ll 1$, we may ignore these corrections.

(c) Visualizing Radiation Coupling Using Feynman's Lever The detailed solutions of Newton's and Maxwell's equations for coupled particles and em fields are complicated. However, for small numbers of particles there is a graphical construction given in the Feynman Lectures (Section II-21) which is very instructive. It provides a way to tell exactly what the fields will be around an arbitrarily moving charge.

Imagine that you are holding a charge and moving it back and forth. Let the charge be attached to a ring which can slide on a long lever arm as shown in Figure 6.5.6(a). Let the lever have a unit vector $(-\hat{\mathbf{e}}_r)$ or pointer pointing in the opposite direction of the lever $\mathbf{r}$ on the other side of its swivel point (0) at origin. Feynman has shown that the $\mathbf{E}$ field at origin at time t depends on the position of the pointer $\hat{\mathbf{e}}'_r$ and lever $\mathbf{r}'$ at a slightly earlier time ($t' = t - r/c$). The time delay is just the time it would take a signal traveling at c to propagate from r at t' to origin at t. The $\mathbf{E}$ field is given by

$$\mathbf{E}(0,t) = \frac{q}{4\pi\varepsilon_0}\left\{\frac{-\hat{\mathbf{e}}'_r}{(r')^2} + \frac{r'}{c}\frac{d}{dt}\left[\frac{-\hat{\mathbf{e}}'_r}{(r')^2}\right] + \frac{1}{c^2}\frac{d^2}{dt^2}[-\mathbf{e}'_r]\right\}$$
$$= \underset{\text{term}}{\text{Coulomb}} + \underset{\text{term}}{\text{induction}} + \underset{\text{term}}{\text{radiation}}. \qquad (6.5.25a)$$

The first term is just the usual Coulomb field. The second term gives rise to a magnetic induction field,

$$\mathbf{B}(0,t) = (\hat{\mathbf{e}}'_r \times \mathbf{E})/c, \qquad (6.5.25b)$$

at origin if the charge has velocity transverse to $\mathbf{r}$. Finally, the third radiation term contributes to $\mathbf{E}(0,t)$ and $\mathbf{B}(0,t)$ in (6.5.25) if the charge has acceleration transverse to $\mathbf{r}$. It is interesting to note that in some ways this term is the reverse of Newton's law. For Newton's law one is given a field $\mathbf{E}$ or

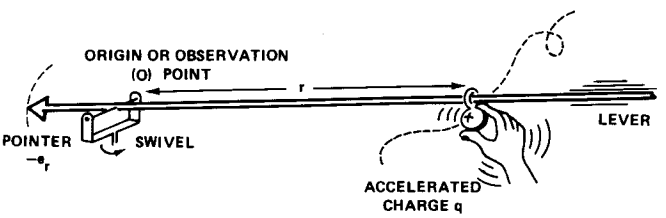

(a)

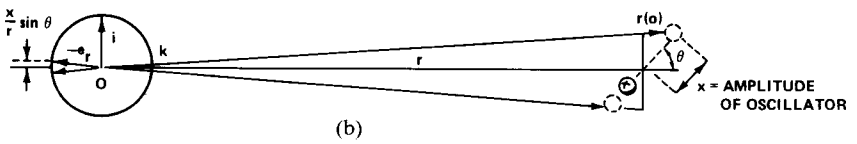

(b)

Figure 6.5.6 Feynman's lever. This construction provides a convenient way to visualize the field due to an accelerated or moving charge.

force $\mathbf{F} = q\mathbf{E}$ and computes the double integral $\mathbf{r} = \int\int(dt^2(q/\mu)\mathbf{E})$ of $\mathbf{E}$ to obtain the particle's position $\mathbf{r}$ in space. For the third term of (6.5.15a) one is given the position $\mathbf{r}$ and computes $\mathbf{E}$ from the double *derivative* of $\hat{\mathbf{e}}'_r$. Note that the radiation term is the only significant term at large distances since it has no $(1/r')^2$ factor to kill it off.

Feynman's lever can tell you a number of things immediately. For example, one can easily see that a charge rotating around in a circle gives rise to circularly polarized radiation for observers along the axis of the circle. One can also see that a uniform *ring* of charge gives *no* radiation no matter how fast it rotates since all the charges in the ring yield canceling levers. We use the lever now to derive the most common radiation problem: a single oscillating charge giving electric dipole radiation.

As seen in Figure 6.5.6(b) a charge oscillating at an angle θ to the radius vector causes the pointer lever to oscillate with an amplitude $(x/r)\sin\theta$. The unit vector is given by

$$-\hat{\mathbf{e}}_r(t) = -\hat{\mathbf{k}} - \hat{\mathbf{i}}\frac{x}{r}\sin\theta e^{-i\omega t}$$

for $r \gg x$. The second derivative required for (6.5.25a) is

$$\frac{d^2}{dt^2}(-\hat{\mathbf{e}}_r(t)) = \hat{\mathbf{i}}\omega^2\frac{x}{r}\sin\theta e^{-i\omega t},$$

and the resulting E field is

$$\mathbf{E}(t) = \hat{\mathbf{i}}\frac{q\omega^2 x\sin\theta}{4\pi\varepsilon_0 c^2}\left(\frac{e^{i(kr-\omega t)}}{r}\right), \tag{6.5.26}$$

where the retardation $(\omega r/c = kr)$ has been put in the exponent.

From this one can find the total energy lost by a oscillating charge to Poynting flux,

$$\mathbf{S} = \mathbf{E}\times\mathbf{B}/\mu_0 = \hat{\mathbf{e}}_r|E|^2/\mu_0 c = \hat{\mathbf{e}}_r\frac{q^2\omega^4x^2\sin^2\theta}{16\pi^2c^3\varepsilon_0}\frac{\cos^2(kr-\omega t)}{r^2}, \tag{6.5.27}$$

and derive the natural decay constant Γ_0 of a free oscillator. The surface integral,

$$\begin{aligned} P(t) &= \int\int d\mathbf{A}\cdot\mathbf{S} = \int_0^{2\pi}d\phi\int_0^{\pi}d\theta\, r^2\sin\theta|S| \\ &= \frac{q^2\omega^4x^2}{16\pi^2c^3\varepsilon_0}\cos^2(kr-\omega t)2\pi\int_0^{\pi}d\theta\sin^3\theta \\ &= \frac{q^2\omega^4x^2}{6\pi c^3\varepsilon_0}\cos^2(kr-\omega t) \end{aligned} \tag{6.5.28}$$

is the total power being pumped into radiation at each instant. The time average of the squared cosine factor is $\frac{1}{2}$, and this gives the average power loss

$$\langle P\rangle = \frac{q^2\omega^4 x^2}{12\pi c^3\varepsilon_0}. \tag{6.5.29}$$

We notice that $\langle P\rangle$ is proportional to the fourth power of frequency and to the square of the amplitude x. Since the energy of a damped harmonic oscillator is $(m\omega^2|x|^2/2)$ its power loss by (6.5.4) is also proportional to x^2; i.e.,

$$\langle P\rangle = -\frac{d}{dt}\langle m\omega^2 a^2 e^{-2\Gamma t}/2\rangle = 2\Gamma\langle m\omega^2 x^2/2\rangle.$$

Comparing this to (6.5.29) one derives

$$\Gamma = \frac{q^2\omega^2}{12\pi c^3\varepsilon_0 m} \tag{6.5.30}$$

for the decay constant just due to radiation.

For an electron in an atom that oscillates at the 600 THz frequency of green light for which $\omega = 3.77 \times 10^{15}$ rad · Hz one has $\Gamma = 4.4 \times 10^7\ \mathrm{s}^{-1}$. The atom's energy will decay by 95% in time $t = 3/(2\Gamma) = 3.4 \times 10^{-8}$ s. This is a typical atomic lifetime. It sounds short but that is enough time for about 20 million oscillations! For a 6 THz infrared transition ($\omega = 3.77 \times 10^{13}$rad · Hz) the lifetime is 3.4×10^{-4} s; still pretty short but enough for two billion oscillations. In terms of heartbeats that is about as long as the average human life.

Because more rapidly oscillating charges radiate more quickly, it follows that higher-frequency stimulating radiation will be scattered more quickly by oscillators they stimulate. This is why higher-frequency light is scattered more in air. The scattering process which makes our sky blue is called Rayleigh scattering, and we consider it in more detail now. The Rayleigh scenario goes as follows. First an atomic oscillator responds according to (6.5.5a) and (6.5.5c) to incoming E field $E_0 e^{ikz-\omega t}$ with an amplitude

$$x(z,t) = \frac{qE_0/\mu}{\omega_0^2 - \omega^2 - 2i\Gamma\omega} e^{i(kz-\omega t+\rho)} \tag{6.5.31a}$$

$$\simeq \left(qE_0/\mu\omega_0^2\right)e^{i(kz-\omega t)} \qquad (\text{for } \omega \ll \omega_0). \tag{6.5.31b}$$

The DC approximation (6.5.12) is given in the second line. Then the oscillator radiates or Rayleigh-scatters this energy at the rate (6.5.29)

$$\langle P\rangle = \frac{q^2\omega^4|x|^2}{12\pi c^3\varepsilon_0} = \frac{q^2\omega^4}{12\pi c^3\varepsilon_0}\left|\frac{qE_0/\mu}{\omega_0^2 - \omega^2 - 2i\Gamma\omega}\right|^2. \tag{6.5.32}$$

Scattering theorists like to factor this result in a funny way so that three types of contributions are exposed:

$$\langle P \rangle = \left[\frac{1}{2}\varepsilon_0 c E_0^2\right] \cdot \left[\pi\left(\frac{q^2}{4\pi\varepsilon_0 mc^2}\right)^2\right]\left[\frac{8\omega^4}{3|\omega_0^2 - \omega^2 - 2i\Gamma\omega|^2}\right]$$

$$= [S] \cdot \left[\pi r_{\text{classical}}^2\right]\left[\frac{8\omega^4}{3\left(\omega_0^2 - \omega^2\right)^2 + 12\Gamma^2\omega^2}\right]. \qquad (6.5.33)$$

The first factor is Poynting energy flux per unit area. The second factor is the so-called classical electronic cross-section $\pi r_{\text{classical}}^2 = 2.5 \times 10^{-29}$ m^2, which involves the classical electron radius $q^2/(4\pi\varepsilon_0 mc^2)$. (This is the radius at which dipolar electronic coulomb energy equals the rest mass mc^2 of the electron.) The third factor is a dimensionless frequency enhancement factor for the Rayleigh cross-section, which is approximated by $8\omega^4/3\omega_0^4$ when $\omega \ll \omega_0$. It indicates how an electron can appear to "swell up" and scatter more radiation when its oscillation amplitude is amplified.

(d) Four Points of the Response Phasor Using Feynman's methods one can visualize some of the *mechanisms* behind the Lorentz susceptibility formula (6.5.15) and Figure 6.5.4. It is possible to see (1) how light gets slowed down when its frequency ω is below resonance ($\omega < \omega_0$), (2) how it gets absorbed near resonance ($\omega \simeq \omega_0$), and (3) how it speeds up above resonance ($\omega > \omega_0$). It is also possible to understand a fourth case involving *l*ight *a*mplification by *s*timulated *e*mission or LASER processes. These four cases correspond to four values 0°, 90°, 180°, and 270°, respectively, for the response phasor lag ρ. These four points of the phasor are as important to modern spectroscopy as the four points of the compass are to navigation.

Figure 6.5.7 shows an incremental slab containing N dipoles per cubic meter responding according to (6.5.31a) to the incoming radiation. We need to find the electric field $(z_0 - z)$ meters downstream at an observation point

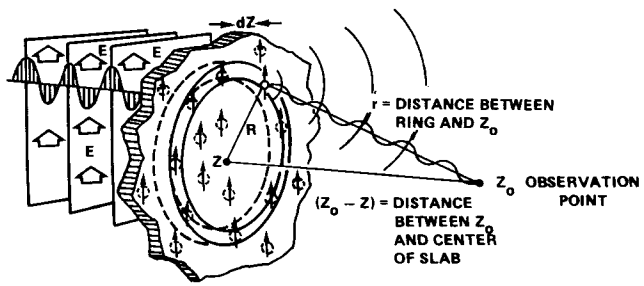

Figure 6.5.7 Incremental slab responding to plane-wave radiation.

z_0. This would be the sum of the original stimulating field $E_0 e^{i[k(z-z_0)-\omega t]}$ plus all the extra little fields broadcast by the dipoles in the slab. Let us label the extra response field by E^R. The contribution dE^R to E^R due just to the dipoles in the ring of volume $2\pi R\,dR\,dz$ in Figure 6.5.7 is

$$dE^R(z_0) = \frac{q\omega^2 x(z, t - r/c)}{4\pi\varepsilon_0 c^2 r} N 2\pi R\,dR\,dz$$

$$= \frac{q\omega^2 |x| e^{i(kz-\omega t)+\rho+\omega r/c)}}{4\pi\varepsilon_0 c^2 r} N 2\pi R\,dR\,dz,$$

according to (6.5.26). Here we take $x \sin\theta \simeq x$ and include the retardation $\omega r/c$ in the exponent.

The figure shows that $r^2 = R^2 + (z_0 - z)^2$. If z is fixed at slab center then $2r\,dr = 2R\,dR$. This simplifies the integral over the ring radius R to give the response generated at z_0.

$$E^R(z_0, t) = \frac{2\pi N\,dz\,q\omega^2|x|}{4\pi\varepsilon_0 c^2} e^{i(kz-\omega t+\rho)} \int_{R=0}^{R=\infty} \frac{R\,dR\,e^{i\omega r/c}}{r}$$

$$= \frac{N\,dz\,q\omega^2|x|}{2\varepsilon_0 c^2} e^{i(kz-\omega t+\rho)} \int_{r=z_0-z}^{\infty} dr\,e^{ikr}$$

$$= \frac{N\,dz\,q\omega^2|x|}{2\varepsilon_0 c^2} e^{i(kz-\omega t+\rho)} \frac{e^{ikr}}{ik}\bigg|_{z_0-z}^{\infty}. \tag{6.5.34}$$

Now we pull a well-known swindle and set $e^{ik\infty} = 0$. This can be justified by more careful analysis which shows how the distant oscillators cancel. The result is

$$E^R(z_0, t) = |E^R| e^{i(kz-\omega t+\rho)} e^{\pi i/2} e^{ik(z_0-z)}$$

$$= |E^R| e^{i(kz_0-\omega t+\rho+\pi/2)}, \tag{6.5.35a}$$

where

$$|E^R| = \frac{N\,dz\,q\omega^2|x|}{2\varepsilon_0 c^2 k}. \tag{6.5.35b}$$

The main result in (6.5.35a) is the extra phase lag of $\pi/2$ beyond that of the response lag ρ. (The response phase lag is given by (6.5.5f).)

This result is used to draw the four cases in Figure 6.5.8. Each case shows phasors for the stimulating E wave, the polarization wave of the responding slab oscillators with phase lag ρ, the resulting downstream response generated wave E^R with phase lag $\rho + \pi/2$, and, finally, the sum wave $E + E^R$.

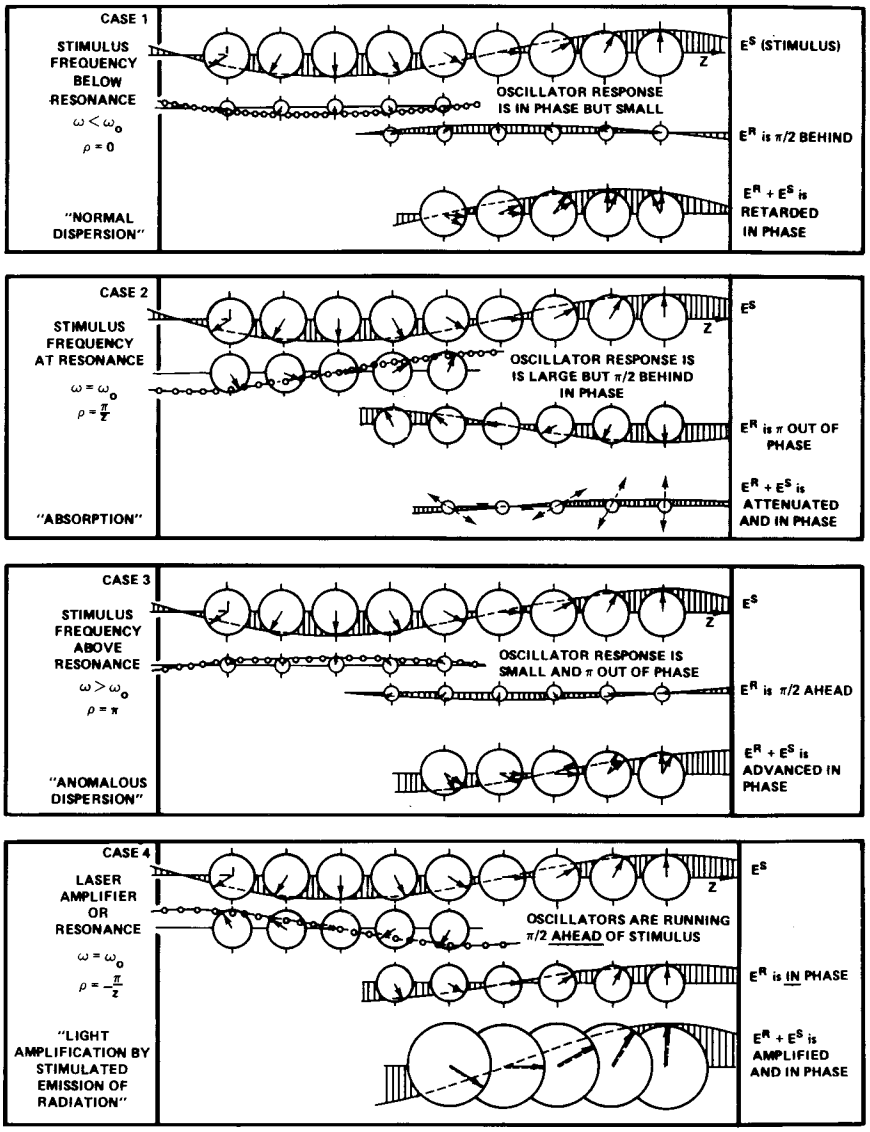

Figure 6.5.8 The Four points for the response compass.

In normal dispersion (case 1) the oscillators are responding weakly but in phase ($\rho \simeq 0$). They broadcast a weak E^R signal which adds a small component at 90° to the original E-field phasors and so the sum is a slightly retarded wave of the same amplitude. This retardation accumulates arithmetically or linearly from slab to slab and so it amounts to a reduction in phase velocity.

In case 2 the oscillators are resonating strongly and 90° behind the stimulus ($\rho \simeq 90°$). This means that the E^R tends to attenuate the E field since the extra 90° lag swings it around to be 180° out of phase. This attenuation accumulates geometrically or exponentially from slab to slab since the response in each slab is proportional to the total field coming from the preceding one. This exponential decay of amplitude is sometimes stated as Beer's law. Note that the original E field is not simply eaten up. It keeps *going forever, but it stimulates traveling companions which are out of phase* with it. Destruction is accomplished through creation.

Just above resonance ($\omega > \omega_0$) corresponds to anomalous dispersion as shown in case 3 of Figure 6.5.8. Here the phase velocity exceeds that of light in a vacuum. It should be noted that the plasma effects mentioned after Eq. (6.5.22) are not accounted for by the thin slab model which ignores the surface charges produced by dipoles on the edges. Such effects are important in condensed matter but usually ignorable in the gas phase.

In case 4 of Figure 6.5.8 the oscillating dipoles are feeding energy into the E field since they have negative phase lag $\rho - 90° = 270°$; i.e., they *lead* the stimulating field by 90°. Consequently, the E field grows exponentially as in a laser amplifier. It is interesting to note that classical Lorentz theory can account for many laser effects. It is only necessary to replace the oscillator number N by the difference $N = N_l - N_u$ between the number N_l of atoms in the lower laser level (l) and the number N_u of atoms in the upper level (u). When N_u exceeds N_l this is called a population inversion and N in (6.5.15) becomes negative as does the phase lag ρ. The resonance frequency ω_0 is the quantum energy difference $(E_u - E_l)/h$ in all these classical analyses. In Chapter 8 we will see how the Lorentz model and phasor picture is generalized when we introduce the quantum phasor.

C. Two Types of Spectroscopy for Vibration Analysis

(a) Infrared Absorption Spectroscopy An experimental apparatus which gives infrared spectra is sketched in Figure 6.5.9. The output of the

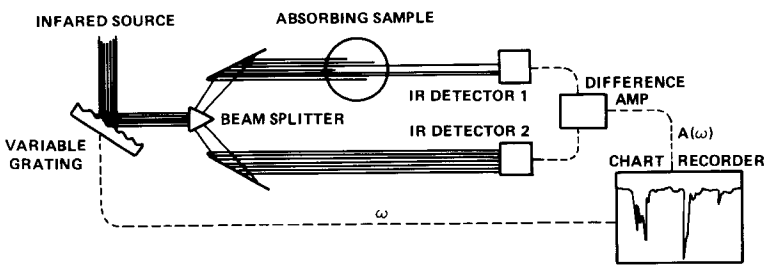

Figure 6.5.9 Infrared spectrometer.

machine is the difference in intensity between the absorbed beam and a reference beam as a function of the input frequency ω.

As explained in the preceding sections, light is absorbed when its frequency is near that of a resonance of some motion that gives an oscillating dipole moment. For a given frequency, the absorption coefficient Im k increases with the magnitude of the induced dipole moment $\boldsymbol{p} = \alpha\varepsilon_0\mathbf{E}$, but vanishes if $\mathbf{p}$ is zero. For infrared frequencies, it is important to see what dipole moments can arise from the motion of ions for a few simple examples and to derive some general rules about them.

Suppose the atoms of UF_6 (recall Section 4.4) are rigid ions, and the F ions have charge q_F while the U has charge q_U. Then the dipole moment vector is the vector sum of the charge positions $\mathbf{r}_i$ with respect to the center of charge at that position:

$$\mathbf{p} = \sum_i q_i \mathbf{r}_i. \tag{6.5.36}$$

Now suppose the UF_6 octahedron is distorted according to the base state $|c_3^{T_{1u}}\rangle$ as pictured in Figure 6.5.10. (Recall Figure 4.4.36, which shows $|c_1^{T_{1u}}\rangle$ with amplitude A.) Then the dipole components are, using Eq. (6.5.36),

$$p_x = 0, \qquad p_y = 0, \qquad p_z = 6q_F(MA) - q_U(6mA).$$

Note that p_z is proportional to the amplitude A of this distortion, and that all components of the dipole vector are zero when UF_6 is the octahedral equilibrium configuration. Furthermore, similar calculations show that the dipole moments due to $|A_{1g}\rangle$, $\left|\begin{matrix}E_g\\ m\end{matrix}\right\rangle$, $\left|\begin{matrix}T_{2g}\\ m\end{matrix}\right\rangle$, and $\left|\begin{matrix}T_{2u}\\ m\end{matrix}\right\rangle$ are all identically zero.

However, it is usually easier to tell by symmetry analysis which motions are capable of giving a particular dipole moment component. This is done by

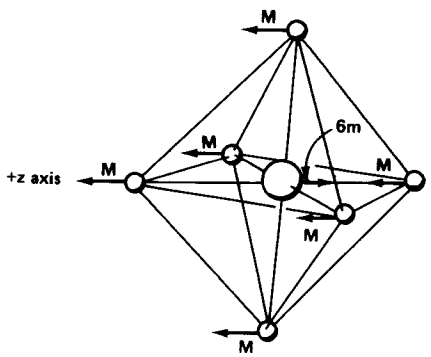

Figure 6.5.10 First-order infrared activity. This is an example of a vibrational motion giving rise to a dipole moment. The moment varies linearly with the normal coordinate, but also depends upon the charges on the central ion and the six octahedrally located ions.

studying the expansion of symmetry-defined dipole components p_m^γ in terms of the normal coordinates x_i^α.

$$p_m^\gamma(\cdots x^\alpha \cdots) = [p_m^\gamma(\cdots 0 \cdots)] + \sum_{\alpha,i} x_i^\alpha \left[\frac{\partial p_m^\gamma}{\partial x_i^\alpha}(\cdots 0 \cdots)\right] + \frac{1}{2}\sum_{\alpha,i}\sum_{\beta,j} x_i^\alpha x_j^\beta \left[\frac{\partial^2 p_m^\gamma}{\partial x_i^\alpha \partial x_j^\beta}(\cdots 0 \cdots)\right] \cdots . \quad (6.5.37)$$

Symmetry definition of dipole components is the same as that of ordinary vector components according to the definition given in Eq. (6.5.36). For O_h we have $p_z \equiv p_3^{T_{1u}}$, $p_y \equiv p_2^{T_{1u}}$, and $p_x \equiv p_1^{T_{1u}}$. For C_{3v} we have $p_z = p^{(1)}$, $p_x = p_1^{(3)}$, and $p_y = p_2^{(3)}$.

All the constant factors in the brackets in Eq. (6.5.37) are derived from the equilibrium configuration ($x_i^\alpha \equiv 0$) and therefore are invariant to symmetry operations. One needs to find which of these constants or which combinations of these constants are independent or nonzero. It is precisely the same problem we solved when writing tensor relations in Section 6.3, only now we have one such problem for each order $N = 0, 1, 2, \ldots$ in the expansion.

The zeroth-order problem is easy. Clearly, $[p_m^\gamma(\cdots 0 \cdots)]$ must vanish unless there is a dipole component p^γ that is a scalar (p^{A_1}). The O_h vector irrep T_{1u} accounts for all three dipole components; none are scalar. Therefore, nothing with O_h symmetry has a permanent electric moment. On the other hand, for C_{3v} we have $p_z = p^{(1)} = p^{A_1}$; that is, the z component of the dipole belongs to the scalar irrep. Therefore, NH_3 could have a dipole moment along its z axis, and this is observed.

The first-order problem is also easy. In order to be invariant, the quantity $[\{\partial p_m^\gamma/\partial x_i^\alpha\}(\cdots 0 \cdots)]$ must have $\alpha = \gamma$. This tells us whether it is possible for a mode x^α to have an associated dipole moment. For UF_6, which has O_h symmetry, this is possible only for $\alpha = T_{1u}$. This is called an INFRARED SELECTION RULE. Only the T_{1u} modes of UF_6 can be seen when the spectrograph is tuned to their eigenfrequencies. All other modes are "first-order infrared forbidden." For C_{3v} symmetry (viz., NH_3) and (1) and (3) type modes, which account for all NH_3 modes (recall Figures 3.7.2 and 3.7.3) are infrared active. Only (2) type modes would be forbidden.

The second- and higher-order terms are a little more difficult to understand. These will be needed to account for the variation of ionic charge with interatomic separation. Generally, the dipole moment will not increase linearly with x_i^α forever. The only higher order terms that can be nonzero are those which can make the vector irrep (γ) through a Clebsch-Gordon coupling. The quadratic terms must be of the form

$$p_m^\gamma = \cdots + k^\gamma \left(\sum_{i,j} \mathscr{C}_{ijm}^{\alpha\beta\gamma} x_i^\alpha x_j^\beta\right) + \cdots , \quad (6.5.38)$$

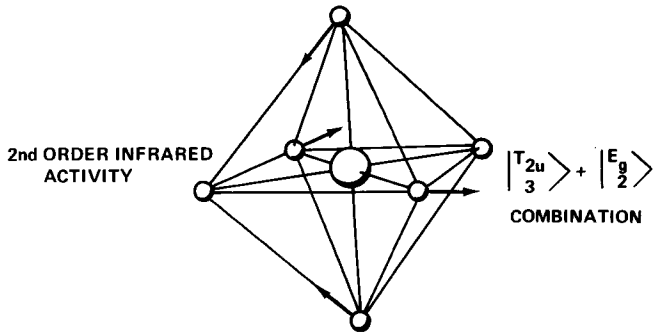

Figure 6.5.11 Second-order infrared activity. This is an example of combination of normal coordinates giving rise to dipole moment. It depends on the product of the normal coordinates. It is also necessary that the charge difference between an octahedral ion and the central ion should depend on the distance between them.

where

$$k^\gamma = \frac{1}{2}\sum_{i,j} \mathscr{C}_{ijm}^{\alpha\beta\gamma}\left[\frac{\partial^2 p_m^\gamma}{\partial x_i^\alpha\, \partial x_j^\beta}(\cdots 0 \cdots)\right]$$

is independent of m.

In this way a particular combination of normal coordinates may give rise to a dipole moment even though neither one of them could do it separately. Consider, for example, the infrared inactive modes $x_3^{T_{2u}}$ and $x_2^{E_g}$ of UF_6. Since $\mathscr{C}_{323}^{T_{2u}E_gT_{1u}} = -1$ it may be possible for the combination of these two to make a $p_z(p_3^{T_{1u}})$ dipole component. Indeed, from Figure 6.5.11 we may visualize this possibility. It should be clear that this second-order dipole moment depends on how much the charge on the F ions varies with their distance from the U ion.

The frequencies associated with second- or higher-order products $x_i^\alpha x_j^\beta \cdots$ may be the sums or difference $|\pm\omega^\alpha \pm \omega^\beta \pm \cdots|$ of the respective eigenfrequencies and are called OVERTONES or COMBINATION TONES. Understanding their detailed behavior requires quantum mechanics.

(b) Rayleigh and Raman Scattering We mentioned that the polarizability of electrons by optical frequency radiation is much greater than that of the vibrational modes. This is particularly so for larger molecules. Now we will give a more detailed discussion of the polarizability of the electron clouds around various arrangements of ions or atoms.

For objects more complicated than the simple charge-ball model it is necessary to discuss other components of polarizability. The polarizability of nonspherical charge clouds may vary with the direction of **E**, and the induced dipole moment **p** may not point in the same direction as **E**.

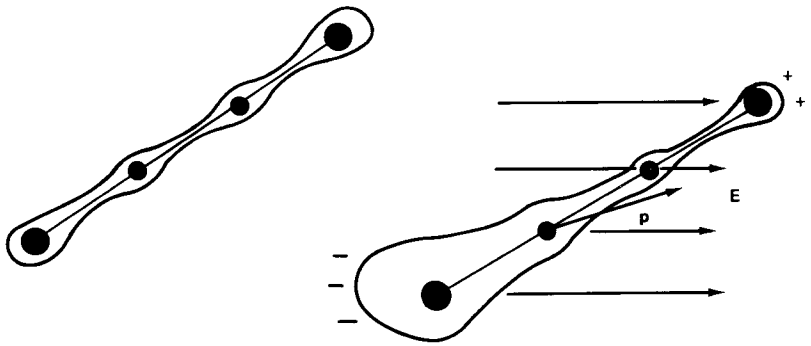

Figure 6.5.12 Electronic polarizability may be anisotropic.

For example, consider a long thin molecule with some electrons that can move more easily along its z axis than in the x or y directions. An electric field **E** applied at a random angle to the axis will produce a dipole vector nearly parallel to the axis as shown in Figure 6.5.12.

In order to describe the general linear polarization, the simple relation $p = \alpha\varepsilon_0$ is replaced by the following tensor relation:

$$\mathbf{p} = \varepsilon_0 \vec{\vec{\alpha}} \cdot \mathbf{E},$$

$$\begin{pmatrix} p_x \\ p_y \\ p_z \end{pmatrix} = \varepsilon_0 \begin{pmatrix} \alpha_{xx} & \alpha_{xy} & \alpha_{xz} \\ \alpha_{yx} & \alpha_{yy} & \alpha_{yz} \\ \alpha_{zx} & \alpha_{zy} & \alpha_{zz} \end{pmatrix} \begin{pmatrix} E_x \\ E_y \\ E_z \end{pmatrix}. \tag{6.5.39}$$

The radiation arising from the oscillating dipole **p** induced by an oscillating **E** through a changing $\vec{\vec{\alpha}}$ is the RAYLEIGH AND RAMAN-SCATTERED LIGHT. A basic experimental setup which may detect this is sketched in Figure 6.5.13.

The vector of the **E** field coming to the collecting optics from a single dipole $\mathbf{p}(t)$ can be given by rewriting Feynman's lever formulas (6.5.25) and (6.5.26) as follows:

$$\mathbf{E} = \frac{1}{4\pi\varepsilon_0 c^2} \frac{(\ddot{\mathbf{p}}(t - \mathbf{r}/c) \times \hat{\mathbf{r}}) \times \hat{\mathbf{r}}}{r} e^{ikr}, \tag{6.5.40}$$

or if we assume $\mathbf{p}(t - \mathbf{r}c) = \mathbf{p}(+)e^{-i\omega t}$, by

$$\mathbf{E} = -\frac{\omega^2}{4\pi\varepsilon_0 c^2} \frac{(\mathbf{p}(+) \times \hat{\mathbf{r}}) \times \hat{\mathbf{r}}}{r} e^{ikr}. \tag{6.5.41}$$

The energy flux S was given in (6.5.27).

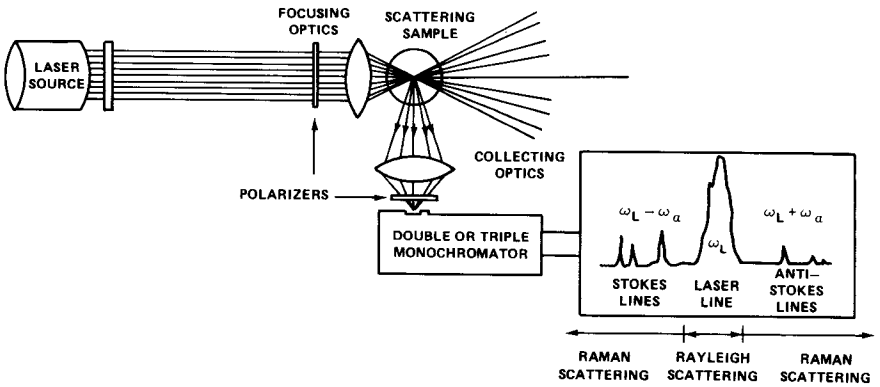

Figure 6.5.13 Raman spectrometer.

The frequency spectrum, polarization, and intensity of scattered light depends upon the incoming **E** field and the polarizability tensor $\overleftrightarrow{\alpha}$ according to the foregoing and Eq. (6.5.39). The most important effects come from the changing of the $\overleftrightarrow{\alpha}$ components as the scattering molecules expand and contract while vibrating. One may express this dependence on atomic motion by the following expansion of $\overleftrightarrow{\alpha}$ in terms of normal coordinates:

$$\alpha_{uv}(\cdots x_i^\alpha \cdots) = [\alpha_{uv}(\cdots 0 \cdots)] + \sum_{\alpha,i} x_i^\alpha \left[\frac{\partial \alpha_{uv}}{\partial x_i^\alpha}(\cdots 0 \cdots)\right] + \frac{1}{2}\sum_{\alpha,i}\sum_{\beta,j} x_i^\alpha x_j^\beta \left[\frac{\partial^2 \alpha_{uv}}{\partial x_i^\alpha \, \partial x_j^\beta}(\cdots 0 \cdots)\right]. \quad (6.5.42)$$

For symmetry analysis it is more convenient to use the symmetry-defined tensor components α_m^γ instead of the Cartesian components α_{uv},

$$\overleftrightarrow{\alpha} = \sum_{u,v} \alpha_{uv} \hat{x}_u \hat{x}_v = \sum_{\gamma,m} \alpha_m^\gamma \mathbf{T}_m^\gamma, \quad (6.5.43)$$

just as was done for the stress or strain tensors. The expansion of each of these,

$$\alpha_m^\gamma(\cdots x_i^\alpha \cdots) = [\alpha_m^\gamma(\cdots 0 \cdots)] + \sum_{\alpha,i} x_i^\alpha \left[\frac{\partial \alpha_m^\gamma}{\partial x_i^\alpha}(\cdots 0 \cdots)\right] + \frac{1}{2}\sum_{\alpha,i}\sum_{\beta,j} x_i^\alpha x_j^\beta \left[\frac{\partial^2 \alpha_m^\gamma}{\partial x_i^\alpha \, \partial x_j^\beta}(\cdots 0 \cdots)\right], \quad (6.5.44)$$

can be treated term by term using the same ideas that worked for the dipole expansion in the preceding section.

The first term, like all the coefficients in brackets evaluated at $x = 0$, is invariant to symmetry operations. It can be nonzero only for the components α_m^γ for which $(\gamma) =$ (scalar). This is called the RAYLEIGH-SCATTERING term. According to Eqs. (6.5.39) and (6.5.41), it gives a dipole moment and outgoing light with the same frequency as the incoming (laser) source. For O_h symmetry we have that $[\alpha^{A_{1g}}(\cdots 0 \cdots)]$ is the only nonzero component, and so the Rayleigh polarizability tensor is a unit tensor $\overleftrightarrow{\mathbf{1}}$. In this case the Rayleigh polarization must be the same as that of the incoming light.

The second terms give what is called the FIRST-ORDER or FUNDAMENTAL RAMAN SCATTERING. Each oscillating normal coordinate

$$x_i^\alpha = x_i^\alpha(+)e^{i\omega_\alpha t} + x_i^\alpha(-)e^{-i\omega_\alpha t} \tag{6.5.45}$$

gives the following contribution to the oscillating dipole:

$$\begin{aligned}\mathbf{p} &= \sum_{\gamma, m} \alpha_m^\gamma \mathbf{T}_m^\gamma \cdot \mathbf{E} e^{i\omega t} \\ &= \sum_{\gamma, m} \cdots + \left[\frac{\partial \alpha_m^\gamma}{\partial x_i^\alpha}(\cdots 0 \cdots)\right] \\ &\quad \times \left(x_i^\alpha(+)e^{i(\omega+\omega_\alpha)t} + x_i^\alpha(-)e^{i(\omega-\omega_\alpha)t}\right)\mathbf{T}_m^\gamma \cdot \mathbf{E} + \cdots .\end{aligned} \tag{6.5.46}$$

This depends on the constants in the brackets being nonzero for some irrep (γ). If for some (γ), $[(\partial \alpha_m^\gamma / \partial x_i^\alpha)(\cdots 0 \cdots)]$ is nonzero, then the spectrograph in Figure 6.5.13 may record a bump at frequency $\omega - \omega^\alpha$ called the α-STOKES LINE, and possibly another bump at $\omega + \omega^\alpha$ called the α-ANTI-STOKES LINE. However, if no tensor component α_m^γ exists such that $\gamma = \alpha$, then the bracket constants must be zero for that mode $\binom{\alpha}{i}$. In this case we say that the spectral lines $\omega \pm \omega^\alpha$ are RAMAN INACTIVE or FORBIDDEN.

For example, there are three triply degenerate frequencies of UF_6 which cannot show up in the ordinary Raman spectrum, namely, $\omega_\alpha^{T_{2u}}$, and the two $\omega^{T_{1u}}$ vibrations. To be Raman active, an O_h vibration mode x_i must belong to one of the $\binom{\gamma}{m}$ irreps that are used to define a second-rank symmetric tensor $\overleftrightarrow{\alpha}$, namely A_{1g}, E_g, or T_{2g}.

Consider now the detailed form of some Raman-active modes. In Figure 6.5.14 we show how the expansion of the polarizability tensor gives various contributions. We can visualize various effects in the drawings below.

The main idea is that if the molecule expands in some direction then the polarizability for that direction increases. The symmetry analysis keeps track of the precise ratios of the polarizability components for each case, and tells which components must vanish. We have shown only one component of each

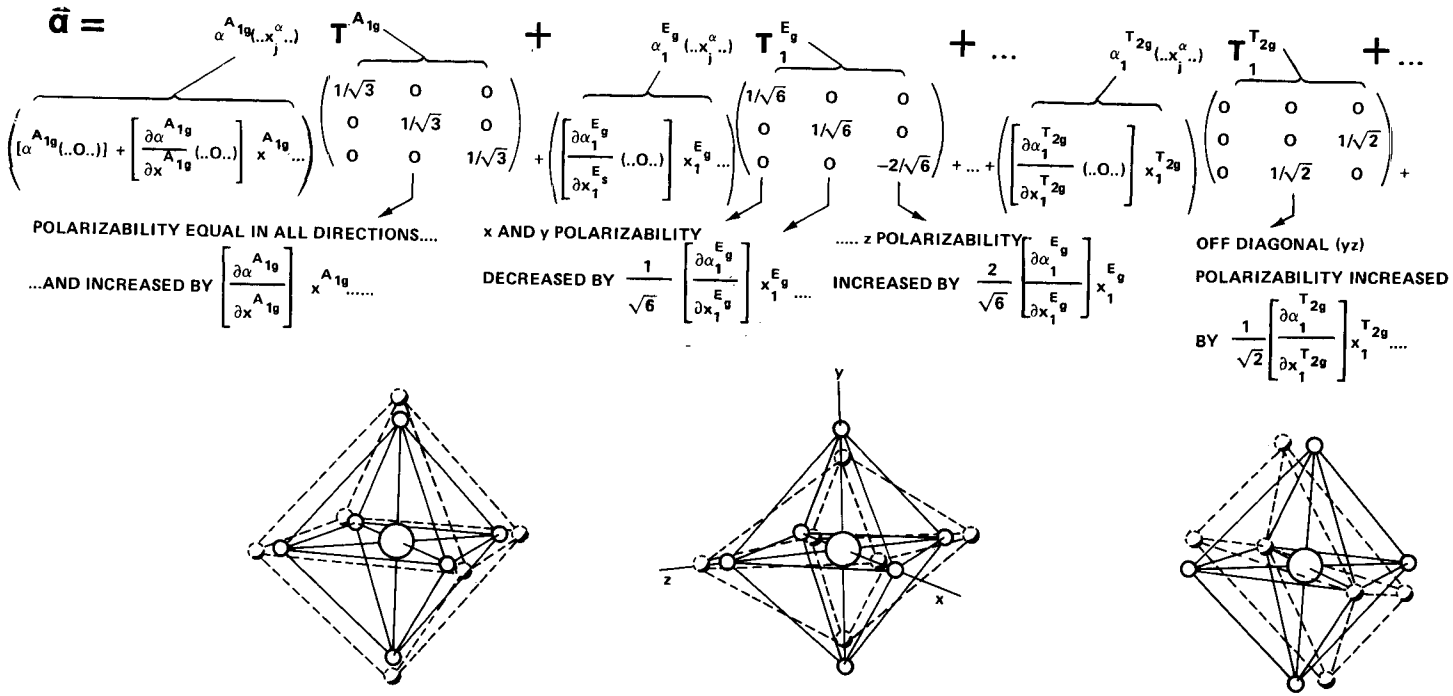

Figure 6.5.14 Linear (first order) effects of modes A_{1g}, $E_g(1)$, and $T_{2g}(1)$ on polarizability.

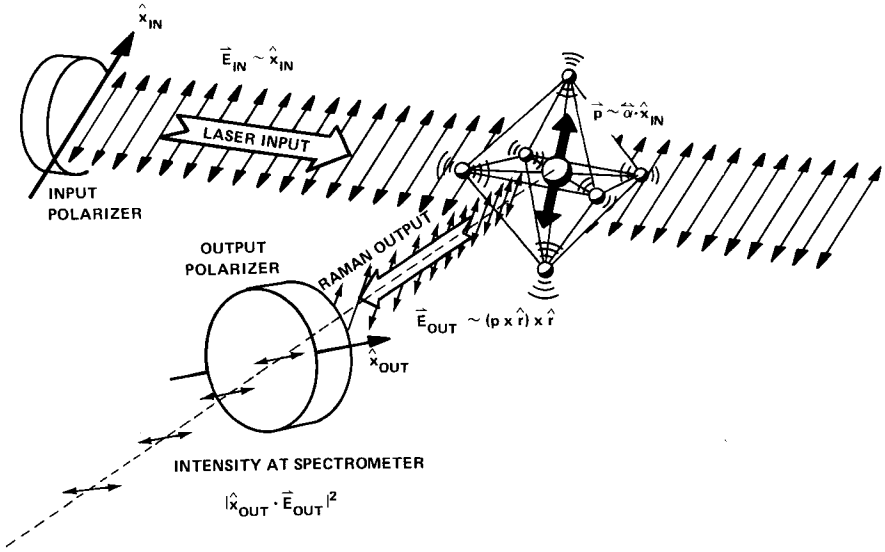

Figure 6.5.15 Geometry of raman polarization experiment.

Raman-active mode in the figure. You might find it instructive to look at some of the others, particularly $\begin{pmatrix} E_g \\ 2 \end{pmatrix}$. Note that the bracket constants such as $[\partial \alpha_2^{E_g} / \partial x_2^{E_g}(\cdots 0 \cdots)]$ for the other components must equal those of the first component. (Recall the tensor theorem.)

The second-order terms in Eq. (6.5.44) or any higher-order terms may be treated in exactly the same way for the analogous expansion of the dipole moment in the preceding section. The main difference here is that any mode x_i^α can contribute to the polarizability of a second-order term of the form $(\sum_i C_{ii}^{\alpha\alpha^{A_1}} x_i^\alpha x_i^\alpha T^{A_1})$. However, during one vibration period for the rise and fall of x_i^α, this contribution rises twice. Hence, these terms lead to spectral lines of overtone Raman scattering with frequency $\omega_{\text{laser}} \pm 2\omega^\alpha$. In this way inactive modes can be observed, although their contributions are usually quite weak unless they are encouraged by stimulation or resonance techniques.

Each of the different Raman processes have more or less distinctive forms for their contribution to the polarizability tensor, as shown by the examples in Figure 6.5.14. This means it is possible to distinguish one type of mode from another by adjusting polarizations at the laser and at the slit in Figures 6.5.13 and 6.5.15. This is certainly true for a solid for which the crystal axis remains fixed with respect to the experiment. However, it is also true for gas and liquid molecules even though they are rotating.

Figure 6.5.15 shows how the output polarization will depend upon the polarization of the input beam and the polarizability tensor $\vec{\vec{\alpha}}$. This is derived

in the following, where the proportionality constants in Eq. (6.5.41) are deleted:

$$\begin{aligned}\text{output amplitude} &\sim \hat{\mathbf{x}}_{\text{out}} \cdot \mathbf{E}_{\text{out}} \sim \hat{\mathbf{x}}_{\text{out}} \cdot [(\hat{\mathbf{p}} \times \hat{\mathbf{r}}) \times \hat{\mathbf{r}}] \\ &= (\hat{\mathbf{x}}_{\text{out}} \cdot \hat{\mathbf{r}})(\mathbf{p} \cdot \hat{\mathbf{r}}) - (\hat{\mathbf{x}}_{\text{out}} \cdot \mathbf{p})(\hat{\mathbf{r}} \cdot \hat{\mathbf{r}}) \\ &= -(\hat{\mathbf{x}}_{\text{out}} \cdot \mathbf{p}) \\ &\sim -(\hat{\mathbf{x}}_{\text{out}} \cdot \vec{\alpha} \cdot \hat{\mathbf{x}}_{\text{in}}).\end{aligned} \tag{6.5.47}$$

If you can ignore all but one type of symmetry-defined tensor $\mathbf{T}^{\gamma}$ in the expansion of α, then you will observe the polarization dependence that is peculiar to the γ-type modes. For example, if only the T_{2g} modes are excited, and you only observe the light scattered with the $\omega^{T_{2g}}$ frequency shift, then the output intensity is the square of the following output amplitude:

$$\langle \hat{\mathbf{x}}_{\text{out}} \cdot \vec{\alpha} \cdot \hat{\mathbf{x}}_{\text{in}} \rangle^{T_{2g}} = \overbrace{x_{\text{out}}\, y_{\text{out}}\, z_{\text{out}}} \begin{pmatrix} 0 & \alpha & \alpha \\ \alpha & 0 & \alpha \\ \alpha & \alpha & 0 \end{pmatrix} \begin{pmatrix} x_{\text{in}} \\ y_{\text{in}} \\ z_{\text{in}} \end{pmatrix}. \tag{6.5.48}$$

By adjusting the polarization and beam angles between $\hat{\mathbf{x}}_{\text{out}}$ and $\hat{\mathbf{x}}_{\text{in}}$ it is possible to distinguish T_{2g} resonances from others. The A_{1g} resonances, for example, have an isotropic polarization response since their α tensor is proportional to the unit matrix.

6.6 MULTIPLY EXCITED QUANTUM VIBRATION STATES

The quantum description of molecular vibrations was introduced in Section 4.4. That discussion contained a derivation of the eigenstate

$$\frac{\cdots (a_i^{\dagger\alpha})^{n_i^{\alpha}} \cdots (a_j^{\dagger\beta})^{n_j^{\beta}} \cdots | \cdots 0 \cdots 0 \cdots \rangle}{\sqrt{\cdots n_i^{\alpha}! \cdots n_j^{\beta}! \cdots}} \equiv | \cdots n_i^{\alpha} \cdots n_j^{\beta} \cdots \rangle \tag{6.6.1}$$

of the harmonic Hamiltonian: $H = \sum_{i,j} \hbar\omega_{\alpha}(a_i^{\dagger\alpha} a_i^{\alpha} + \frac{1}{2}\mathbf{1})$ where the quantum numbers $n_i^{\alpha} = 1, 2, \ldots$ are the number of excitations of the mode of type $\binom{\alpha}{i}$. [In solid-state physics one speaks of n_i^{α} as the number of $\binom{\alpha}{i}$ PHONONS.]

An introduction to the excited or multiphonon vibration spectrum was given in Section 4.4.D. The first, second, third, ... excited states of a mode belonging to a one-dimensional irrep (for example, $\alpha = A_{1g}$ in XF_6) are all singly degenerate with energies $E_0 + n^{\alpha}\hbar\omega_{\alpha}$. This is just like the ordinary one-dimensional oscillator spectrum. The excited states of a mode belonging to a two-dimensional irrep (for example, $\alpha = E_g$ in XF_6) have degeneracies $(2, 3, 4, \ldots, n + 1)$ for levels $E_0 + (\hbar\omega_{\alpha}, 2\hbar\omega_{\alpha}, 3\hbar\omega_{\alpha}, \ldots, n\hbar\omega_{\alpha})$. A mode

belonging to a triply degenerate irrep (for example, $\alpha = T_{1u}, T_{2u}, \ldots$, etc. in XF_6) has excited-state energies of $E_0 + \hbar\omega_\alpha$, $E_0 + 2\hbar\omega_\alpha$, $E_0 + 3\hbar\omega_\alpha, \ldots$, $E_0 + n\hbar\omega_\alpha$, with degeneracies $3, 6, 10, \ldots, (n+1)(n+2)/2$, respectively. This is the three-dimensional oscillator spectrum.

This can be generalized for any irrep dimension l^α. The resulting degeneracies are the combination coefficients in Pascal's triangle as given by Eq. (4.4.64). Now Clebsch-Gordon coupling analysis can be used to discuss the form of the wave functions and spectral splitting of multiphonon configurations.

Anharmonicity Splitting

The large degeneracies of excited degenerate vibration modes come from a harmonic Hamiltonian. However, for any molecular or solid complex, the harmonic part is only the first of many terms in an approximation that must have higher-order potentials in order to describe what happens when the system is very excited. The $\Sigma_{\alpha,i}(x_i^\alpha)^2$ terms by themselves are the harmonic oscillator potential, while any higher terms $(x_i^\alpha)^3, (x_i^\alpha)^4, \ldots$ are said to make the oscillator ANHARMONIC.

Now, only those anharmonicities are permitted which have the same (G) symmetry of the physical system. (The harmonic terms obviously have G symmetry.) By systematically constructing all independent scalar polynomials,

$$\sum_{j,k,\ldots} \mathscr{C}_{i_1 i_2 j}^{\alpha_1 \alpha_2 \gamma} \mathscr{C}_{j j_3 k}^{\gamma \alpha_3 \beta} \cdots \mathscr{C}_{l i_n}^{\delta \alpha_n 0} \cdot x_{i_1}^{\alpha_1} x_{i_2}^{\alpha_2} x_{i_3}^{\alpha_3} \cdots x_{i_n}^{\alpha_n}, \tag{6.6.2}$$

using G coupling coefficients, one will find all the independent anharmonic terms of a given order. The final coupling $(\mathscr{C}_{l i_n}^{\delta \alpha_n 0})$ must give a scalar.

One effect of anharmonic terms will be the splitting of the degeneracy of the multiply excited (overtone or combination tone) vibration levels. Consider, for example, the six states of harmonic eigenvalue $E_0 + 2\hbar\omega_{T_{2u}}$,

$$|0 \cdots (2)_{T_{2u}} \cdots 0\rangle = a_i^{\dagger T_{2u}} a_j^{\dagger T_{2u}} |0 \cdots 0 \cdots 0\rangle / \sqrt{2} \tag{6.6.3}$$

in an O_h system such as XF_6. These belong to the $2v_6$ level in Figure 4.4.8. From these we can make states of definite O_h symmetry using coupling coefficients:

$$\left|(2)_{T_{2u}} {}^{\gamma}_{m}\right\rangle = \sum_{i,j} \mathscr{C}_{ijm}^{T_{2u} T_{2u} \gamma} a_i^{\dagger T_{2u}} a_j^{\dagger T_{2u}} |0 \cdots 0 \cdots 0\rangle / \sqrt{2}\,. \tag{6.6.4}$$

To first order, these will be eigenstates in the presence of anharmonic potentials. Note that we obtain just six symmetrized-outer-product bases A_{1g}, E_g (1 and 2), and T_{2g} (1, 2, and 3) because of the commutation symmetry $a_i^\dagger a_j^\dagger = a_j^\dagger a_i^\dagger$. By adjoining one more $a_k^{\dagger T_{2u}}$ factor, we see that 10 third-order states appear. The resulting anharmonic splittings are indicated in Figure 6.6.1(a).

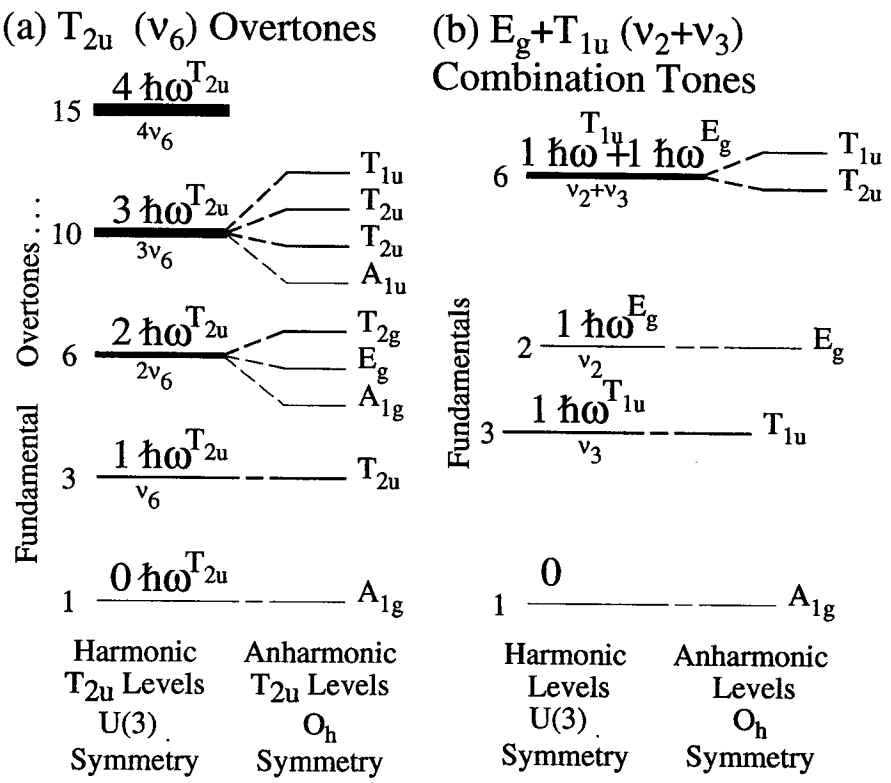

Figure 6.6.1 Examples of multiple vibration levels. Harmonic and anharmonic eigenvalues are indicated. (a) Overtone levels. (b) Combination tone levels.

The combination-tone levels arise from the coupled products in the same way, as seen in Figure 6.6.1(b). Note that the commutation symmetry $a_i^{\dagger\alpha}a_j^{\dagger\beta} = a_j^{\dagger\beta}a_i^{\dagger\alpha}$ does not eliminate any terms when $\alpha \neq \beta$.

To gain some appreciation of the complexity of overtone and combination levels one should examine the level diagrams for SF_6, UF_6, and SiF_4 in Figures 6.6.2(a–c) by R. S. McDowell and B. J. Krohn at Los Alamos. The spectroscopy upon which they are based is described in some of the references given at the end of Chapter 4 and in Chapter 7. The spectroscopic notation for the fundamental levels discussed in Chapter 4 (recall Figures 4.4.5 and 4.4.6) is $\nu_1 = A_{1g}$, $\nu_2 = E_g$, $\nu_3 = T_{1u}$(high), $\nu_4 = T_{1u}$(low), $\nu_5 = T_{2g}$, and $\nu_6 = T_{2u}$. The center of the figure is devoted to the ν_3 overtone ladder which provides a pathway for infrared laser dissociation of the molecule. The need to investigate dissociation and apply it to isotope separation was the driving force behind much of the initial high-resolution spectroscopy of UF_6, SF_6, and related molecules. The overtone levels for UF_6 are shown for comparison in Figure 6.6.2(b), and SiF_4 levels are displayed in Figure 6.6.2(c).

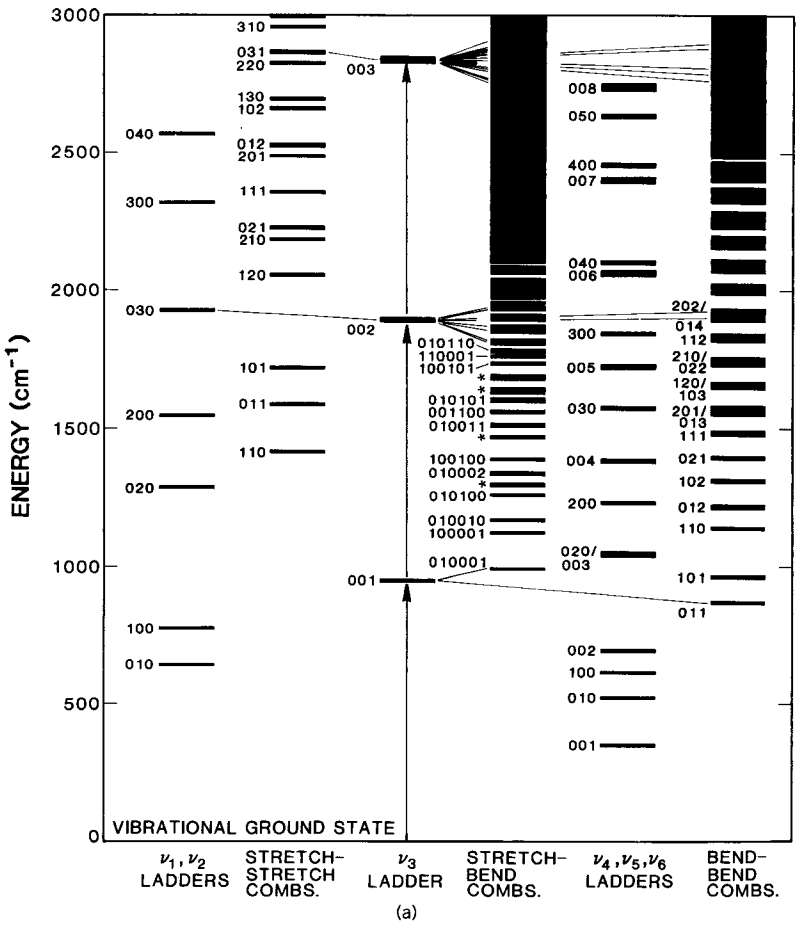

Figure 6.6.2a Vibrational levels in SF_6 below 3000 cm^{-1}, illustrating intramolecular energy transfer in multiple photon excitation of the lower ν_3 ladder. The level energies are based on the ν_i and x_{ii} constants of McDowell and Krohn. In the fourth column the levels are labeled with the vibrational quantum numbers $v_1v_2v_3v_4v_5v_6$; in the first three columns with $v_1v_2v_3$ (v_4, v_5, and v_6 understood to be zero); and in the last two columns with $v_4v_5v_6$ ($v_1 = v_2 = v_3 = 0$). The four levels marked with asterisks are (in order of decreasing energy) 010020/010003, 100011/001002/020001, 001010/100002, and 100010/001001; also, in column six, 031 falls between 202 and 014. Anharmonic splittings of higher vibrational manifolds were arbitrarily assumed to be 1 cm^{-1} between sublevels, except for $2\nu_3$ and $3\nu_3$, for which the sublevel positions of Patterson, Krohn, and Pine were used. Each sublevel was given a width of 12 cm^{-1} to indicate rotational broadening. There are approximately 327 vibrational levels between 0 and 3000 cm^{-1}, comprising about 5540 sublevels. Also shown are typical near-resonant collisional pathways out of the ν_3 ladder for which the centers of the vibrational manifolds are detuned by less than 80 cm^{-1}. (After R. S. McDowell and B. J. Krohn, unpublished.)

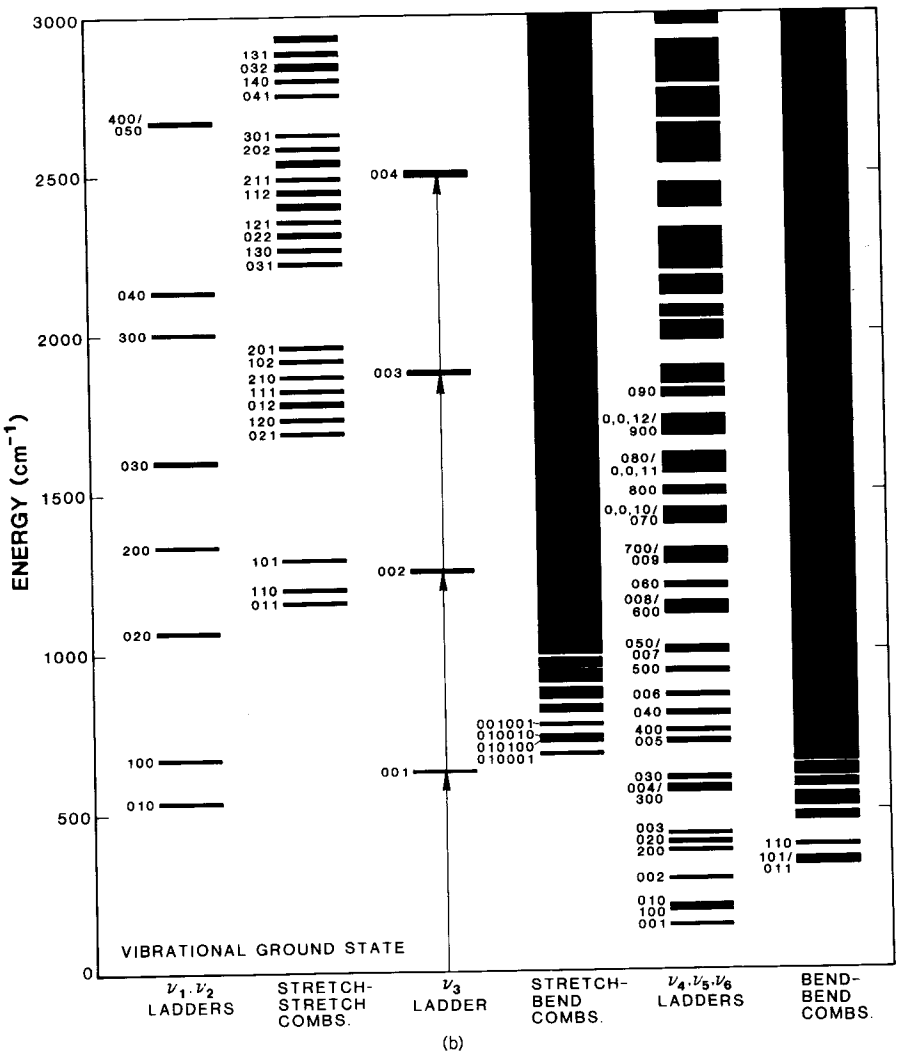

Figure 6.6.2b Vibrational energy levels of UF_6 below 3000 cm^{-1}. The level energies are based on the ν_i and x_{ij} constants of Adlridge et al., except that $x_{33} = -0.7$ cm^{-1}. The levels are labeled as in Figure 6.6.1. Anharmonic splittings were assumed to be 1 cm^{-1} between sublevels, except for the ν_3 ladder, for which the sublevel positions of Krohn et al., were used. Each sublevel was given a width of 12 cm^{-1} to indicate rotational broadening. There are approximately 1015 vibrational levels between 0 and 2000 cm^{-1}, comprising about 120,700 sublevels. For a given amount of ν_3 excitation, higher bending levels are more accessible for UF_6 than for SF_6. (After R. S. McDowell and B. J. Krohn, unpublished.)

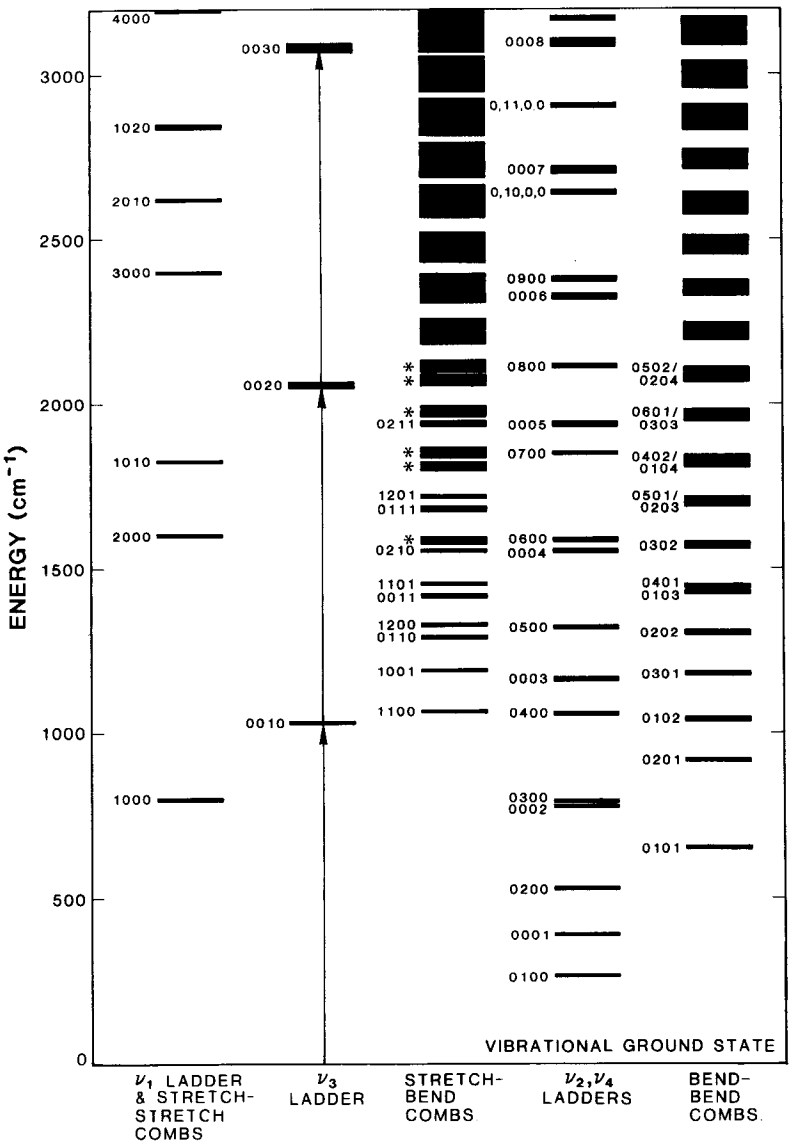

Figure 6.6.2c Vibrational energy levels of SiF_4 below 3200 cm^{-1}. The level energies are based on the ν_i and x_{ij} constants of McDowell et al., and are labeled with the vibrational quantum numbers $v_1v_2v_3v_4$. The six levels marked with asterisks in column three are (in order of decreasing energy) 2200/1500/1202, 1110/0410/0112, 2001/1301/1003, 2100/1400/1102, 0310/0012, and 1300/1002. Anharmonic splittings were assumed to be 1 cm^{-1} between sublevels, except for $2\nu_3$ and $3\nu_3$, for which the sublevel positions of Patterson and Pine were used. Each sublevel was given a width of 12 cm^{-1} to indicate rotational broadening. There are approximately 185 vibrational levels between 0 and 3200 cm^{-1}, comprising about 2185 sublevels. (After R. S. McDowell and B. J. Krohn, unpublished.)

A desire to understand the general problem of intramolecular vibrational energy redistribution (IVER) has stimulated research on vibrational overtone and combination states of many molecules. In order to reduce the complexity of the problem, many researchers have chosen to examine simpler molecules and anharmonic vibrational models. Since diatomic molecules seem to be too simple to show IVER effects one must consider triatomic molecules—such as H_2O, H_2S, or O_3, or weakly bound triatomic clusters such as HFAr.

One of the most famous triatomic anharmonic vibrational potential models is the third-order C_{3v} symmetric potential constructed from the two-vector normal coordinates $\{x \equiv q_1^E, y \equiv q_2^E\}$. Using coupling coefficients for the group C_{3v} we have

$$V = \lambda(x^3 - 3xy^2).$$

This is known as the Henon-Heiles potential function. Breaking the symmetry to C_2 yields the Barbannis potential:

$$U = \lambda x^3 - 3uxy^2.$$

This recovers the C_{3v} symmetry when $u = \lambda$. Some effects of nonlinear and anharmonic potentials are discussed in Chapter 7 and references.

6.7 INTRODUCTION TO THEORY OF SYMMETRY STABILITY

So far it has been assumed that the Hamiltonian or equations of motion of various systems had a certain symmetry. By making various models subject to the symmetry constraint one could relate and predict various properties of the systems which the models represent. However, such an approach cannot give you much of a clue about how the symmetry came about in the first place, i.e., why the electronic and electromagnetic forces hold some configuration in a symmetric form. Now by relaxing the assumptions about these Hamiltonians somewhat it is possible to gain a little insight into what forms may or may not be stable under various conditions.

This involves an interaction between nuclear (or vibrational) and electronic motion which is called VIBRONIC motion. This section contains an introduction to vibronic Hamiltonians and their symmetry properties. This leads to the Jahn-Teller theory of symmetry stability.

A. Symmetry Analysis of Vibronic Hamiltonians

In the models of molecular electronic orbitals given in Chapters 2–5 and later in Chapter 7 Section 7.6 some approximate electronic eigensolutions are derived for electrons tunneling or orbiting around several fixed potential wells. The potential wells represent the nuclei of a molecule, and so the

electronic levels were derived for one fixed position of nuclei. On the other hand, the models of nuclear motion in molecular vibrations were based on the assumption of internuclear potential functions or "spring constants." The internuclear potential represents the combined effect of nuclear Coulomb repulsion and electronic bonding energy. The bonding energy depends on the eigenvalue of the electronic ground-state eigenfunction.

In Section 4.3.D various changes of energy or positions of octahedral potentials were seen to shift or split the energy eigenvalues. (Recall Figures 4.3.5 and 4.3.7.) One can imagine that each electronic energy eigenvalue ε^γ of a molecule is plotted as a function $\varepsilon^\gamma(\cdots x_i^\alpha \cdots)$ of the nuclear positions or normal coordinates x_i^α. If the internuclear repulsion potential $Z(\cdots x_i^\alpha \cdots)$ is added, there results an effective potential

$$V^\gamma(\cdots x_i^\alpha \cdots) = \varepsilon^\gamma(\cdots x_i^\alpha \cdots) + Z(\cdots x_i^\alpha \cdots)$$

for each electronic state. The BORN-OPPENHEIMER APPROXIMATION amounts to picking just one of these effective potentials for the nuclear vibration Hamiltonian. For molecules in their electronic ground states one picks the ground state V^γ. This is a good approximation as long as the splitting between different $V^\gamma, V^{\gamma'}, \ldots$ is much greater than the fundamental vibration energies resulting from each effective potential. In other words, a single electronic level provides an effective nuclear potential as long as the nuclei move slowly compared to the electrons.

Now it is clear that the Born-Oppenheimer approximation may break down for any ε^γ belonging to degenerate electronic levels or multidimensional ($l^\gamma > 1$) irreps. The possibility of electronic degeneracy signals the need for a vibration-electronic or vibronic Hamiltonian which strongly effects the stability of the molecule. The question of stability is: "What values of x_i^α are stable local minima for $V^\gamma(\cdots x_i^\alpha \cdots)$?" or more to the point: "Is a stable minimum of $V^\gamma(\cdots x_i^\alpha \cdots)$ found at the symmetry configuration where $x_i^\alpha = 0$?"

To answer this, imagine that the total Hamiltonian $H(\cdots \mathbf{r}_e \cdots x_i^\alpha \cdots)$ operator for the nuclei and electrons can be expanded in powers of the nuclear coordinates x_i^α.

$$H(\cdots \hat{r}_e \cdots x_i^\alpha \cdots) = H^0(r) + \sum_{\alpha,i} H_i^\alpha(r) x_i^\alpha + \sum_{\gamma,m} H[\alpha\beta]_m^\gamma(r)[x^\alpha x^\beta]_m^\gamma + \cdots. \quad (6.7.1a)$$

Here each $H(r)$ operator factor is a function only of the electronic operators, and we use a bracket notation to abbreviate the quadratic Clebsch-Gordon combinations of nuclear coordinates:

$$[x^\alpha x^\beta]_m^\gamma = \sum_{i,j} \mathscr{C}_{ijk}^{\alpha\beta\gamma} x_i^\alpha x_j^\beta. \quad (6.7.1b)$$

Higher-order (anharmonic) terms in this expansion will be important in general, but, for now, we will only consider terms of second order or less. The Hamiltonian $H(\cdots \mathbf{r} \cdots \mathbf{x} \cdots)$ being considered contains all the kinetic energy terms $(\cdots P_e^2/2m_e \cdots P_N^2/2M_N \cdots)$ for n_e electrons and n_N nuclei, all the Coulomb potentials of interaction between then $1/|\mathbf{r}_e - \mathbf{r}_{e'}| \cdots 1/|\mathbf{x}_N - \mathbf{x}'_N| \cdots 1/|\mathbf{r}_e - \mathbf{x}_N|)$, and nuclear and electronic spin operators, too, if they are important.

Assuming the external environment is isotropic, such a Hamiltonian is completely invariant to all rigid spatial rotations from the group O_3 discussed in Chapter 5. Also, it is invariant to all $n_e! n_{N_1}! n_{N_2}! \cdots$ permutations of identical particles. Together, this amounts to an enormous symmetry, in general, which is larger than the ordinary molecular point symmetry G which the nuclei will have if $(x_i^\alpha = 0)$ is a stable minimum.

Indeed, there is more physical symmetry in fundamental descriptions of nature than is readily apparent from most of the objects which we observe. Hidden symmetry is a fascinating subject because it usually involves more fundamental and simpler principles which explain complex spectral effects. Elementary examples of hidden symmetry were introduced in connection with spontaneous symmetry breaking in Section 4.3.C. The "global" symmetry discussed there corresponds to hidden symmetry, while the "local" symmetry corresponds here to the molecular point symmetry G of a stable molecule. Most molecules become "frozen" into stable G-symmetric forms and never get to realize the full freedom of their hidden symmetry.

It is important to establish some criteria for determining whether a particular molecular symmetry G or a G-symmetric arrangement is stable. To do this we imagine, again, putting the nuclei in a G-symmetric position long enough for all the electrons to settle down into some ground-state orbital that transforms according to irrep $\mathscr{D}^\gamma$ of G. Then, using this assumption of a (γ) orbital, the fact that $H(\cdots \mathbf{r} \cdots, \cdots x_i^\alpha \cdots)$ has G symmetry (at least!), and Eq. (6.7.1a), we may derive an energy submatrix for the electronic substates $|{}^\gamma_m\rangle$:

$$\begin{pmatrix} \left\langle {}^\gamma_1 \middle| H \middle| {}^\gamma_1 \right\rangle & \left\langle {}^\gamma_1 \middle| H \middle| {}^\gamma_2 \right\rangle \cdots \\ \left\langle {}^\gamma_2 \middle| H \middle| {}^\gamma_1 \right\rangle & \left\langle {}^\gamma_2 \middle| H \middle| {}^\gamma_2 \right\rangle \cdots \\ \vdots & \vdots \end{pmatrix}. \tag{6.7.2}$$

Since $H(\cdots \mathbf{r} \cdots, \cdots x_i^\alpha \cdots)$ has G symmetry, we must have that the purely electronic operator factors $H_i^\alpha(r), H[\alpha\beta]_n^\delta(r), \ldots$ transform as irreducible tensorial operators with irrep labels $\binom{\alpha}{i}, \binom{\delta}{n}, \ldots$, respectively. That is, each term in Eq. (6.7.1a) is a G scalar. This allows one to expand and

evaluate each energy submatrix component using the Wigner-Eckart theorem:

$$\left\langle \begin{matrix}\gamma\\ m\end{matrix}\middle|H\middle|\begin{matrix}\gamma\\ j\end{matrix}\right\rangle = \left\langle \begin{matrix}\gamma\\ m\end{matrix}\middle|H^{A}\middle|\begin{matrix}\gamma\\ j\end{matrix}\right\rangle + \sum_{\alpha,i}\left\langle \begin{matrix}\gamma\\ m\end{matrix}\middle|H_i^{\alpha}\middle|\begin{matrix}\gamma\\ j\end{matrix}\right\rangle x_i^{\alpha} + \sum_{\delta,n}\left\langle \begin{matrix}\gamma\\ m\end{matrix}\middle|H[\alpha\beta]_n^{\delta}\middle|\begin{matrix}\gamma\\ j\end{matrix}\right\rangle [x^{\alpha}x^{\beta}]_n^{\delta} \cdots$$
$$= \mathscr{C}_{jm}^{A\gamma\gamma}\langle\gamma\|A\|\gamma\rangle + \sum_{\alpha,i}\mathscr{C}_{ijm}^{\alpha\gamma\gamma}\langle\gamma\|\alpha\|\gamma\rangle x_i^{\alpha}$$
$$+ \sum_{\delta,n}\mathscr{C}_{njm}^{\delta\gamma\gamma}\langle\gamma\|[\alpha\beta]\delta\|\gamma\rangle[x^{\alpha}x^{\beta}]_n^{\delta} + \cdots . \qquad (6.7.3)$$

B. The Jahn-Teller Theorem

Let us pick once again the example of the XF_6 molecule which we assumed in Section 4.4 had O_h symmetry. The normal cordinates were $x^{A_{1g}}$, x^{E_g}, $x^{T_{1u}}$ (two kinds), $x^{T_{2g}}$, and $x^{T_{2u}}$, as shown in Figure 4.4.4.

Some possibilities for XF_6 electronic orbitals were briefly discussed in Section 4.3. However, the approximate molecular orbital states $|A_{1g}\rangle$, $|_m^{E_g}\rangle$, and $\left|\begin{matrix}T_{1u}\\ m\end{matrix}\right\rangle$ displayed in Figure 4.3.2 were made just for one electron shared between the F atoms. In a more detailed analysis in later chapters involving more electrons and more orbitals, it will be clear that all irreps can show up as orbitals in general. So one must consider each possible (γ) in Eq. (6.7.3).

Case 1. $\gamma = A_{1g}$, A_{1u}, A_{2g}, or A_{2u}

Substituting $\gamma = A_x$ into Eq. (6.7.3), we find that most of the coupling coefficients are zero. All linear terms except $\alpha = A_{1g}$ are ruled out:

$$\langle A_x|H|A_x\rangle = \langle A_x\|A\|A_x\rangle + \langle A_x\|A_{1g}\|A_x\rangle x^{A_{1g}}$$
$$+ \langle A_x\|[\alpha\alpha]A_{1g}\|A_x\rangle[x^{\alpha}x^{\alpha}]^{A_{1g}} \cdots . \qquad (6.7.4)$$

Of the quadratic terms only $\delta = A_{1g}$ or the harmonic terms

$$[x^{\alpha}x^{\alpha}]^{A_{1g}} = (1/\sqrt{l^{\alpha}})\sum_{i=1}^{l^{\alpha}}(x_i^{\alpha})^2$$

remain. The reduced matrix coefficients $\langle A_x\|[\alpha\alpha]A_{1g}\|A_x\rangle$ must now all be positive in order for the molecule to be stable in a symmetric shape. Then the molecule will alter its $x^{A_{1g}}$ coordinate until a minimum is reached for the energy

$$E = \langle A_x\|A_{1g}\|A_x\rangle x^{A_{1g}} + \langle A_x\|[A_{1g}A_{1g}]A_{1g}\|A_x\rangle(x^{A_{1g}})^2$$

at equilibrium position

$$x^{A_{1g}}(0) = -\langle A_x \| A_{1g} \| A_x \rangle / 2\langle A_x \| [A_{1g} A_{1g}] A_{1g} \| A_x \rangle.$$

However, this shift involves no reduction of symmetry, just a change of size for the molecule.

Case 2. $\gamma = E_g$ or E_u

In the 2×2 energy matrix for an E electronic doublet, we find that two motions x_i^α give possibly nonzero linear terms. These are the motions $x^{A_{1g}}$ and $x_j^{E_g}$:

$$\begin{aligned}\langle H \rangle = {} & \langle E \| A \| E \rangle \begin{pmatrix} 1 & 0 \\ 0 & 1 \end{pmatrix} + \langle E \| A_{1g} \| E \rangle \begin{pmatrix} x^{A_{1g}} & 0 \\ 0 & x^{A_{1g}} \end{pmatrix} \\ & + \frac{\langle E \| E_g \| E \rangle}{\sqrt{2}} \begin{pmatrix} x_1^{E_g} & -x_2^{E_g} \\ -x_2^{E_g} & -x_1^{E_g} \end{pmatrix} \cdot \\ & + \langle E \| [EE] A_{1g} \| E \rangle \cdot \begin{pmatrix} [x^E x^E]^{A_{1g}} & 0 \\ 0 & [x^E x^E]^{A_{1g}} \end{pmatrix} \\ & + \frac{\langle E \| [EE] E \| E \rangle}{\sqrt{2}} \begin{pmatrix} [x^E x^E]_1^E & -[x^E x^E]_2^E \\ -[x^E x^E]_2^E & -[x^E x^E]_1^E \end{pmatrix}. \end{aligned} \tag{6.7.5}$$

Extra quadratic terms show up, too; however, just the linear terms in $x_j^{E_g}$ are sufficient to spoil the O_h symmetry in the ordinary sense. As we will see in the following, the equilibrium position is not at $x_j^{E_g} = 0$ if the reduced matrix element $\langle E \| E_g \| E \rangle$ is finite. Of course, this reduced matrix element might turn out to be zero anyway, even though symmetry does not require it; however, this is improbable.

Case 3. $\gamma = T_{1g}, T_{1u}, T_{2g}$, or T_{2u}

In the 3×3 energy matrix for any T electronic orbital we find that the motions $x^{A_{1g}}$, $x_j^{E_g}$, and $x_i^{T_{2g}}$ all are capable of giving nonzero linear terms, in addition to some nonscalar quadratic terms. Again, we find that the equilibrium position is not necessarily $x_j^{E_g} = 0 = x_i^{T_{2g}}$. Of the Cases 1, 2, and 3 we see that of all the electronic states, only the nondegenerate ones (A) are likely to yield an O_h symmetric XY_6 molecule. This is the content of the following theorem.

Jahn-Teller Theorem There will be at least one possible linear term involving a symmetry-breaking motion in the energy expansion for a degenerate

electronic orbital, except for (a) the electronic spin degeneracy of 2 and (b) the axial angular-momentum degeneracy of 2 for linear molecules.

The theorem was first proved by exhaustive study of each symmetry structure possible with all possible molecular configurations: XY_2, XY_3, $XY_4, \ldots, X_2Y_2$, and so on. Since then more elegant proofs have been devised.

C. Dynamic Jahn-Teller and Renner Effects

We now investigate the ($\gamma = E$) case or Case 2 in more detail. Before beginning, one should note that the E-case mathematics serves as a solution for at least two distinct problems. It pertains to the stability of an O_h-symmetric XF_6 molecule with an E_g or E_u orbital, but it also applies to the triangular C_{3v} molecule displayed in Figure 3.3.4. It may be a model for ozone (O_3). This coincidence happens because the coupling coefficients involving the O_h irreps E_g, A_{2g}, and A_{1g} are precisely the same as those for C_{3v} irreps (3) $\equiv E$, (2) $\equiv A_2$, and (1) $\equiv A_1$. This is fortunate because it is easier to visualize the ozone molecule when trying to get a physical feeling for the results.

Let us rewrite the matrix in Eq. (6.7.5) as follows:

$$\langle H \rangle = \begin{pmatrix} jx_1 + k(x_1^2 + x_2^2) + r(x_1^2 - x_2^2) & -jx_2 + 2rx_1x_2 \\ -jx_2 + 2rx_1x_2 & -jx_1 + k(x_1^2 + x_2^2) - r(x_1^2 - x_2^2) \end{pmatrix} \tag{6.7.6a}$$

by dropping the constant term and the irrep superscripts ($x_j^E \equiv x_j$), and by letting

$$j = \langle E \| E \| E \rangle / \sqrt{2} \tag{6.7.6b}$$

be the coefficients of what are the JAHN-TELLER terms, by letting

$$r = \langle E \| [EE] E \| E \rangle / 2 \tag{6.7.6c}$$

be the coefficients of what are called the RENNER terms, and by letting

$$k = \langle E \| [EE] A_1 \| E \rangle / \sqrt{2} \tag{6.7.6d}$$

be the coefficient of the HARMONIC terms. One can leave the harmonic terms out of the matrix while diagonalizing since they just are proportional to the unit matrix. In that case the secular equation is simply

$$\lambda^2 - \left[\left(jx_1 + r(x_1^2 - x_2^2) \right)^2 + (jx_2 - 2rx_1x_2)^2 \right) = 0,$$

and has the following solution:

$$\lambda = \pm\left(j^2\left(x_1^2 + x_2^2\right) + 2jr\left(x_1^3 - 3x_1x_2^2\right) + r^2\left(x_1^2 + x_2^2\right)^2\right)^{1/2}.$$

It is convenient to switch to polar coordinates in the normal-mode space, where

$$x_1^E = \rho\cos\phi, \qquad x_2^E = \rho\sin\phi. \tag{6.7.7}$$

The total energy eigenvalues (we add the harmonic term back now) have the following form:

$$\varepsilon_{\pm} = k\rho^2 \pm \left(j^2\rho^2 + 2jr\rho^3\cos 3\phi + r^2\rho^4\right)^{1/2} = k\rho^2 \pm j\rho \qquad (\text{for } r = 0). \tag{6.7.8}$$

On the right we have eliminated the Renner terms.

We therefore find some rather curious potential-energy functions of the normal coordinates x_1^E, x_2^E or ρ, ϕ, which are sketched in Figures 6.7.1a and 6.7.1b) for $r = 0$ and $r > 0$, respectively.

The electronic eigenstates can be expressed very nicely in terms of the normal coordinate polar angle for the case $r = 0$

$$\begin{aligned} |\varepsilon_+\rangle &= \cos(\phi/2)\left|\begin{matrix}E\\1\end{matrix}\right\rangle - \sin(\phi/2)\left|\begin{matrix}E\\2\end{matrix}\right\rangle, \\ |\varepsilon_-\rangle &= \sin(\phi/2)\left|\begin{matrix}E\\1\end{matrix}\right\rangle + \cos(\phi/2)\left|\begin{matrix}E\\2\end{matrix}\right\rangle. \end{aligned} \tag{6.7.9}$$

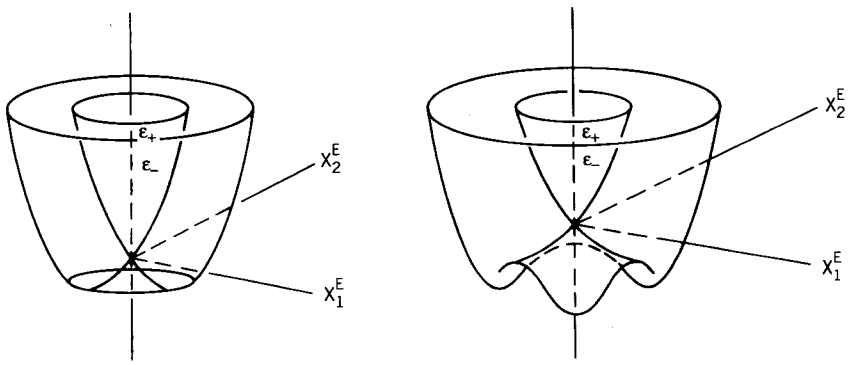

Figure 6.7.1 Potential energy functions of the E-type coordinates. (a) Jahn-Teller terms ($r = 0$). (b) Jahn-Teller and Renner terms ($r > 0$).

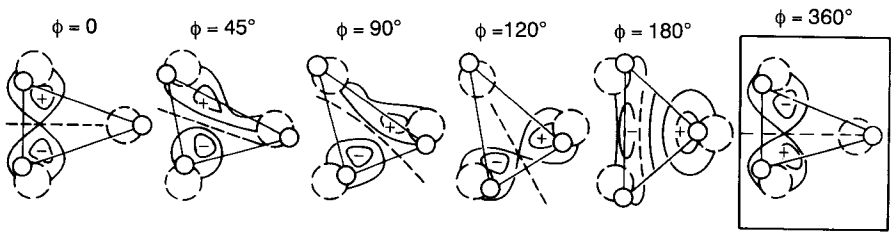

Figure 6.7.2 Electronic state $|\varepsilon_-\rangle$ for various nuclear positions allowed by varying E coordinates.

These are eigenvectors of the electronic matrix [Eq. (6.7.6a)] with $r = 0$:

$$\langle H\rangle = \begin{pmatrix} j\rho\cos\phi & -j\rho\sin\phi \\ -j\rho\sin\phi & -j\rho\cos\phi \end{pmatrix} + k\rho^2 1.$$

In order to visualize this kind of eigenstate, one may imagine the ozone-molecule motions of type (3) or E which were drawn in Figure 3.4.5. Figure 6.7.2 contains sketches of the form of the electronic eigenwave $\langle \cdots \mathbf{r} \cdots |\varepsilon_-\rangle$ for several values of angle ϕ. (We do not know the exact shapes without solving a Schrödinger equation, but symmetry theory gives us a rough idea of form, as explained in Section 2.12.) As we rotate the nuclear distortion ($x_1^E = \rho$, $x_2^E = 0$) into ($x_1^E = \rho\cos\phi$, $x_2^E = \rho\sin\phi$) we see what happens to the electronic wave as shown in Figure 6.7.2. Its progress can be traced by the position of the nodal plane indicated by the dotted line.

One thing to notice is that the electronic wave rotates half as much as the nuclear distortion. A complete rotation $\phi = 360°$ leaves the electronic wave with a minus sign. In Section 5.7.A it was shown that such transformation behavior corresponds to a RAY representation of the symmetry. Half-integral spin states or the states of any two-state system will exhibit this sort of double-valued behavior.

A similar sketch could be made for the electronic state $|\varepsilon_+\rangle$. At $\phi = 0°$ it would be the same as $|\varepsilon_-\rangle$ for $\phi = 180°$. This gives another way to see the multivalued structure. A cross-section of Figure 6.7.1(a) is shown in Figure 6.7.3(a). Note that by going from $\phi = 0°$ to $\phi = 180°$ via the valley, one effectively jumps from the right parabola belonging to state $\left|\begin{matrix}E\\2\end{matrix}\right\rangle$ to the left one belonging to orthogonal electronic state $\left|\begin{matrix}E\\1\end{matrix}\right\rangle$. We have been describing this function as consisting of a top sheet (ε_+) and a bottom sheet (ε_-). This description is probably more suitable, particularly if some perturbation like spin-orbit separates the two sheets as indicated by dotted lines in Figure 6.7.3(b).

By looking again at the various nuclear distortions in Figure 6.7.2 we get some idea what the meaning is of the minima in the (ε_-) energy sheet at

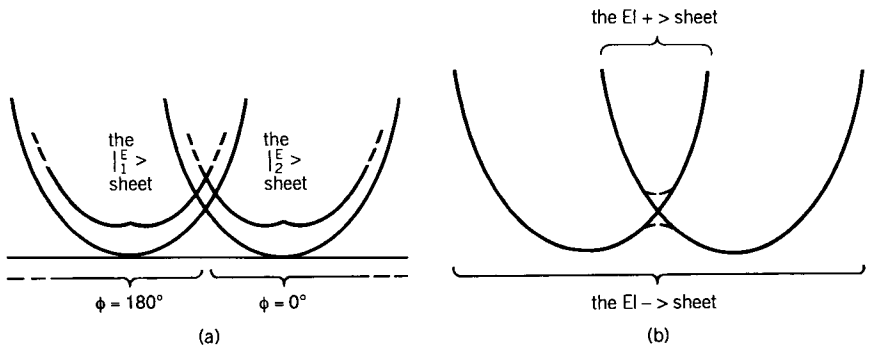

Figure 6.7.3 Different ways to label the cross-sections of the potential surfaces in Figure (6.7.1a). (a) Parabolic potentials due to electronic states $\begin{pmatrix} E \\ 1 \end{pmatrix}$ and $\begin{pmatrix} E \\ 2 \end{pmatrix}$. (b) Separate potential sheets due to excited (+) and ground (−) electronic states.

$\phi = 60°$, 180°, and 300° when the Renner coefficient r is positive [see Figure 6.7.1(b)] or at 0°, 120°, and 240° when r is negative. In particular, the $\phi = 0°$ and $\phi = 120°$ distortions are pictured in Figure 6.7.2. An acute isosceles triangle pointing in one of three directions is stable when $r < 0$. For $\phi = 60°$, 180°, and 300° we find an obtuse isosceles triangle pointing away from these directions.

It might appear that a model Hamiltonian with nonzero j and r terms reduces the molecular symmetry to the Abelian C_{2v} and splits all the electronic and vibrational levels into singlets. This is *not* the case. Let us go back to the beginning by first assuming j and r are zero. With only the scalar harmonic (k) Hamiltonian one has essentially independent electronic and vibration states. One can be rotated without affecting the other.

Suppose the electronic states and classical vibration coordinates being considered transform according to E [or (3)] irreps as before. Then the quantum vibration states transform according to $\beta = A_1; E; E, A_1; \ldots$ for excitation number $N = 0; 1; 2; \ldots$, respectively, according to an accounting explained in the preceding Section 6.6. The quantum states for the whole molecule are then the products,

$$\left| \begin{matrix} E & \beta \\ i & j \end{matrix} \right\rangle = \left| \begin{matrix} E \\ i \end{matrix} \right\rangle_{\text{electron}} \left| \begin{matrix} \beta \\ j \end{matrix} \right\rangle_{\text{nuclei}}, \tag{6.7.10}$$

as indicated on the left of Figure 6.7.4 [see columns (a) and (b)].

In the presence of any electron-vibration interaction represented by j, r, or other terms, it is appropriate to couple the separate electronic and vibrational states to make what are called VIBRONIC states:

$$\left| \begin{matrix} \gamma \\ m \end{matrix} \right\rangle_{\text{vibronic}} = \sum_{i,j} \mathscr{C}_{ijm}^{E\beta\gamma} \left| \begin{matrix} E \\ i \end{matrix} \right\rangle_{\text{electronic}} \left| \begin{matrix} \beta \\ j \end{matrix} \right\rangle_{\text{nuclei}}, \tag{6.7.11}$$

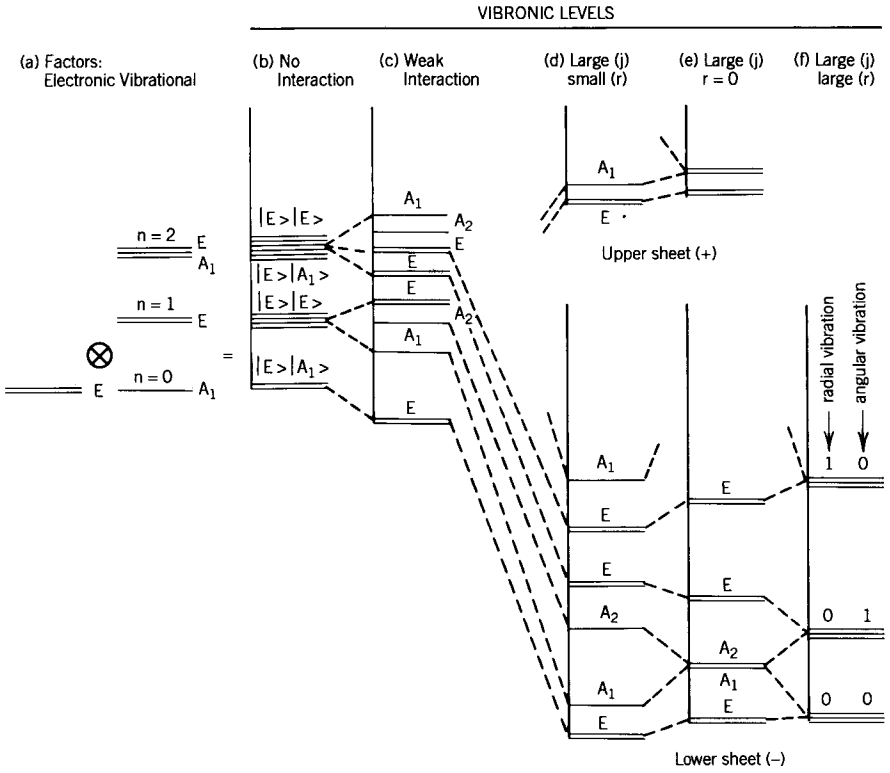

Figure 6.7.4 Vibronic levels arising from the combinations of E-type vibrations with E-type electronic orbitals.

which will, to first order, be eigenstates of the interaction operator. The resulting levels shown in Figure 6.7.4(c) will keep their irrep labels $\begin{pmatrix} \gamma \\ m \end{pmatrix}$ and degeneracy no matter what r or j may be. The E levels will not split, and each vibronic state can be mixed only with others which have the same irrep labels.

Now let us consider the extreme case in which both r and j are large and the nuclear coordinates are essentially "stuck" near the the bottom of one of the three "subvalleys" in Figure 6.7.1(b). The vibration frequency for oscillation in the radial (ρ) direction will be different (presumably higher) than that for the angular (ϕ) direction. Therefore, each state should be singly degenerate. However, this description forces us to consider the corresponding (single) states for each of the configurations in the other two valleys. We then have a total degeneracy of 3 for each level as indicated in Figure 6.7.4(f).

Indeed, we may follow the levels as the constants are changed. For small r, but large j, the angular bumps or saddle points will be reduced; so the three species of vibrational states get mixed with a resulting tunneling and

splitting of the triple degeneracy as indicated in Figure 6.7.4(d). This is similar to the hindered rotation mechanics discussed in Section 2.12. [Recall Figure 2.12.4(a).] This is a good example of spontaneous symmetry breaking. With little or no tunneling the dynamic Jahn-Teller levels collapse into $A_1 + E$ or $E + A_2$ clusters which belong to the $O_1 \uparrow C_{3v}$ or $O_2 \uparrow C_{3v}$ induced representations. In the limit of no tunneling the molecule becomes "frozen" into a local C_v symmetry with an isosceles triangular shape. This is the static Jahn-Teller limit, and the clusters are degenerate. Someone unaware of the hidden C_{3v} symmetry will treat the clusters as singlet levels.

For $r = 0$ the effective potential takes the shape shown in Figure 6.7.1(a). Now a type of free rotation is possible with spectra of the form shown in Figure 6.7.4(e). One may derive a differential equation for the vibronic state in this case and discuss the form of the wave function.

Consider a wave function of the form

$$\Psi_{nl}(\cdots \mathbf{r} \cdots \rho, \phi) = \langle \cdots \mathbf{r} \cdots | \varepsilon_- \rangle \phi_{nl}^-(\rho, \phi) + \langle \cdots \mathbf{r} \cdots | \varepsilon_+ \rangle \phi_{nl}^+(\rho, \phi), \tag{6.7.12}$$

where the electronic parts

$$\langle \cdots \mathbf{r} \cdots | \varepsilon_- \rangle = \sin(\phi/2) \langle \cdots \mathbf{r} \cdots \left| \begin{matrix} E \\ 1 \end{matrix} \right\rangle + \cos(\phi/2) \langle \cdots \mathbf{r} \cdots \left| \begin{matrix} E \\ 2 \end{matrix} \right\rangle,$$

$$\langle \cdots \mathbf{r} \cdots | \varepsilon_+ \rangle = \cos(\phi/2) \langle \cdots \mathbf{r} \cdots \left| \begin{matrix} E \\ 1 \end{matrix} \right\rangle - \sin(\phi/2) \langle \cdots \mathbf{r} \cdots \left| \begin{matrix} E \\ 2 \end{matrix} \right\rangle$$

follow from Eq. (6.7.9), and the nuclear parts

$$\phi_{nl}^{\pm}(\rho\phi) = R_n^{\pm}(\rho) e^{il\phi} \tag{6.7.13}$$

are separated into a radial and angular part. The effective nuclear Hamiltonian is $H = T + V$, where the kinetic part is

$$T = -\frac{\hbar^2}{2}\left[\frac{\partial^2}{\partial\rho^2} + \frac{1}{\rho}\frac{\partial}{\partial\rho} + \frac{1}{\rho^2}\frac{\partial^2}{\partial\phi^2}\right], \tag{6.7.14}$$

and the potential part represents the effect of the electronic states:

$$V = \begin{cases} k\rho^2 + j\rho, & \text{acting on } \phi^+, \\ k\rho^2 - j\rho, & \text{acting on } \phi^-. \end{cases}$$

The angular derivatives in the kinetic part lead to the terms which will mix up

the states from the two energy sheets + and −:

$$\frac{\partial^2}{\partial\phi^2}\langle \cdots \mathbf{r} \cdots |\varepsilon_-\rangle \phi_{nl}^-(\rho,\phi)$$

$$= \frac{\partial^2}{\partial\phi^2}\left(\sin\phi\langle \cdots \mathbf{r} \cdots \left|\begin{matrix}E\\1\end{matrix}\right\rangle + \cos\phi\langle \cdots \mathbf{r} \cdots \left|\begin{matrix}E\\2\end{matrix}\right\rangle\right) R_n^-(\rho)e^{il\phi}$$

$$= \left(-\left(l^2+\tfrac{1}{4}\right)\langle \cdots \mathbf{r} \cdots |\varepsilon_-\rangle + (il)\langle \cdots \mathbf{r} \cdots |\varepsilon_+\rangle\right) R_n^-(\rho)e^{il\phi},$$

$$\frac{\partial^2}{\partial\phi^2}\langle \cdots \mathbf{r} \cdots |\varepsilon_+\rangle \phi_{nl}^+(\rho,\phi)$$

$$= \left(-\left(l^2+\tfrac{1}{4}\right)\langle \cdots \mathbf{r} \cdots |\varepsilon_+\rangle - (il)\langle \cdots \mathbf{r} \cdots |\varepsilon_-\rangle\right) R_n^+(\rho)e^{il\phi}.$$

Using the electronic orthogonality $\langle\varepsilon_+|\varepsilon_-\rangle = 0$, we derive the following equations for the radial functions:

$$\frac{1}{2}\left[-\frac{\partial^2}{\partial\rho^2} - \frac{1}{\rho}\frac{\partial}{\partial\rho} + \frac{l^2+\frac{1}{4}}{\rho^2} + k\rho^2 + j\rho\right] R_n^+(\rho) + i\frac{l}{2\rho^2}R_n^-(\rho) = E_n R_n^+,$$

$$\frac{1}{2}\left[-\frac{\partial^2}{\partial\rho^2} - \frac{1}{\rho}\frac{\partial}{\partial\rho} + \frac{l^2+\frac{1}{4}}{\rho^2} + k\rho^2 - j\rho\right] R_n^-(\rho) - i\frac{l}{2\rho^2}R_n^+(\rho) = E_n R_n^-. \tag{6.7.15}$$

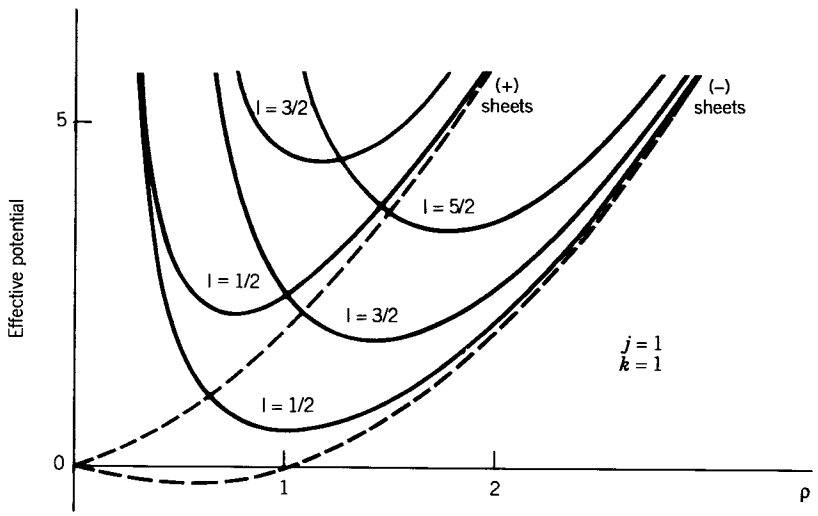

Figure 6.7.5 Effective potential energy surfaces for Jahn-Teller system with various fixed values of vibrational angular momentum ($l = \frac{1}{2}, \frac{3}{2}, \ldots$).

The angular quantum number is restricted to half-integral values $l = 1/2, 3/2, \ldots$ so that wavefunction (6.7.12) will be single valued. [Recall the behavior of the electronic part shown in Fig. (6.7.2)].

For low excited states, we may ignore the coupling terms in Eq. (6.7.15) and obtain the separate solutions

$$\Psi^- = \langle \cdots \mathbf{r} \cdots | \varepsilon_- \rangle R_n^-(\rho) e^{il\phi}, \qquad \Psi^+ = \langle \cdots \mathbf{r} \cdots | \varepsilon_+ \rangle R_n^+(\rho) e^{il\phi}$$

for each energy sheet. (These are Born-Oppenheimer approximate solutions.) Examples of the effective potentials which would give the $R^{\pm}$ functions are plotted in Figure (6.7.5).

ADDITIONAL READING

A standard text on the tensor properties of crystals is by Nye.

J. F. Nye, *Physical Properties of Crystals* Clarendon, Oxford, 1957).

A short elementary introduction to crystal tensor analysis (without much group theory) is the following:

D. R. Lovett, *Tensor Properties of Crystals* (Adam Hilger, Philadelphia, 1989).

An advanced text on crystalline optical properties is the following:

W. A. Wooster, *Tensors and Group Theory for the Physical Properties of Crystals* (Clarendon, Oxford, 1973).

Modern nonlinear optics problems are treated in books by Yariv.

A. Yariv and P. Yeh, *Optical Waves in Crystals* (Wiley, New York, 1984).

A. Yariv, *Quantum Electronics* (Wiley, New York, 1975).

A standard text on light scattering in solids is

M. Born and K. Huang, *Dynamic Theory of Crystal Lattices* Clarendon, Oxford, 1962).

A well-known work on infrared and Raman scattering complements the Herzberg volumes cited earlier at the end of Chapter 3.

E. B. Wilson, J.C. Decius, and P.C. Cross, *Molecular Vibrations: The Theory of Infrared and Raman Spectra* (McGraw-Hill, New York, 1955).

The following are some modern treatments of Raman scattering.

J. Lascombe and P.V. Huong, *Raman Spectroscopy (Linear and Nonlinear)* (Wiley, New York, 1982).

A. Weber (Ed.), *Raman Spectroscopy of Gases and Liquids* (Springer, Berlin, 1978).

G. L. Eesley, *Coherent Raman Spectroscopy* (Pergamon, Oxford, 1981).

The Jahn-Teller effect was first described in the following papers.

H. A. Jahn and E. Teller, "Stability of Polyatomic Molecules in Degenerate Electronic States: I. Orbital Degeneracy," *Proc. R. Soc. London Ser. A*, **161**, 220 (1937). "II. Spin Degeneracy," *Proc. R. Soc. London Ser. A*, **164**, 117 (1938).

These were reprinted in the following volume (which is worth its weight in other precious papers as well).

R. S. Knox and A. Gold, *Symmetry in Solid State* (W. A. Benjamin, New York, 1964).

The Jahn-Teller problem arises in the treatment of crystal fields and orbital bonding which are the subject of the following well-known text. (See also end of Chapter 7).

C. J. Ballhausen, *Introduction to Ligand Field Theory* (McGraw-Hill, New York, 1962).

The Herzberg volume III contains references and discussions of Jahn-Teller and Renner effects.

PROBLEMS

6.1 Use the subgroup chain methods to help compute all the Clebsch-Gordon (CG) coefficients for irreps labeled by subgroup chains:

- **(a)** $D_3 \supset C_2$ (standing wave).
- **(b)** $D_3 \supset C_3$ (moving wave).
- **(c)** $D_4 \supset C_2$.
- **(d)** $D_4 \supset C_4$.

6.2 (a) Use the ($D_3 \supset C_2$) Clebsch-Gordon coefficients (see Problem 6.1) to construct all the possible irreducible tensorial sets of rank- 1 (vectors) and rank- 2 (tensors) that can be made from D_3 base vectors $\hat{x}$, $\hat{y}$, and $\hat{z}$. (Let $\hat{x}$ be along the triangular symmetry axis and vertex, while $\hat{z}$ is normal to plane.)

- **(b)** Construct all the irreducible D_3 polynomials (trigonal harmonics) of degree 1 and 2 using Cartesian coordinates $\hat{x}$, $\hat{y}$, $\hat{z}$.
- **(c)** Construct a third-degree scalar A_1 (invariant) polynomial in x and y. Write it in polar coordinates and sketch its level curves. (This is called the Henon-Heiles potential function.)
- **(d)** Do the same for a third-degree *pseudo*scalar A_2 polynomial in x and y.

6.3 Recall the four fundamental vibrational levels and six states of the X_3 model in Chapter 3. From the ground state...

- **(a)** Which could be excited by x-polarized electric dipole radiation (El_x)?
- **(b)** Which could be excited by z-polarized magnetic dipole radiation (Ml_z)?
- **(c)** Which could be excited by xy-polarized electric quadrupole radiation ($E2_{xy}$)?

6.4 Answer Problem 6.3 for the X_4 model.

6.5 The spectral diagrams for the $(A_{1g}T_{1u}E_g)$ level system in Figures 6.4.1(a) and 6.4.1(b) represent dipole transitions in the presence of a small $O_h \downarrow D_{4h}$ symmetry breaking. Redo these figures for a small *trigonal* $O_h \downarrow D_{3d}$ symmetry breaking.

6.6 Write out the character table of D_{6h} and label group elements and irreps using conventional A, B, E, 1, 2, u, and g labels.

(a) Which irreps transform like polar vectors x, y, and z?

(b) Which irreps transform like axial vectors J_x J_y and J_z?

(c) Which irreps will belong to *genuine* vibrational fundamentals of a hexagonal benzol-like X_6 radical. Account for all motions in 3-space which could have non-zero frequency.

(d) Answer (c) for the benzene molecule, and tell what size matrices would show up in the classical symmetry vibration problem.

(e) Which modes in (d) are infrared-active? Raman-active?